Genetic Mechanisms and Community Dynamics of Bacterial Social Behaviors in Roseobacter member Rhodobacterales strain. Y4I

A Dissertation Presented for the

Doctor of Philosophy

Degree

The University of Tennessee, Knoxville

April C. Armes

December 2021

DEDICATION

To my parents, Ron and Tina Mitchell. They would have been so proud.

ACKNOWLEDGEMENTS

First and foremost, I want to thank my friends and family both blood and chosen. You know who you are. Specifically, I want to thank my brothers, Dusty, Benjamin, and Isaac Mitchell for their support over the years. We might not have always seen eye to eye, but I have always valued your advice and input. I'd also like to thank my 'brothers and sisters' of the Etchison clan for their support. They loved me like family and I love them back as such.

There are several people that I need to acknowledge for helping me evolve into the person I am today. Among them is my advisor, Alison Buchan, who has always been supportive and encouraging of my scientific endeavors. You have been understanding, kind, and caring when I needed it most; and firm, tough-loving, and steadfast when I needed it more. You have supported my career goals to the point of letting me do an internship in the middle of grad school. You have pulled me out of rabbit holes and reigned me in and I'd like to think I've done the same for you. You have been a wonderful mentor and as such have made a major positive impact on my development as a young scientist. Thank you for taking a me and shaping me.

Consisting of a purposely assembled team of all-female amazing scientist, my committee has played a major role in shaping my development over the past several years. You have made meetings something I looked forward to rather than dreaded. You have put up with my strange requests to change the meeting format from a formal presentation to a paper discussion. Thank you for all of your feedback, support, and encouragement throughout the years. Most importantly, thank you for treating me like a colleague rather than a student.

There are several different types of mentorships and few people who can fill all the mentorship roles, but Katie Sipes has done just that for me. Katie, you have been a mentor in your craft (*laughs in bioinformatics*), helped me navigate work and personal conflicts, and have supported through thick and thin. You have always been kind, even when I've been stubborn. You have always treated me with respect and love. I will fondly remember the conversations we've had during our numerous hikes at Ijams or House Mountain, our "basic white girl" photoshoots, and shared laughs in the office. You are my cheerleader, fitness coach, confidant, conference roomie, and best friend. The friendship we share is the type that will always be there despite what distance may be between us. I could not imagine having gone through the last several years without your friendship.

I would be remiss if I did not acknowledge the support I have received from my husband Joseph. It is a comfort to know that you have always had my back. We have faced a lot of loss and a lot of love together. We've navigated personal tragedies, natural disasters, and hardships together. Each time, we have come out stronger together. There isn't anyone else I'd rather be in an emergency situation with. I have enjoyed all of our adventures together, our mutual enjoyment of spoopy things, and co-parenting our fur-babies. Thank you for your partnership, love, and support. I love you forever and always.

Last, but far from least, I want to acknowledge my pets for their comfort and love. My three dogs: Artemis, Apollo, and Nyx and my two cats: Switch and Ronnie Levi Sebastian ('Levi'). Specifically, Levi, who has actively participated in 'helping' me with graduate school from the start. He has helped me grade exams, read papers, analyze data, write manuscripts, and supervised me during the Covid-19 pandemic. It is my opinion that he is deserving of an honorary PhD for his contributions to my work.

ABSTRACT

Quorum sensing (QS) allows bacterial populations to coordinate gene expression, typically in a cell density-dependent manner. Through the production and recognition of small diffusible signaling molecules, called autoinducers, bacteria can elicit group-level behaviors. Prevalent classes of autoinducers in Proteobacteria are *N*-acyl-homoserine lactones (AHL). Exchanges of AHLs in bacterial social engagements allow the regulation of cooperative and competitive interactions contributing to biofilm formation. Biofilms have both clinical and ecological relevance. In marine ecosystems, microbial biofilms contribute to biofouling of equipment, bioremediation of pollutants and transform organic matter which influences global biogeochemical cycles. Early microbial colonizers, such as representatives of the marine Roseobacter Clade, are hypothesized to 'set the stage' for biofilm structure, function, and dynamics via AHL-mediated QS. A necessary first step in understanding how bacterial social behaviors, such as cooperation and competition, influence interactions within biofilms are performing genetic analysis on primary surface colonizers. In Chapter 2, the QS systems of a competitive primary surface colonizer within the Roseobacter Clade, Rhodobacterales strain Y4I, are characterized. The work presented in this chapter demonstrates QS in Y4I is hierarchical. The findings provide a mechanistic understanding of physiological processes important in revealing genetic mechanisms facilitating competitiveness in Roseobacters. Chapter 3 highlights how QS within a microbial biofilm influences community structure and dynamics. The findings within suggests that inactivation of QS in a dominant community member, Y4I, result in increased community cooperation. These data support the hypothesis that primary surface colonizers 'set the stage' for community structure and dynamics in marine ecosystems. In Chapter 4, a model of the DNA regulatory binding site for QS was built to probe Roseobacter genomes for QS-regulated genes. The results presented in this chapter illuminate the genetic diversity within the *Phaeobacter-Leisingera* subclade of Roseobacters. Together, the works presented in this dissertation provide the necessary framework for espousing genetic understanding of QS to culture-based studies using multispecies biofilms. Furthermore, this dissertation provides a rudimentary motif model for probing QS-regulated genes within genomes.

TABLE OF CONTENTS

LIST OF TABLES

LIST OF SUMMPLEMETAL TABLES

LIST OF FIGURES

LIST OF SUPPLEMENTAL FIGURES

Chapter 1 : INTRODUCTION

A version of this introduction was originally written by Alison Buchan, April Mitchell (Armes), W. Nathan Cude, and Shawn Campagna and is published in Stress and Environmental Regulation of Gene Expression and Adaptation in Bacteria.

Alison Buchan, April Mitchell, W. Nathan Cude, and Shawn Campagna. "Acyl-homoserine lactone-based quorum sensing in members of the marine bacterial Roseobacter clade: complex cell-to-cell communication controls multiple physiologies" *Stress and Environmental Regulation of Gene Expression and Adaptation in Bacteria (2016): 225-233*

My contribution to the published version of this chapter was to provide an updated review of the role of quorum sensing in Roseobacter biology and discussion of the integration of master regulatory, CtrA, into the Roseobacter QS regulatory network. Included in the excerpt version below not in the original publication is the addition of bacterial biofilm formation via regulators such as CtrA and the global secondary messenger cyclic-di-GMP.

I. Background

Bacteria have evolved a variety of genetic mechanisms to mediate behaviors in response to environmental signals. One of these mechanisms, frequently referred to as quorum sensing (QS), is dependent upon the concentration of bacterially produced, diffusible chemical cues. Bacteria capable of producing these signal molecules release them into the local environment where they can be sensed by bacteria of the same or different species resulting in regulation of gene expression in a manner that depends upon signal concentration and potentially other environmental cues. In this way, bacterial communities use these signaling systems to communicate, cooperate and/or compete with one another as a form of social interaction. It is hypothesized that QS allows these bacterial consortia to behave as pseudo-multicellular organisms. Phylogenetically diverse bacteria use QS systems to coordinate gene expression (1, 2). QS networks have been implicated in bacterial behaviors including bioluminescence, host colonization, biofilm formation, coordinated motility (i.e., swarming) and virulence (1).

Several classes of small molecule signals are known to mediate intraspecies signaling in bacteria. These signals often upregulate their own production and have been termed autoinducers (1, 3, 4). The major class of intraspecies signal in Proteobacteria are *N*-acylhomoserine lactones (AHLs) (2). Canonical AHL-QS systems produce and respond to AHLs via two proteins, LuxI and LuxR, respectively. The genes encoding these proteins are most often located adjacent to one another on the bacterial chromosome (1). LuxI family proteins synthesize AHLs via cyclization of S-adenosyl methionine (SAM), forming a lactone ring, to which an acylated carbon chain, derived from fatty acid biosynthesis, is conjugated (3). Acyl chain length and saturation, combined with the presence or absence of oxidation at the third carbon, by either a hydroxyl or carbonyl group, allows for species or group specificity (1, 3). LuxR proteins represent a large family of proteins, all of which are response regulators (5). Those LuxR proteins that function in QS systems mediate gene expression required for communal behavior in response to intracellular concentrations of their cognate AHLs (5, 6). Activated LuxR proteins, that is LuxRs bound to their cognate AHLs, typically upregulate *luxI* transcription by binding to a DNA regulatory element termed 'lux box' which enhances the rate of AHL synthesis. Activated LuxR proteins also modulate expression of other genes, including those involved in secondary metabolite production, motility, biofilm formation, and others (1, 2, 5).

II. Bacterial Biofilms

Bacteria switch between motile, or swimming, and sessile lifestyles. Of these two prominent modalities, many bacteria in environmental ecosystems prefer life in the form of a biofilm (7). Biofilms consist of a microbial consortium suspended in an extracellular polymeric substance. Biofilm formation begins by the sensing of a surface, biotic or abiotic in nature. This action, usually referred to as mechanosensing, typically involves external cues such as torque of a flagellum as it encounters a surface establishing a reversible attachment (8). Involved in this "swim-or-stick" decision is typically a response regulator that is activated by environmental stimuli. In the alpha-proteobacterium, *Caulobacter crescentus*, this response regulator is known as the master regulator CtrA. In addition to the "swim-stick" switch, the CtrA phosophorelay system also regulates cell cycle, polar cell division, and flagellar biosynthesis (9–11). This system is highly conserved amongst Alphaproteobacteria and its role in lifestyle switch between motile or sessile modalities has been demonstrated in several Roseobacters (discussed further below)(12).

Another regulator of biofilm formation is the global secondary messenger bis-(3'-5')-cyclic dimeric guanosine monophosphate (c-di-GMP). Like the CtrA phosphorelay system, intracellular levels of c-di-GMP respond to environmental stimuli. Once a concentration threshold is reached the induction of genes, including those promoting biofilm formation, are upregulated in diverse bacteria (13). C-di-GMP can regulate the production of most known extracellular matrix components on transcriptional, post transcriptional, or posttranslational levels (12). Furthermore, central metabolism and intracellular pools of c-di-GMP have been linked through glutamate-induced cyclase activity in some bacteria (e.g., *Pseudomonas aeruginosa* (14)). In a group of marine Alphaproteobacteria, known as the Roseobacter clade, c-di-GMP has been suggested to mediate biofilm formation, likely through the regulation of the CtrA phosphorelay system and integration of cell-to-cell QS (15, 16).

III. The Roseobacter lineage

Members of the Roseobacter clade fall within the Rhodobacteraceae family of the Alphaproteobacteria class and are well represented across diverse marine habitats, from coastal to open oceans and from sea ice to sea floor. The lineage encompasses a large, phylogenetically diverse group of bacteria. At present, the clade contains well over 50 described genera and thousands of uncharacterized isolates and clone sequences (17). It has been proposed that the clade can be parsed into five deeply branching subclades based on a phylogenetic analysis of 70 concatenated conserved single-copy genes (18). The first described members of the group were *Roseobacter litoralis* and *Roseobacter denitrificans*, both pink-pigmented bacteriochlorophyll-*a* producers (19). Subsequent cultivation of clade members, however, revealed that most strains are neither pink nor bacteriochlorophyll-*a* producers. With very few exceptions, the Roseobacter clade is exclusively marine or hypersaline (17, 20). High natural abundances of Roseobacters were first demonstrated in the coastal waters of the southeastern US in the late 1990s using culture-independent approaches (21). Subsequent studies based on culture collections, 16S rRNA gene clone libraries, and single cell analyses, reveal that Roseobacters are found in almost all marine environments sampled (22). Molecular-based approaches targeting 16S rRNA genes demonstrate that the Roseobacter clade is one of the major marine bacterial groups, typically comprising upwards of 20% of coastal and 15% of mixed layer ocean bacterioplankton communities (22). Members have been found to be free-living or particle-associated, or in commensal relationships with marine phytoplankton, invertebrates and vertebrates (22). Furthermore, representatives of this clade stand out as one of the most readily cultivated of the major marine lineages (23). These isolated representatives are serving as the foundation for an improved understanding of marine bacterial ecology and physiology. Many of these studies are facilitated by the wealth of genome data that is available for both cultured and uncultured representatives.

Genome sequences of cultivated Roseobacter strains reveal relatively large genomes (~4.5 Mb) with gene content that suggests versatility may be driving this cosmopolitan group's ecological success (24). Evidence from environmental, microbiological, genomic and metagenomic studies point to the involvement of members of the Roseobacter lineage in several key biogeochemical processes, including mineralization of plant-derived compounds and transformations of reduced inorganic and organic sulfur compounds (22, 25). Another trait characteristic of Roseobacter clade strains is the production of secondary metabolites, including AHLs (26). Several recent studies have begun to examine the contribution of QS to the physiology of cultivated representatives (discussed below).

The role of quorum sensing in Roseobacter biology. The first evidence of QS in Roseobacters demonstrated AHL production in representative strains isolated from marine snow using an *Agrobacterium tumefaciens* bioreporter strain (27). Subsequent studies have provided evidence that QS is involved in the colonization of both living organisms and non-living surfaces in marine environments and have shown the involvement of QS in a variety of physiologies, from secondary metabolite production to cellular morphology (28–31). Furthermore, as primary and aggressive surface colonizers, members of the Roseobacter clade are hypothesized to set the stage for microbial biofilm structure, function, and dynamics via QS-mediated interactions (32). Despite the prevalence of QS in this clade, only a few representative Roseobacters have been the primary focus of experimental studies of QS and none of these representatives are currently being utilized to determine the effect of QS on microbe-microbe interactions within a multispecies biofilm.

AHLs characterized from Roseobacter isolates possess some of the longest acyl side chains recognized with lengths ranging from C_4 to C_{18} and possessing differing degrees of saturation and oxidation (26, 33). Relatively common among Alphaproteobacteria, long chain AHLs are hydrophobic in nature, often causing them to partition in cell membranes where they may not be as readily available as diffusible signaling molecules (34). QS signal efflux pumps have been identified in other Proteobacteria, but similar mechanisms have yet to be identified in Alphaproteobacteria. Thus, the biological implications of membrane "sequestering" of QS molecules are not yet fully appreciated. In addition, it has been noted that long chain AHLs are more stable than their shorter chain counterparts in alkaline environments, such as the world's oceans. Thus, it has been recently suggested that the slight alkalinity of seawater may be a driving force in shaping the AHL repertoire of Roseobacters (35).

Culture-based studies indicate that Roseobacters are the primary symbiont producers of AHLs in marine sponges and *Ruegeria* sp. KLH11 has been established as a model for sponge-associated Roseobacters (36). KLH11 contains two sets of *luxRI* homologs, designated *ssaRI* and *ssbRI.* This strain also possesses an orphan, or solo, *luxI,* designated *sscI,* in its genome (30, 37). SsaI, SsbI, and SscI predominantly produce long chain saturated and unsaturated AHLs ranging in size from C12 to C16. SsaI produces 3O-AHL variants whereas SsbI and SscI produce 3OH-AHLs (30). The binding affinity of signaling molecules to LuxR homologs is influenced by modifications at the third carbon, and this may allow KLH11 to finely tune its metabolism to cellular density and AHL diversity (38). Similarly, the algal symbiont *Dinoroseobacter shibae* DFL12 is another representative of the Roseobacter clade reported to have two *luxRI*-like cassettes as well as an *luxI* orphan, designated *luxRI1, luxRI2,* and *luxI3,* respectively (39). Deletion of *luxI1* has been shown to affect the regulation of the other two QS systems, indicating the regulatory network in *D. shibae* is organized in a hierarchical fashion (40). QS in *D. shibae* has also been demonstrated to regulate the *cckA-chpT-ctrA* regulatory circuit, which mediates the cell cycle in this strain and influences cellular morphology (40). *D. shibae* populations show variation in cell morphology which is hypothesized to contribute to fitness in changing environments (41).

Integration of QS and cell cycle regulatory mechanisms, such as the *cckA-chpT-ctrA* circuit and the secondary global messenger c-di-GMP, in Roseobacters is an emerging area of research. While the specific mechanistic details of the interactions have yet to be elucidated, it has been shown in *D. shibae* that not only is the *cckA-chpT-ctrA* regulatory circuit impaired in QS mutants but that AHL production is impaired in a *ctrA* mutant (31). Thus, the regulatory network of these two systems is clearly connected, in at least some Roseobacters. The extent to which this integration of networks is present amongst the larger collection of Roseobacters has been probed bioinformatically. CtrA, which functions as

a master regulator in many Alphaproteobacteria has a conserved binding site that can be recognized by genome analysis (31). Wang et al. (2014), found CtrA binding sites within the *luxRI* cassettes of five of the ten Roseobacters genomes analyzed. *O. antarcticus* 307 possesses CtrA binding sites in both of its *luxRI* cassettes. *R. denitrificans, R. litoralis, R. pomeroyi,* and *D. shibae* were all predicted to have a single CtrA binding site within one *luxRI* cassette found within these strains (31). Additionally, QS-mediated physiologies, such as surface attachment and biofilm formation, is often modulated through intracellular signaling of the global secondary messenger c-di-GMP. Concentrations of c-di-GMP are often influenced by environmental cues and cell-to-cell signaling in bacteria (12). In *Rugeria mobilis*, c-di-GMP has been demonstrated to regulate biofilm formation and the production of the QS-mediated antimicrobial, tropodithietic acid (TDA) (42). Thus, there is strong indication that the integration of these networks is common amongst, but not absolutely conserved, in Roseobacters.

AHL-based quorum sensing systems are prevalent in cultured Roseobacter representatives. The inventory of chemical signals produced by Roseobacters is anticipated to be large and result in complex signaling pathways in lineage members. Some of these pathways may be involved in interspecies interactions that influence biogeochemical cycles. For instance, uncharacterized Roseobacters have been shown to be epibionts of *Trichodesmium* and AHL-based interactions between *Trichodesmium* and select epibionts has been shown to stimulate phosphorus acquisition in this marine cyanobacterium (43, 44). Additionally, it has been suggested but not yet demonstrated that QS plays a role in the switch from mutualistic to antagonistic behavior in *P. gallaeciensis* against the bloom-forming marine phytoplankton species *Emiliana huxleyi* (45). Furthermore, as critical mediators of the decomposition of vascular plant material in coastal oceans, which is an essential process within the global carbon cycle, Roseobacters colonize and mediate transformation of plant-derived aromatic compounds in marine ecosystems. However, the role of QS in colonization, composition of biofilm community members, and interactions has yet to be elucidated for marine ecosystems. Social behaviors regulated by QS between Roseobacters is anticipated to be essential in the varied relationships these bacteria have with marine primary producers and undoubtedly influence global biogeochemical cycles via the marine food web through these interactions. Given the abundance, genetic repertoire, and metabolic capabilities among Roseobacters, the establishment of a genetically characterized model for use in synthetic community studies is of upmost importance for our understanding of the role QS plays in influencing biofilm dynamics. Moreover, while the breadth of QS in Roseobacters has been probed bioinformatically, attempts to pair QS regulatory elements with physiologies associated with bacterial social behaviors has not yet been made.

IV. Research Objectives

Despite numerous studies detailing various physiological aspects of Roseobacter clade members, QS systems have only been a focus in a limited number of strains. Furthermore, relatively little is understood of the genetic and physiological mechanisms underlying biofilm formation and microbial competition within this clade. Due to its prolific surface colonization, dominance in synthetic microbial communities, and ability to readily outcompete strains in pairwise and multi-species communities (46, 47), Rhodobacterales strain Y4I shows promise as an emerging model organism to better understand the roles QS play in Roseobacter physiology. Elucidating the genetic hierarchy regulating competitive physiologies in a member of the Roseobacter clade, such as Y4I, is an important first step to our understanding of how these dominate marine microorganisms regulate social behaviors. Many studies have explored how social behaviors mediated by QS influence community

cooperation and competition within microbial biofilms and the role of these interactions in the diversity and stability of microbial communities (48). However, these studies have failed to encompass ecologically relevant microbial communities and their interactions, especially those in marine ecosystems. Thus, understanding the role of QS in interspecies interactions within marine associated biofilms has been relatively unexplored. Understanding the regulatory elements influencing biofilm community dynamics aids our ability to utilize Roseobacters as model organisms for marine ecology. Bacterial social behaviors, such as community cooperation and competition, within microbial biofilms are often mediated by QS (49). QS utilizes a special class of transcriptional regulators bound to their cognate signaling molecule that interact with DNA binding domains (5). Despite the prevalence for QS in Roseobacter clade members, few studies have demonstrated direct transcriptional regulation of population level behaviors within members of this clade. Recent genomic evidence suggests up to 87% of sequenced Roseobacter genomes contain at least one QS systems (35). Of those, 56% contain multiple at least one copy of each gene and are considered capable of QS-mediated behaviors (20). Yet the bioinformatic tools available to identify DNA regulatory elements, such as the lux box, within the Roseobacter clade are lacking. The establishment of clade-specific regulatory element (termed 'roseo box') will allow us to query genomic data for social behaviors regulated by QS allowing us to design hypothesis-driven experiments with representatives of the environmentally relevant Roseobacter clade.

The work presented in this dissertation broadly seeks to resolve the gaps in knowledge regarding the regulation, interactions, and prevalence of bacterial social behaviors in Roseobacters, using strain *Rhodobacterales* sp strain Y4I as a representative for competitive social behaviors. Prior work has demonstrated that QS plays a regulatory role in antimicrobial biosynthesis, but many open questions regarding the multi-layered control system remain. Chapter 2 of this dissertation further characterizes the QS regulatory network governing these competitive social behaviors in Y4I, such as antimicrobial production and prolific surface colonization. In Chapter 3, the contribution of QS and indigoidine production to interactions, such as cooperation and competition, within a five-member Roseobacter synthetic biofilm community is explored. Finally, Chapter 4, uses a bioinformatic approach to examine the prevalence of bacterial social behaviors within the Roseobacter clade by identifying DNA binding regions for LuxR family proteins. Collectively, the work presented in this dissertation provides the necessary framework for understanding bacterial social behaviors and their regulation using a Roseobacter model.

References

1. Fuqua C, Parsek MR, Greenberg EP. 2001. Regulation of Gene Expression by Cell-to-Cell Communication: Acyl-Homoserine Lactone Quorum Sensing. Annu Rev Genet 35:439–468.
2. Case RJ, Labbate M, Kjelleberg S. 2008. AHL-driven quorum-sensing circuits: their frequency and function among the Proteobacteria. ISME J 2008 24.
3. Schaefer AL, Hanzelka BL, Eberhard A, Greenberg EP. 1996. Quorum sensing in *Vibrio fischeri*: Probing autoinducer-LuxR interactions with autoinducer analogs. J Bacteriol 178:2897–2901.
4. Shiner EK, Rumbaugh KP, Williams SC. 2005. Interkingdom signaling: Deciphering the language of acyl homoserine lactones. FEMS Microbiol Rev. Oxford Academic.
5. Fuqua C, Winans SC, Greenberg EP. 1996. Census and Concensus in Bacterial Ecosystems: The LuxR-LuxI Family of Quorum-Sensing Transcriptional Regulators. Annu Rev Microbiol 50:727–751.
6. Fuqua WC, Winans SC, Greenberg EP. 1994. Quorum sensing in bacteria: The LuxR-LuxI family of cell density- responsive transcriptional regulators. J Bacteriol 176:269–275.
7. Flemming H-C, Wingender J, Szewzyk U, Steinberg P, Rice SA, Kjelleberg S. 2016. Biofilms: an emergent form of bacterial life. Nat. Rev. 9: 563-575.
8. Belas R. 2014. Biofilms, flagella, and mechanosensing of surfaces by bacteria. Trends Microbiol 22:517–27.
9. Laub MT, Chen SL, Shapiro L, McAdams HH. 2002. Genes directly controlled by CtrA, a master regulator of the *Caulobacter* cell cycle. Proc Natl Acad Sci 99:4632–4637.
10. Aldridge P, Paul R, Goymer P, Rainey P, Jenal U. 2003. Role of the GGDEF regulator PleD in polar development of *Caulobacter crescentus*. Mol Microbiol 47:1695–1708.
11. Angelastro PS, Sliusarenko O, Jacobs-Wagner C. 2010. Polar localization of the CckA histidine kinase and cell cycle periodicity of the essential master regulator CtrA in *Caulobacter crescentus* . J Bacteriol 192:539–552.
12. Römling U, Galperin MY, Gomelsky M. 2013. Cyclic di-GMP: the First 25 Years of a Universal Bacterial Second Messenger. Microbiol Mol Biol Rev 77:1–52.
13. Valentini M, Filloux A. 2016. Biofilms and Cyclic di-GMP (c-di-GMP) signaling: Lessons from *Pseudomonas aeruginosa* and other bacteria. J Biol Chem 291:12547–12555.
14. Roy AB, Sauer K. 2014. Diguanylate cyclase NicD-based signalling mechanism of nutrient-induced dispersion by *Pseudomonas aeruginosa*. Mol Microbiol 94:771–793.
15. Su Y, Tang K, Liu J, Wang Y, Zheng Y, Zhang X-H. 2019. Quorum Sensing System of *Ruegeria mobilis* Rm01 Controls Lipase and Biofilm Formation. Front Microbiol 9:3304.
16. Koppenhöfer S, Wang H, Scharfe M, Kaever V, Wagner-Döbler I, Tomasch J. 2019. Integrated Transcriptional Regulatory Network of Quorum Sensing, Replication Control, and SOS Response in *Dinoroseobacter shibae* . Front Microbiol 10:803.
17. Buchan A, LeCleir GR, Gulvik CA, González JM. 2014. Master recyclers: features and functions of bacteria associated with phytoplankton blooms. Nat Rev Microbiol 12:686–698.
18. Newton RJ, Griffin LE, Bowles KM, Meile C, Gifford S, Givens CE, Howard EC, King E, Oakley CA, Reisch CR, Rinta-Kanto JM, Sharma S, Sun S, Varaljay V, Vila-Costa M, Westrich JR, Moran MA. 2010. Genome characteristics of a generalist marine bacterial lineage. ISME J 4:784–798.
19. Shiba T. 1991. *Roseobacter litoralis* gen. nov., sp. nov., and *Roseobacter denitrificans* sp. nov., Aerobic Pink-Pigmented Bacteria which Contain Bacteriochlorophyll a. Syst Appl Microbiol 14:140–145.
20. Liang KYH, Orata FD, Boucher YF, Case RJ. 2021. Roseobacters in a Sea of Poly- and Paraphyly: Whole Genome-Based Taxonomy of the Family Rhodobacteraceae and the

Proposal for the Split of the "Roseobacter Clade" Into a Novel Family, Roseobacteraceae fam. nov. Front Microbiol 0:1635.
21. González JM, Moran MA. 1997. Numerical dominance of a group of marine bacteria in the α-subclass of the class Proteobacteria in coastal seawater. Appl Environ Microbiol 63:4237–4242.
22. Buchan A, González JM, Moran MA. 2005. Overview of the marine *Roseobacter* lineage. Appl Environ Microbiol 71:5665–5677.
23. Giovannoni SJ, Rappé MS. 2000. Evolution, diversity, and molecular ecology of marine prokaryoteso Title, p. 47–84. *In* Kirchman, DL (ed.), Microbial Ecology of the Oceans. John Wiley & Sons, Inc., New York.
24. Moran MA, Belas R, Schell MA, González JM, Sun F, Sun S, Binder BJ, Edmonds J, Ye W, Orcutt B, Howard EC, Meile C, Palefsky W, Goesmann A, Ren Q, Paulsen I, Ulrich LE, Thompson LS, Saunders E, Buchan A. 2007. Ecological genomics of marine roseobacters. Appl Environ Microbiol 73:4559–4569.
25. Gonzalez JM, Mayer F, Moran MA, Hodson RE, Whitman WB. 1997. *Sagittula stellata* gen. nov., sp. nov., a Lignin-Transforming Bacterium from a Coastal Environment. Int J Syst Bacteriol 47:773–780.
26. Cude WN, Buchan A. 2013. Acyl-homoserine lactone-based quorum sensing in the Roseobacter clade: Complex cell-to-cell communication controls multiple physiologies. Front Microbiol 4:336.
27. Gram L, Grossart H-P, Schlingloff A, Kiørboe T. 2002. Possible quorum sensing in marine snow bacteria: production of acylated homoserine lactones by Roseobacter strains isolated from marine snow. Appl Environ Microbiol 68:4111–6.
28. Dang H, Lovell CR. 2002. Seasonal dynamics of particle-associated and free-living marine Proteobacteria in a salt marsh tidal creek as determined using fluorescence in situ hybridization. Environ Microbiol 4:287–295.
29. Berger M, Neumann A, Schulz S, Simon M, Brinkhoff T. 2011. Tropodithietic Acid Production in *Phaeobacter gallaeciensis* Is Regulated by N-Acyl Homoserine Lactone-Mediated Quorum Sensing. J Bacteriol 193:6576–6585.
30. Zan J, Cicirelli EM, Mohamed NM, Sibhatu H, Kroll S, Choi OO, Uhlson CL, Wysoczynski CL, Murphy RC, Churchill MEA, Hill RT, Fuqua C. A complex LuxR-LuxI type quorum sensing network in a roseobacterial marine sponge symbiont activates flagellar motility and inhibits biofilm formation. Mol Microbiol 85:916–933.
31. Wang H, Ziesche L, Frank O, Michael V, Martin M, Petersen J, Schulz S, Wagner-Döbler I, Tomasch J. 2014. The CtrA phosphorelay integrates differentiation and communication in the marine alphaproteobacterium *Dinoroseobacter shibae*. BMC Genomics 15:130.
32. Dang H, Lovell CR. 2016. Microbial Surface Colonization and Biofilm Development in Marine Environments. Microbiol Mol Biol Rev 80:91–138.
33. Buchan A, Mitchell A, Nathan Cude NW, Campagna S. 2016. Acyl-Homoserine Lactone-Based Quorum Sensing in Members of the Marine Bacterial Roseobacter Clade: Complex Cell-to-Cell Communication Controls Multiple Physiologies. Stress Environ Regul Gene Expr Adapt Bact 1:225–233.
34. Schaefer AL, Taylor TA, Beatty JT, Greenberg EP. 2002. Long-chain acyl-homoserine lactone quorum-sensing regulation of *Rhodobacter capsulatus* gene transfer agent production. J Bacteriol 184:6515–6521.
35. Zan J, Liu Y, Fuqua C, Hill R. 2014. Acyl-Homoserine Lactone Quorum Sensing in the Roseobacter Clade. Int J Mol Sci 15:654–669.
36. Taylor MW, Schupp PJ, Baillie HJ, Charlton TS, De Nys R, Kjelleberg S, Steinberg PD. 2004. Evidence for acyl homoserine lactone signal production in bacteria associated with marine sponges. Appl Environ Microbiol 70:4387–4389.
37. Zan J, Choi O, Meharena H, Uhlson CL, Churchill MEA, Hill RT, Fuqua C. 2015. A solo luxi-type gene directs acylhomoserine lactone synthesis and contributes to motility

control in the marine sponge symbiont *Ruegeria* sp. KLH11. Microbiol (United Kingdom) 161:50–56.
38. Koch B, Liljefors T, Persson T, Nielsen J, Kjelleberg S, Givskov M. 2005. The LuxR receptor: The sites of interaction with quorum-sensing signals and inhibitors. Microbiology 151:3589–3602.
39. Wagner-Döbler I, Ballhausen B, Berger M, Brinkhoff T, Buchholz I, Bunk B, Cypionka H, Daniel R, Drepper T, Gerdts G, Hahnke S, Han C, Jahn D, Kalhoefer D, Kiss H, Klenk HP, Kyrpides N, Liebl W, Liesegang H, Meincke L, Pati A, Petersen J, Piekarski T, Pommerenke C, Pradella S, Pukall R, Rabus R, Stackebrandt E, Thole S, Thompson L, Tielen P, Tomasch J, Von Jan M, Wanphrut N, Wichels A, Zech H, Simon M. 2010. The complete genome sequence of the algal symbiont *Dinoroseobacter shibae*: A hitchhiker's guide to life in the sea. ISME J 4:61–77.
40. Patzelt D, Wang H, Buchholz I, Rohde M, Gröbe L, Pradella S, Neumann A, Schulz S, Heyber S, Münch K, Münch R, Jahn D, Wagner-Döbler I, Tomasch J. 2013. You are what you talk: quorum sensing induces individual morphologies and cell division modes in *Dinoroseobacter shibae*. ISME J 7:2274–2286.
41. Veening JW, Smits WK, Kuipers OP. 2008. Bistability, epigenetics, and bet-hedging in bacteria. Annu Rev Microbiol. Annu Rev Microbiol.
42. D'Alvise PW, Magdenoska O, Melchiorsen J, Nielsen KF, Gram L. 2014. Biofilm formation and antibiotic production in *Ruegeria mobilis* are influenced by intracellular concentrations of cyclic dimeric guanosinmonophosphate. Environ Microbiol 16:1252–1266.
43. Hmelo LR, Mooy BAS Van, Mincer TJ. 2012. Characterization of bacterial epibionts on the cyanobacterium *Trichodesmium*. Aquat Microb Ecol 67:1–14.
44. Van Mooy BAS, Hmelo LR, Sofen LE, Campagna SR, May AL, Dyhrman ST, Heithoff A, Webb EA, Momper L, Mincer TJ. 2012. Quorum sensing control of phosphorus acquisition in *Trichodesmium* consortia. ISME J 6:422–429.
45. Seyedsayamdost MR, Case RJ, Kolter R, Clardy J. 2011. The Jekyll-and-Hyde chemistry of Phaeobacter gallaeciensis. Nat Chem 3:331–335.
46. Cude WN, Mooney J, Tavanaei AA, Hadden MK, Frank AM, Gulvik CA, May AL, Buchan A. 2012. Production of the antimicrobial secondary metabolite indigoidine contributes to competitive surface colonization by the marine roseobacter *Phaeobacter sp.* strain Y4I. Appl Environ Microbiol 78:4771–4780.
47. Quigley LNM, Edwards A, Steen AD, Buchan A, Fagervold SK. 2019. Characterization of the Interactive Effects of Labile and Recalcitrant Organic Matter on Microbial Growth and Metabolism. Front Microbiol 10:1–15.
48. Liu W, Røder HL, Madsen JS, Bjarnsholt T, Sørensen SJ, Burmølle M. 2016. Interspecific Bacterial Interactions are Reflected in Multispecies Biofilm Spatial Organization. Front Microbiol 7:1366.
49. Li Y-H, Tian X-L. 2016. Quorum Sensing and Bacterial Social Interactions in Biofilms: Bacterial Cooperation and Competition, p. 1195–1205. *In* Stress and Environmental Regulation of Gene Expression and Adaptation in Bacteria. John Wiley & Sons, Inc., Hoboken, NJ, USA.

Chapter 2 : CYCLIC DI-GMP IS INTEGRATED INTO A HIERARCHAL QUORUM SENSING NETWORK REGULATING ANTIMICROBIAL PRODUCTION AND BIOFILM FORMATION IN ROSEOBACTER CLADE MEMBER

A version of this chapter was originally written by April C. Armes and Alison Buchan and has been published by *Frontiers in Marine Science*:

April C. Armes and Alison Buchan. "Cyclic-di-GMP is integrated into a hierarchal quorum sensing network regulating antimicrobial production and biofilm formation in Roseobacter Clade member *Rhodobacterales* sp. Y4I." *Frontiers in Marine Science* (2021).

A.C.A. and A. B. conceived and designed the experiments for quantitative Reverse-Transcriptase Polymerase Chain Reaction (qRT-PCR) and surface attachment and biofilm formation assays. A.C. A. conceived and designed experiments for acyl-homoserine lactone (AHL) add-back assays and bis-(3'-5')-cyclic dimeric guanosine monophosphate (c-di-GMP) analysis. A.C.A. conducted the experiments, carried out data analysis, generated figures, and wrote the manuscript. The manuscript was edited by A.C.A and A. B.

I. Abstract

Microbial biofilms associated with marine particulate organic matter carry out transformations that influence local and regional biogeochemical cycles. Early microbial colonizers are often hypothesized to "set the stage" for biofilm structure, dynamics, and function via N-acetylated homoserine lactone (AHL)-mediated quorum sensing (QS). Production of AHLs, as well as antimicrobials, contributes to the colonization success of members of the Roseobacter clade. One member of this group of abundant marine bacteria, Rhodobacterales sp.Y4I, possesses two QS systems, *phaRI* (QS1) and *pgaRI* (QS2). Here, we characterize mutants in both QS systems to provide genetic evidence that the two systems work in hierarchical fashion to coordinate production of the antimicrobial indigoidine as well as biofilm formation. A mutation in *pgaR* (QS2) results in decreased expression of genes encoding both QS systems as well as those governing the biosynthesis of indigoidine. In contrast, mutations in QS1 did not significantly influence gene expression of QS2. Addition of exogenous AHLs to QS1 and QS2 mutants led to partial restoration of indigoidine production (45-60% of WT) for QS1 but not QS2. Mutational disruptions of QS1 had a more pronounced effect on biofilm development than those in QS2. Finally, we demonstrate that c-di-GMP levels are altered in QS and indigoidine biosynthesis Y4I mutants. Together, these results indicate that *pgaRI* (QS2) is at the top of a regulatory hierarchy governing indigoidine biosynthesis and that the global regulatory metabolite, c-di-GMP, is likely integrated into the QS circuitry of this strain. These findings provide mechanistic understanding of physiological processes that are important in elucidating factors driving competitiveness of roseobacters in nature.

II. Introduction

Cell-to-cell signaling known as quorum sensing (QS) allows bacterial populations to coordinate gene expression. This coordination of gene expression typically occurs in a cell density dependent manner, through the production and recognition of small diffusible signaling molecules. A prevalent class of these molecules in Gram-negative Proteobacteria are *N*-acylhomoserine lactones (AHLs) (1). AHL-based QS characteristically involves a two-component system consisting of a transcriptional regulator (denoted by -*R*) and an AHL synthase (designated as -*I)*. When bound to their cognate transcriptional regulator, AHLs can elicit global changes in gene expression (2). In model biofilm forming representatives, QS has been shown to genetically regulate surface attachment and biofilm formation (3, 4). Surface attachment and biofilm formation is also often modulated through intracellular signaling of a global secondary messenger of bis-(3'-5')-cyclic dimeric guanosine monophosphate (c-di-GMP). Concentrations of c-di-GMP are influenced by environmental cues as well as cell-to-cell signaling in bacteria (5). Indeed, c-di-GMP signaling is integrated in QS regulatory systems in model biofilm bacteria, such as *Pseudomonas aeruginosa* (6). Integration of this intracellular signaling molecule into QS architectures more tightly links cellular physiology with adaptive behaviors.

Members of the Roseobacter clade are competitive surface colonizers in diverse marine niches. This lineage of heterotrophic Alphaproteobacteria represent one of the most phylogenetically coherent, yet physiologically diverse, groups of marine bacteria. Roseobacters are among the most abundant, metabolically active, and aggressive surface colonizers in marine ecosystems (7). As such, members of this clade inhabit a wide range of niches and readily colonize surfaces both abiotic and biotic in nature, *e.g.* sinking particulate organic matter (8), *Trichodesmium* colonies (9), and polymer test surfaces (10). Recent genomic evidence suggests up to 87% of sequenced Roseobacter genomes contain at least one QS systems. Of those, half contain multiple QS systems (11). Despite the prevalence of QS systems identified in Roseobacter genomes, these systems have been studied in a limited number of strains.

Rhodobacterales sp*.* Y4I shows promise as an emerging model organism to better understand the roles QS play in Roseobacter physiology. Isolated from a coastal marsh ecosystem in the southeastern United States, Y4I has been shown to be a competitive surface colonizer, prolific biofilm former, and a dominant member in mixed species mesocosm experiments (12, 13). Specifically, Y4I has been shown to have a competitive advantage against other marine bacteria, including members of its own clade, when grown on a surface. This fitness advantage has been demonstrated to be linked to the production of the blue-pigmented, redox reactive antimicrobial indigoidine (12)*.* Indigoidine is regulated by two QS systems, *phaRI* (QS1) and *pgaRI* (QS2), in this strain. Previous studies demonstrated a disruption of either QS system influences both indigoidine and AHL production. However, the contributions of each QS system to production of indigoidine were ambiguous due to the expression of a leaky phenotype in a QS1 mutant (14). In addition, the regulatory network governing indigoidine biosynthesis is complex, particularly given that surface attachment is a prerequisite for its production, suggesting that cellular mechanisms beyond QS alone may play a role in coordinated cellular responses to environmental conditions. Here, we assess the hierarchical organization of these two QS systems to coordinate production of the antimicrobial indigoidine and biofilm formation. We also present evidence that the secondary global messenger, c-di-GMP, is integrated into the complex regulatory network governing surface attachment and indigoidine production.

III. Materials and Methods

Strains, growth conditions, and maintenance

Rhodobacterales sp. Y4I was previously isolated from an estuary off the coast of Georgia in the southeastern United States (15, 16). Insertional mutants in either the indigoidine synthase gene, *igiD*::Tn5-Km^R (formerly Y401BD4), or QS transcriptional regulators, *phaR*::Tn5-Km^R (formerly Y412AE6) and *pgaR*::Tn5-Km^R (formerly Y411CE4) were previously generated using a mini Tn5 transposon system (12). *Aliivibrio fischeri* ES114 (ATCC 700601) was kindly provided by Eric Stabb (University of Illinois). Unless otherwise noted, all Y4I and *A. fischeri* strains were routinely grown in YTSS (per liter: 15g Sea Salts (Sigma) or Instant Ocean (Thermo Fisher Scientific), 4g tryptone, 2.5g yeast extract) and incubated at 30°C and 25°C, respectively. *Escherichia coli* BW20767, which is *pir*$^+$, was maintained on Luria-Bertani (LB) and routinely grown at 37°C on LB unless otherwise noted (17).

Construction of phaI mutant using insertional mutagenesis

Insertional mutagenesis of the *phaI* (QS1) gene of strain Y4I was achieved using the pKNOCK-Km^R plasmid (18). Briefly, an internal fragment of *phaI* (302 bp) was PCR amplified using primers Y4I_3464_for and Y4I_3464_rev (**Supplementary Table 2.1**) and ligated into the PCR cloning vector TA TOPO pCR 2.1 (Invitrogen, Carlsbad, CA) following manufacturer's guidelines. The *phaI*-containing plasmid was digested with *Bam*HI and *Xho*I, liberating the *phaI* fragment with compatible cohesive ends suitable for ligation into linearized pKNOCK-Km^R. The *phaI*-pKNOCK-Km^R plasmid was introduced into Y4I via biparental mating with *E. coli* strain BW20767. Counterselection for transconjugants was achieved on marine basal medium (MBM) with 2 mM *p*-hydroxybenzoate (POB) as the sole carbon source and kanamycin (50 µg/mL) (per liter: 1.5% (wt/vol) Sigma Sea Salts, 2.38 µM K2HPO4, 13.35 mM NH4Cl, 71 mM Tris-HCl (pH 7.5), 68 µM Fe-EDTA, trace metals and vitamins) at 30°C (19). The resulting mutant was PCR confirmed using primers phaIF and phaIR. Orientation of pKNOCK insert was confirmed using two primer sets: (i) phaIF and pKNOCK_746 and (ii) phaIR and pKNOCK_895 (**Supplementary Table 2.1**). Finally, the mutant was verified by sequencing of the *phaI* gene and designated *phaI*::pKNOCK.

Gene expression assays

RNA was isolated from cellular biomass scraped from agar (1.5%) plates and suspended in 1.5mL of β-mercaptoethanol–RLT buffer (Qiagen, Germantown, MD). The suspension was transferred to a 2.0 mL screw cap tube containing 0.2 g of low-binding 200 µm zirconium beads (OPS Diagnostics, LLC, Lebanon, NJ). The vial was then subjected to vortex mixing at 13,000 rpm for 10 minutes and incubated in the water bath (70°C) for 5 minutes. Cell debris was pelleted and lysate was transferred into a clean 1.5 mL tube. Nucleic acids were precipitated using 700 µL volume of 70% ethanol. The lysate was then transferred to a RNeasy Mini spin column and RNA was isolated following the RNeasy minikit protocol (Qiagen, Germantown, MD). Turbo DNase (Invitrogen) was used to remove DNA from samples. Reverse transcriptase (RT) was performed using Moloney murine leukemia virus (M-MLV) reverse transcriptase following manufacture's guidelines (Invitrogen). No RT controls were included to identify any residual DNA contamination in RNA samples. Nucleic acid concentration was measured using a Nanodrop spectrophotometer (Nanodrop Technologies, Inc, Wilmington, DE). Total RNA was diluted to 6 ng/µL for use in assays.

Quantitative reverse transcription PCR (qRT-PCR) was used to assess gene expression of *igiD*, *phaR*, *pgaR, phaI*, and *pgaI* in strains grown on agar plates for 24 hr.

Position of gene disruptions and location of qPCR primer binding sites are presented in Supplementary Table2. Amplified products ranged in size from 150 bp to 240 bp. All assays are normalized to three reference genes (*rpoC, alaS*, and *map*; **Supplementary Table 2.1**). qRT-PCR data analysis and the normalized relative transcripts quantities were calculated using the qBASE method (20).

Viable cell counts and total biomass on surface attached cultures

To assess viability of surface attached cells, we inoculated a 96-well polystyrene plate (Costar, Corning Incorporated Corning, NY) containing a sterilized 4mm glass bead (Pyrex, Corning Incorporated Corning, NY) with Y4I variants at ~1 x 10^4 cells/mL and incubated at 30° C. Y4I variants were inoculated in biological and technical triplets. A duplicate of each plate was made to assess total biomass described below. Following 20, 44, and 48 hrs, the glass bead was extracted from wells and cells were dislodged from beads as previously described (12). Briefly, beads containing cell biomass were transferred to 2 mL plastic screw cap tubes containing 940 µL of 20% YTSS (per liter: 15 g Instant Ocean, 0.8 g tryptone, 0.5 g yeast extract) and 60 µL of 10% Tween20, submerged in a sonicating water bath and sonicated for 6 minutes at 40 kHz. Samples were then vortexed for ~30 s and diluted to perform viable cell counts.

Total biomass on surface attached cultures was assessed by performing a crystal violet stain on glass beads. Briefly, liquid was removed from wells containing glass beads. The beads were rinsed with 1.5 % sea salt solution (Instant Ocean), then extracted and moved to a clean 96-well plate containing 100 µL YTSS. Uninoculated glass beads served as a control. Crystal violet (25 µL) was added to all wells in the 96-well plate containing beads and incubated for 30 minutes at room temperature. Liquid was aspirated out of wells and stained beads were washed ~3X with 1.5% sea salt solution. Following wash, 200 µL of 95% EtOH was added to each well and allowed to sit for 1 hr to allow crystal violet to solubilize. Following solubilization, liquid was transferred to a clean 96-well plate and diluted 1:10 with 95% EtOH. Absorbance was read at 600 nm using a microplate reader (Bio Tek Instruments, Inc., Synergy HT Multi-Mode Microplate Reader, SN 270212).

Cyclic-di-GMP extraction and quantification

Cyclic-di-GMP was extracted from cell biomass in liquid and growth on agar cultures using procedure adapted from (21). For broth grown cultures, Y4I variants were grown in liquid YTSS at 30° C overnight, shaking in the dark. Cultures were reinoculated in YTSS and allowed to grow for 24 hrs under the same conditions. Following 24 hrs, 10 mL of culture was pelleted by centrifugation (3 min at 8000 rpm). Supernatant was decanted, biomass was resuspended in 1 mL 1.5% sea salt solution and transferred to a 1.5 mL microcentrifuge tube. Biomass was pelleted again, and supernatant was removed by pipetting. For surface attached cultures, Y4I variants were grown in liquid YTSS at 30° C overnight, shaking in the dark. Liquid cultures were spotted (50 µL) onto YTSS agar and incubated for 24 hrs at 30° C. Biomass was scrapped from agar using cell scrappers and transferred to a 1.5 mL microcentrifuge tube. For Y4I variants in either growth medium technical replicates were combined, if necessary, to achieve an approximate biomass of ~0.04 g. Biomass was then suspended in 100 µL extraction buffer (40% methanol, 40% acetonitrile, and 0.1 M of N formic acid) per 0.04 g of biomass. Cell slurries were then incubated at -20° C for 30 minutes. Following incubation, cells slurries were centrifuged at 4° C (13000 rpm for 3 minutes) to remove insoluble material. Lysate was neutralized with 4 µL of 15% ammonium bicarbonate per 100 µL of sample and transferred to a clean 1.5 mL microcentrifuge tube. Cyclic-di-GMP was extracted from pellet again using 50 µL of extraction buffer per 0.04 g of initial biomass. Incubated for 30 minutes at -20° C,

centrifuged at 4° C at 13000 rpm for 3 minutes, and neutralized with 4 µL 15% ammonium bicarbonate and lysates were combined. Following extraction, samples were dried, and shipped for processing to the Mass Spectrometry and Metabolomics Core (Michigan State University). Samples were resuspended in ~160 µL of mobile phase A [(10 mM tributylamine +15 mM acetic acid) in 97:3/H_20:MeOH]. Fluorinated c-di-GMP (Difluoro 3'3'-c-di-GMP, InVivoGen, San Diego, CA) was added as internal standard prior to being analyzed using mass spectrometry.

Growth Inhibition assays

Growth inhibition of *A. fischeri* by Y4I variants was assessed as previously reported (12, 14). Briefly, *A. fischeri* was grown overnight (23°C) to an optical density (OD) of 1.5 – 2.0 at 540 nm. Cultures of *A. fischeri* were diluted 1000-fold and spread plated on to YTSS. Plates containing *A. fischeri* lawn were allowed to dry prior to spotting with Y4I variants. Y4I variants were grown to an OD of 0.6 at 540 nm and 10 µl spot plated on *A. fischeri* lawns and incubated at 27°C as growth rates of the two organisms are comparable at this temperature (12). Zones of clearing around Y4I strains was assessed at 48 hrs post inoculation.

Exogenous AHL add-back assay and indigoidine quantification

To test whether addition of exogenous AHLs could restore indigoidine production, we performed AHL add-back assays and measured indigoidine production in each Y4I variant. Y4I and variants were diluted from overnight cultures to an OD_{540nm} of approximately 0.2. This optical density corresponds to early exponential phase in Y4I strains. Cultures were then incubated at 30° C until late exponential phase (OD_{540nm} ~1.3) was reached. At this time, a final concentration of 13 nM 3OHC12:1-HSL was added to the liquid cultures. Technical replicates containing no added 3OHC12:1-HSL served as controls. All cultures were incubated at 30° C for approximately 16 hrs until cultures reached stationary phase (OD_{540nm} ~2.0). Following incubation, cultures were spot plated, in triplicate, onto YTSS agar containing a final concentration of 800 nM C8-HSL. All cultures were also spot plated on YTSS agar containing no C8-HSL. Spot plates were incubated at 30°C for 24 hrs (**Supplementary Figure 2.1**). Following incubation, one set of technical replicates was sacrificed to quantify indigoidine as outlined previously (12). Briefly, cells were scrapped from plates and solubilized in dimethyl sulfoxide (DMSO). To obtain purified pigment, the cells were lysed via sonication and cell debris were collect via centrifugation. Pigmented supernatant was passed through a 0.2 µm filter and transferred to a clean tube. Two microliters aliquots of the solubilized pigment were measured on a Nanodrop spectrometer (Thermo Fisher Scientific) at 612 nm. 3OHC12:1-HSL and C8-HSL were synthesized locally as described previously (14).

Statistical analysis

All data was analyzed and visualized using GraphPad Prism8 (GraphPad Software, La Jolla California USA, www.graphpad.com). Two-way ANOVA with Dunnett's test was performed on gene expression assay data. One-way ANOVA with Tukey's test was used to determine statistical significance in quantitative biofilm assays and cyclic-di-GMP analysis. One-way ANOVA using Dunnett's test was used to determine statistical significance on AHL add-back assays. Mixed effects analysis was performed on viable cell counts and total biomass assays using Dunnett's and Tukey's, respectively, for post-hoc analyses. Outliers were identified with 95% confidence using a robust nonlinear repression model (ROUT) (22).

IV. Results

Rhodobacterales sp. Y4I possesses two QS systems: *phaRI* (QS1) and *pgaRI* (QS2). We have previously demonstrated that disruption of *pgaR* (QS2) results in undetectable levels of its cognate AHL, C8-HSL, which is synthesized by PgaI (14). This result indicates that the insertional mutation in *pgaR* leads to downstream effects on *pgaI* expression. Indeed, this is confirmed by the gene expression data presented in a subsequent section. In contrast, disruption of *phaR* (QS1) results in detectable, albeit decreased levels, of its cognate AHL, 3OHC12:1-HSL. In addition, indigoidine production is impaired, but not abolished, in this mutant (14). Thus, to fully elucidate the relative contributions of each QS system and to define the regulatory architecture governing indigoidine biosynthesis, we first generated a AHL synthase mutant in the QS1 system (*phaRI*) in the marine isolate, *Rhodobacterales* sp. Y4I. We then assessed various phenotypes of this and previously generated mutants.

The *phaI* mutant does not produce indigoidine and demonstrates increased biofilm formation. Unlike the *phaR*::Tn5-Km^R (QS1) mutant, *phaI*::pKNOCK (QS1) does not produce detectable levels of its cognate AHL (data not shown) nor does it produce any visible levels of indigoidine, even after several days of incubation. Consistent with this phenotype, the mutant is unable to inhibit the growth of *A. fischeri* (**Table 2.1**). We also assessed whether insertional mutagenesis of *phaI* results in growth defects. Growth of *phaI*::pKNOCK in liquid culture was comparable to that of wildtype (**Supplementary Figure 2.2A**). Given that Y4I forms prolific biofilms and mutants in QS1, QS2, and the indigoidine synthase gene (*igiD*) previously demonstrated increased biofilm formation compared to wildtype, we tested biofilm formation in *phaI*::pKNOCK. The *phaI* mutant has significantly increased biofilm formation relative to wildtype as well as the other mutants assayed (**Supplementary Figure 2.2B**).

Disruption in *pgaRI* (QS2) leads to a system wide decrease in QS and *igiD* gene expression. To examine the QS regulatory network governing indigoidine biosynthesis in Y4I, we performed gene expression assays via qRT-PCR on the following five genes: *igiD* (indigoidine synthase); *phaR* and *-I* (QS1); and *pgaR* and *-I* (QS2) (**Figure 2.1**). A disruption in the *luxR* homolog of QS2 (*pgaRI*) resulted in decreased expression in all genes surveyed: a nearly 5-fold decrease in its own gene, more than 10-fold decrease in the *luxI* homolog of QS2, a 4-fold decrease in *phaR,* and a 2-fold decrease in *phaI*. Furthermore, this disruption in *pgaR* led to more than 1000-fold decrease in *igiD* expression (**Figure 2.1A**).

Insertional disruption of *phaR* (QS1) resulted in a 2500-fold decrease of its own expression, but only a ~3-fold decrease in expression of *phaI*. Expression of *igiD* showed a 2-fold decrease compared to wildtype (**Figure 2.1B**). Insertional mutagenesis in *phaI* resulted in an 8-fold decrease in expression of its own gene and a 4-fold decrease in *igiD* expression (**Figure 2.1C**). In the *igiD*::Tn5-Km^R mutant, expression of QS1 *lux* homologs genes (*phaRI*) showed a 2-fold reduction for both genes, while expression of the *luxR* homolog in QS2 (*pgaR*) remained at wildtype levels. Insertional disruption of *igiD* resulted in a nearly 4-fold increase in *pgaI* (QS2) gene expression (**Figure 2.1D**).

Disruption of either QS1 gene (*phaR* and *-I*) led to greater variance in expression of the other assayed genes. For both mutants, a consistent variation is seen in the *pgaI* gene expression: in *phaR*::Tn5-Km^R, *pgaI* transcripts from more than 10-fold decrease to a nearly 2-fold increase in across biological replicates (**Figure 2.1B**). In *phaI*::pKNOCK, *pgaI* transcripts range from a 5-fold decrease to a 5-fold increase across replicates (**Figure 2.1C**). Variability within this mutant is consistent across multiple experimental assays, including biofilm formation, motility, and spontaneous pellicle formation (aka flocking) in liquid cultures (data not shown).

Exogenous Addition of AHLs Partially Restore Indigoidine Production in QS1 Mutants. Given AHL concentrations are decreased in all QS mutants, we next tested to see if we could chemically complement these mutants with the exogenous addition of AHLs. To mimic previously characterized AHL concentrations in Y4I during different phases of growth (14), 13 nM 3OHC12:1-HSL was added to liquid cultures during late exponential phase (OD_{540nm} ~1.3). When cultures reached stationary phase (~16 hr following 3OHC12:1-HSL addition), they were spotted onto agar plates containing a concentration of 800 nM C8-HSL. To assess whether one AHL was driving indigoidine production, we also included 3OHC12:1-HSL and C8-HSL alone controls (**Supplemental Figure 2.1 and Figure 2.2**). To determine whether exogenous addition of AHLs was able to rescue indigoidine production phenotype, we compared the absorbance of our AHL treated mutants to that of the no AHL control in our indigoidine null mutant (*igiD*::Tn5-Km^R) (**Figure 2**). To assess significance in rescuing indigoidine production, we compared AHL treatments to no AHL treatments within mutant genotypes (**Figure 2**).

Exogenous addition of AHLs did not produce any significant response in indigoidine production in wildtype, the indigoidine null mutant or the *pgaR* (QS2) mutant (**Figure 2.2A,B,E**). Addition of 3OHC12:1-HSL (QS1) alone does not significantly restore pigment production in the *phaR* mutant, providing additional support for the non-functionality of PhaR in that strain (**Figure 2.2C**). Both *phaI* and -*R* (QS1) mutants show some restoration of indigoidine production when supplied with exogenous C8-HSL. When supplied with either AHL, but not both, the *phaI* mutant shows significantly increased indigoidine production. Interestingly, C8-HSL addition restores indigoidine production to 33% that of wildtype in the *phaI* mutant compared to the chemical complement of its own AHL (3OHC12:1-HSL) which restored production to 22% that of wildtype. Addition of both AHLs in combination resulted in less than 10% wildtype levels of indigoidine production in this mutant background (**Figure 2.2D**).

Temporal Analysis Reveals Potential Role for QS in Biofilm Regulation. We next assessed whether alterations in the QS pathways also lead to differences in rates of surface colonization and biofilm formation. The indigoidine biosynthesis mutant was included for reference in these assays. Quantification of viable surface attached cells over a 68-hr period revealed all mutants were impaired in their ability to either attach or grow on the surface during the initial growth phase (20 hr). However, those differences were insignificant during later sampling efforts (**Figure 2.3A**). In contrast, quantification of biofilm biomass showed the opposite trend. All mutants were indistinguishable from wildtype at the 20 hr timepoint, but variation between and among wildtype and the mutants became pronounced with time. For example, both *phaR* (QS1) and *pgaR* (QS2) mutants show significantly elevated biofilm biomass relative to wildtype at 44 hr, but these biofilms were not significantly different by the final time point (68 hr). Conversely, *phaI* (QS1) mutant was indistinguishable from wildtype until the final time point, at which point it was 32-42% greater than wildtype and all other variants (**Figure 2.3B**).

Cyclic-di-GMP is higher in surface attached cultures and influenced by QS. In many biofilm forming bacteria the global secondary messenger, c-di-GMP, is integrated into the regulatory network dictating the transition between motile and sessile lifestyles (5). Thus, we wanted to investigate intracellular c-di-GMP concentrations in Y4I and the panel of QS and indigoidine mutants. C-di-GMP concentrations are significantly increased in agar grown Y4I cultures relative to broth cultures (**Figure 2.4A**). Furthermore, all mutants have significantly reduced c-di-GMP concentrations, ranging from 15-33% of wildtype levels when strains are grown in liquid culture and 4-23% of wildtype when grown on agar surfaces (**Figure 2.4B,C**).

V. Discussion

N-acyl homoserine lactone -based QS networks are prevalent in members of the Roseobacter clade where they regulate physiologies predicted to be central to the ecological success of group members (11, 23). The high incidence of multiple QS systems in individual strains presents opportunity for different QS network architectures and signaling circuities to have evolved, the extent of which has not been fully evaluated for Roseobacters. From studies of diverse microbes, three defined QS network architectures have been proposed and provide a valuable comparative framework: (i) 'One-to-One' system, in which a single receptor responding to a single signal controls the entire QS response; (ii) 'Many-to-One' parallel circuit, in which information contained in multiple autoinducers are integrated together to control the QS response; and (iii) 'Many-to-One' hierarchical system, in which many QS receptors are connected in a signaling cascade (24). Of the handful of Roseobacters that have been genetically characterized with regards to QS, two appear to employ a hierarchal regulatory circuit: *Ruegeria mobilis* KLH11 (25) and *Dinoroseobacter shibae* (26). A third, *Phaeobacter inhibens*, appears to employ a parallel regulatory circuit to regulate the production of the antimicrobial trophodithietic acid (27). Here, we propose that Y4I uses a 'Many-to-One' hierarchal QS circuit to mediate indigoidine production and biofilm formation. We also provide evidence for integration of a global regulatory metabolite (c-di-GMP) into this QS circuitry.

Several lines of evidence suggest that QS2 (*pgaRI*) is at the top of the hierarchical regulatory network that integrates input from QS1 to govern indigoidine biosynthesis. Expression of both QS systems and the indigoidine synthase gene, *igiD*, is negatively influenced when the QS2 transcriptional regulator (*pgaR*) is disrupted. This mutant is also null for its cognate AHL. In contrast, disruption of either QS1 component (*phaR* or *-I*) has no significant effect on gene expression of QS2 components, though *pgaI* expression shows considerable and consistent variation across biological replicates in both QS1 mutants. We postulate that the variation in *pgaI* expression is a manifestation of global scale misregulation resulting in some degree of stochasticity within these mutants. This suggests a role for the QS1 system in regulatory homeostasis in this strain. Generation and study of a *pgaI* mutant would further support this finding.

The phenotypic response of the mutants to exogenous AHL additions provide further evidence for the predominant role of QS2 as well as cross-signaling between the two QS systems. With regards to indigoidine production, the QS2 mutant (*pgaR*) is unresponsive to any of the AHL additions. However, both QS1 mutants can be partially restored for this phenotype. When supplied with exogenous C8-HSL (QS2), indigoidine production is evident in both QS1 (*phaRI*) mutants. Addition of its own cognate AHL (3OHC12:1-HSL) results in partial restoration of indigoidine in the *phaI* mutant. However, addition of both AHLs does not restore pigment production. That both AHLs in combination are unable to chemically complement indigoidine production is intriguing. One explanation for this result could lie in the promiscuous nature of AHLs and their receptors. Alternations in the length and degree of saturation in acyl chain structures impact binding affinity of the transcriptional regulator, influencing the genetic response (28, 29). Simultaneous addition of both AHLs may oversaturate the system, resulting in promiscuous binding of the transcriptional regulators and disruption of the regulatory network. Indeed, addition of AHL structural analogs is a proposed mechanism for combating bacterial pathogens reliant on QS for virulence (30). Genetic complementation of these mutants would enhance confidence in the results and help elucidate the mechanism underlying the results presented here.

The two QS mutants exhibit temporal differences regarding biofilm formation, indicating a role for this regulatory network in surface colonization and biofilm dynamics in

Y4I. This finding is consistent with studies in other bacteria where QS can influence all stages of biofilm progression: from attachment and recruitment to maturation and dispersal (31, 32). By monitoring Y4I biofilm formation over the course ~70 h, the cyclical nature of this growth modality is evident. Comparison between and amongst mutant and wildtype strains reveals a degree of asynchronicity in the biofilm mass of QS mutants, supporting a role for QS in mediating periodic biofilm dispersal. QS-regulated biofilm dispersion has been proposed to prevent overcrowding in the sponge symbiont *R. mobilis* (11). Furthermore, induction of biofilm dispersal via QS in *P. inhibins* is thought to contribute to the switch between mutualism (attachment) and pathogenesis (dispersion) with its host (27). The production of the Y4I QS1 signal (3OHC12:1-HSL) is biphasic across the growth cycle, highest during lag and late stationary phases of growth. A previous interpretation of these data was that this AHL represents an important signal when cell growth is relatively static and, thus, may impart information on metabolic status (14). This interpretation combined with data presented here suggests a role for cellular metabolic status in biofilm dynamics, particularly dispersion. Indeed, this topic has recently gained attention for pathogenic microbes (33).

C-di-GMP is integrated into QS network

The global secondary messenger, c-di-GMP, relays information in response to metabolic state and environmental cues. This metabolite has been shown to modulate biofilm dispersal in many bacteria (33, 34). Consistent with the general paradigm (5), intracellular c-di-GMP concentrations in Y4I correlate with growth modality: they are elevated in surface-grown cultures relative to liquid cultures. C-di-GMP concentrations are not only altered in Y4I strains with disruptions in either QS system but also the indigoidine biosynthesis mutant, suggestive of a direct link between these secondary metabolites. In fact, glutamate has been shown to play a key role in biofilm formation by regulating intercellular pools of c-di-GMP in *P. aeruginosa* (35, 36). In Y4I, glutamate is an essential precursor for indigoidine (12, 37, 38). Thus, the integration of c-di-GMP and QS signaling pathways may provide an avenue for convergence of information on cellular status from different central metabolic pathways in Y4I.

Integration of c-di-GMP with bacterial regulatory signaling pathways is not uncommon. For example, in several Alphaproteobacteria, c-di-GMP contributes to the regulation of the biphasic swim-stick switch controlled by the CtrA phosphorelay "master regulator" system (26, 39–42). It is plausible that c-di-GMP and the CtrA phosphorelay system are also integrated into the QS regulatory network architecture governing indigoidine biosynthesis in Y4I. Indeed, we have found a putative DNA binding half-site for the master regulator, CtrA, located in the QS2 (*pgaRI*) operon (**Supplementary Figure 2.3**). Furthermore, integration of the CtrA and QS has been demonstrated in other roseobacters. In *R. mobilis*, QS regulates the lifestyle switch from motile (swim) to sessile (stick) by controlling the expression of CtrA (43). Previous studies have shown that c-di-GMP is also integrated into the QS of *D. shibae* (44) and regulates the expression of *ctrA* in a related alphaproteobacterium, *Rhodobacter capsulatus* (45). Thus, integration of these central signaling pathways may be a mechanism utilized by members of the Roseobacter clade to aid in their colonization success.

In an effort to better contextualize the regulatory network architecture that may govern these key Roseobacter physiologies in marine ecosystems, we present a working model that integrates the key players discussed here (**Figure 2.5**). Implicit in this model is a connection between metabolism and physiology. Quorum sensing molecules are dependent on metabolic precursors (46). Additionally, c-di-GMP, a key intermediate linked to metabolic state has been demonstrated to regulate QS, either directly or indirectly, in

Alphaproteobacteria (31, 41, 47). We postulate this mechanism of regulation applies to the QS networks in Y4I. We also hypothesize a role for the CtrA phosphorelay system in regulating surface growth associated physiologies, including attachment, mechanosensing, flagella and biofilm formation in Y4I (48). We anticipate future studies will more fully elucidate the extent and nature of c-di-GMP and CtrA to antimicrobial production and biofilm in this strain.

Ecological Context of QS Signaling Dynamics

Quorum sensing has been shown to contribute to competitive physiologies, such as biofilm formation and antimicrobial production, in members of the Roseobacter clade (e.g.(27, 49, 50)and reviewed in Zan et al., 2014). Here, we provide evidence that Y4I employs a hierarchical QS circuit to mediate biofilm formation and indigoidine production. At the top of the hierarchical network in Y4I is one of the most common marine signaling molecules: C8-HSL (12, 51–55). It is intriguing that this dominant AHL, which is produced by a number of aquatic microorganisms, including *A. fischeri* and *Aliivibrio anguillarum,* is also required for indigoidine biosynthesis in Y4I, which inhibits the growth of both of these species (14, 56, 57). Given the universality of C8-HSL, the exploitation of this ubiquitous signaling molecule by Y4I may be central to its successful competitive strategies.

References

1. Papenfort K, Bassler BL. 2016. Quorum sensing signal-response systems in Gram-negative bacteria. Nat Rev Microbiol 14:576–588.
2. Williams P, Winzer K, Chan WC, Cámara M. 2007. Look who's talking: communication and quorum sensing in the bacterial world. Philos Trans R Soc Lond B Biol Sci 362:1119–34.
3. Hammer BK, Bassler BL. 2003. Quorum sensing controls biofilm formation in *Vibrio cholerae*. Mol Microbiol 50:101–104.
4. Schuster M, Peter Greenberg E. 2006. A network of networks: Quorum-sensing gene regulation in *Pseudomonas aeruginosa*. Int J Med Microbiol 296:73–81.
5. Römling U, Galperin MY, Gomelsky M. 2013. Cyclic di-GMP: the First 25 Years of a Universal Bacterial Second Messenger. Microbiol Mol Biol Rev 77:1–52.
6. Lin Chua S, Liu Y, Li Y, Jun Ting H, Kohli GS, Cai Z, Suwanchaikasem P, Kau Kit Goh K, Pin Ng S, Tolker-Nielsen T, Yang L, Givskov M. 2017. Reduced Intracellular c-di-GMP Content Increases Expression of Quorum Sensing-Regulated Genes in *Pseudomonas aeruginosa*. Front Cell Infect Microbiol 7:451.
7. Brinkhoff T, Giebel H-A, Simon M. 2008. Diversity, ecology, and genomics of the Roseobacter clade: a short overview. Arch Microbiol 189:531–539.
8. Farnelid H, Turk-Kubo K, Ploug H, Ossolinski JE, Collins JR, Van Mooy BAS, Zehr JP. 2019. Diverse diazotrophs are present on sinking particles in the North Pacific Subtropical Gyre. ISME J 13:170–182.
9. Van Mooy BAS, Hmelo LR, Sofen LE, Campagna SR, May AL, Dyhrman ST, Heithoff A, Webb EA, Momper L, Mincer TJ. 2012. Quorum sensing control of phosphorus acquisition in *Trichodesmium* consortia. ISME J 6:422–429.
10. Dang H, Lovell CR. 2000. Bacterial primary colonization and early succession on surfaces in marine waters as determined by amplified rRNA gene restriction analysis and sequence analysis of 16S rRNA genes. Appl Environ Microbiol 66:467–75.
11. Zan J, Liu Y, Fuqua C, Hill R. 2014. Acyl-Homoserine Lactone Quorum Sensing in the Roseobacter Clade. Int J Mol Sci 15:654–669.
12. Cude WN, Mooney J, Tavanaei AA, Hadden MK, Frank AM, Gulvik CA, May AL, Buchan A. 2012. Production of the antimicrobial secondary metabolite indigoidine contributes to competitive surface colonization by the marine roseobacter *Phaeobacter sp.* strain Y4I. Appl Environ Microbiol 78:4771–4780.
13. Quigley LNM, Edwards A, Steen AD, Buchan A, Fagervold SK. 2019. Characterization of the Interactive Effects of Labile and Recalcitrant Organic Matter on Microbial Growth and Metabolism. Front Microbiol 10:1–15.
14. Cude WN, Prevatte CW, Hadden MK, May AL, Smith RT, Swain CL, Campagna SR, Buchan A. 2015. *Phaeobacter sp.* strain Y4I utilizes two separate cell-to-cell communication systems to regulate production of the antimicrobial indigoidine. Appl Environ Microbiol 81:1417–1425.
15. Buchan A, Neidle EL, Moran MA. 2004. Diverse Organization of Genes of the B-Ketoadipate Pathway in Members of the Marine Roseobacter Lineage. Appl Environ Microbiol 70:1658–68.
16. Slightom RN, Buchan A. 2009. Surface colonization by marine roseobacters: integrating genotype and phenotype. Appl Environ Microbiol 75:6027–37.
17. Metcalf WW, Jiang W, Daniels LL, Kim S-K, Haldimann A, Wanner BL. 1996. Conditionally Replicative and Conjugative Plasmids Carrying *lacZα* for Cloning, Mutagenesis, and Allele Replacement in Bacteria. Plasmid 35:1–13.
18. Alexeyev MF. 1999. The pKNOCK Series of Broad-Host-Range Mobilizable Suicide Vectors for Gene Knockout and Targeted DNA Insertion into the Chromosome of Gram-Negative Bacteria. Biotechniques 26:824–828.

19. Gonzalez JM, Mayer F, Moran MA, Hodson RE, Whitman WB. 1997. *Sagittula stellata* gen. nov., sp. nov., a Lignin-Transforming Bacterium from a Coastal Environment. Int J Syst Bacteriol 47:773–780.
20. Hellemans J, Mortier G, De Paepe A, Speleman F, Vandesompele J. 2007. qBase relative quantification framework and software for management and automated analysis of real-time quantitative PCR data. Genome Biol 8:19.
21. O'Neal L, Ryu M, Gomelsky M, Alexandre G. 2017. Optogenetic Manipulation of Cyclic Receptor Activity in *Azospirillum*. J Bacteriol 199:1–18.
22. Motulsky HJ, Brown RE. 2006. Detecting outliers when fitting data with nonlinear regression – a new method based on robust nonlinear regression and the false discovery rate. BMC Bioinformatics 7:123.
23. Cude WN, Buchan A. 2013. Acyl-homoserine lactone-based quorum sensing in the Roseobacter clade: Complex cell-to-cell communication controls multiple physiologies. Front Microbiol 4:336.
24. Hawver LA, Jung SA, Ng W-L. 2016. Specificity and complexity in bacterial quorum-sensing systems. FEMS Microbiol Rev 40:738–52.
25. Zan J, Cicirelli EM, Mohamed NM, Sibhatu H, Kroll S, Choi OO, Uhlson CL, Wysoczynski CL, Murphy RC, Churchill MEA, Hill RT, Fuqua C. 2012. A complex LuxR-LuxI type quorum sensing network in a roseobacterial marine sponge symbiont activates flagellar motility and inhibits biofilm formation. Mol Microbiol 85:916–933.
26. Koppenhöfer S, Wang H, Scharfe M, Kaever V, Wagner-Döbler I, Tomasch J. 2019. Integrated Transcriptional Regulatory Network of Quorum Sensing, Replication Control, and SOS Response in *Dinoroseobacter shibae* . Front Microbiol 10:803.
27. Beyersmann PG, Tomasch JJ, Son K, Stocker R, Göker M, Wagner-Döbler I, Simon M, Brinkhoff T. 2017. Dual function of tropodithietic acid as antibiotic and signaling molecule in global gene regulation of the probiotic bacterium *Phaeobacter inhibens*. Sci Rep 7:730.
28. Rajput A, Kaur K, Kumar M. 2016. SigMol: repertoire of quorum sensing signaling molecules in prokaryotes. Nucleic Acids Res 44:634–639.
29. Churchill MEA, Chen L. 2011. Structural Basis of Acyl-homoserine Lactone-Dependent Signaling. Chem Rev 111:68–85.
30. LaSarre B, Federle MJ. 2013. Exploiting Quorum Sensing To Confuse Bacterial Pathogens. Microbiol Mol Biol Rev 77:73–111.
31. McDougald D, Rice SA, Barraud N, Steinberg PD, Kjelleberg S. 2012. Should we stay or should we go: Mechanisms and ecological consequences for biofilm dispersal. Nat Rev Microbiol 10:39–50.
32. Dang H, Lovell CR. 2016. Microbial surface colonization and biofilm development in marine environments. Microbiol Mol Biol Rev 80:91–138.
33. Rumbaugh KP, Sauer K. 2020. Biofilm dispersion. Nat Rev Microbiol. 10:571-586
34. Valentini M, Filloux A. 2016. Biofilms and Cyclic di-GMP (c-di-GMP) signaling: Lessons from *Pseudomonas aeruginosa* and other bacteria. J Biol Chem 291:12547–12555.
35. Roy AB, Petrova OE, Sauer K. 2012. The Phosphodiesterase DipA (PA5017) Is Essential for *Pseudomonas aeruginosa* Biofilm Dispersion. J Bacteriol 194:2904–2915.
36. Roy AB, Sauer K. 2014. Diguanylate cyclase NicD-based signalling mechanism of nutrient-induced dispersion by *Pseudomonas aeruginosa*. Mol Microbiol 94:771–793.
37. Kuhn R, Starr MP, Kuhn DA, Bauer H, Knackmuss H-JJ. 1965. Indigoidine and other bacterial pigments related to 3,3′-bipyridyl. Arch Mikrobiol 51:71–84.
38. Day PA, Villalba MS, Herrero OM, Arancibia LA, Alvarez HM. 2017. Formation of indigoidine derived-pigments contributes to the adaptation of *Vogesella sp.* strain EB to cold aquatic iron-oxidizing environments. Antonie van Leeuwenhoek, Int J Gen Mol Microbiol 110:415–428.
39. Paul R, Weiser S, Amiot NC, Chan C, Schirmer T, Giese B, Jenal U. 2004. Cell cycle-dependent dynamic localization of a bacterial response regulator with a novel di-

guanylate cyclase output domain. Genes Dev 18:715–727.
40. Boutte CC, Henry JT, Crosson S. 2011. ppGpp and polyphosphate modulate cell cycle progression in Caulobacter crescentus. J Bacteriol 194:28–35.
41. D'Alvise PW, Magdenoska O, Melchiorsen J, Nielsen KF, Gram L. 2014. Biofilm formation and antibiotic production in *Ruegeria mobilis* are influenced by intracellular concentrations of cyclic dimeric guanosinmonophosphate. Environ Microbiol 16:1252–1266.
42. Su Y, Tang K, Liu J, Wang Y, Zheng Y, Zhang X-H. 2019. Quorum Sensing System of *Ruegeria mobilis* Rm01 Controls Lipase and Biofilm Formation. Front Microbiol 9:3304.
43. Zan J, Heindl JE, Liu Y, Fuqua C, Hill RT. 2013. The CckA-ChpT-CtrA Phosphorelay System Is Regulated by Quorum Sensing and Controls Flagellar Motility in the Marine Sponge Symbiont *Ruegeria* sp. KLH11. PLoS One 8:e66346.
44. Wang H, Ziesche L, Frank O, Michael V, Martin M, Petersen J, Schulz S, Wagner-Döbler I, Tomasch J. 2014. The CtrA phosphorelay integrates differentiation and communication in the marine alphaproteobacterium *Dinoroseobacter shibae*. BMC Genomics 15:130.
45. Leung MM, Brimacombe CA, Beatty JT. 2013. Transcriptional regulation of the *Rhodobacter capsulatus* response regulator CtrA. Microbiology 159:96–106.
46. Goo E, An JH, Kang Y, Hwang I. 2015. Control of bacterial metabolism by quorum sensing. Trends Microbiol 23:567–576.
47. Hengge R. 2009. Principles of c-di-GMP signalling in bacteria. Nat Rev Microbiol 7:263–273.
48. Poncin K, Gillet S, De Bolle X. 2018. Learning from the master: targets and functions of the CtrA response regulator in *Brucella abortus* and other alpha-proteobacteria. FEMS Microbiol Rev. NLM (Medline).
49. Berger M, Neumann A, Schulz S, Simon M, Brinkhoff T. 2011. Tropodithietic Acid Production in *Phaeobacter gallaeciensis* Is Regulated by N-Acyl Homoserine Lactone-Mediated Quorum Sensing. J Bacteriol 193:6576–6585.
50. Rao D, Webb JS, Kjelleberg S. 2006. Microbial colonization and competition on the marine alga *Ulva australis* . Appl Environ Microbiol 72:5547–55.
51. Mohamed NM, Cicirelli EM, Kan J, Chen F, Fuqua C, Hill RT. 2008. Diversity and quorum-sensing signal production of Proteobacteria associated with marine sponges. Environ Microbiol 10:75–86.
52. Gromek SM, Suria AM, Fullmer MS, Garcia JL, Gogarten JP, Nyholm S V., Balunas MJ. 2016. *Leisingera* sp. JC1, a Bacterial Isolate from Hawaiian Bobtail Squid Eggs, Produces Indigoidine and Differentially Inhibits *Vibrios*. Front Microbiol 7:1342.
53. Wagner-Döbler I, Thiel V, Eberl L, Allgaier M, Bodor A, Meyer S, Ebner S, Hennig A, Pukall R, Schulz S. 2005. Discovery of Complex Mixtures of Novel Long-Chain Quorum Sensing Signals in Free-Living and Host-Associated Marine Alphaproteobacteria. ChemBioChem 6:2195–2206.
54. Ziesche L, Rinkel J, Dickschat JS, Schulz S. 2018. Acyl-group specificity of AHL synthases involved in quorum-sensing in Roseobacter group bacteria. Beilstein J Org Chem 14:1309–1316.
55. Krupke A, Hmelo LR, Ossolinski JE, Mincer TJ, Van Mooy BAS. 2016. Quorum Sensing Plays a Complex Role in Regulating the Enzyme Hydrolysis Activity of Microbes Associated with Sinking Particles in the Ocean. Front Mar Sci 3:55.
56. García-Aljaro C, Vargas-Cespedes GJ, Blanch AR. 2012. Detection of acylated homoserine lactones produced by *Vibrio spp.* and related species isolated from water and aquatic organisms. J Appl Microbiol 112:383–389.
57. Verma SC, Miyashiro T. 2013. Quorum Sensing in the Squid-*Vibrio* Symbiosis. Int J Mol Sci 14:16386–16401.

Appendix: Tables

Table 2.1 Y4I variant phenotypes

	WT	***pgaR*::Tn5-Km^R**	***phaR*::Tn5-Km^R**	***phaI*::pKNOCK**	***igiD*::Tn5-Km^R**
Indigoidine Production[a]	+	-	+/-	-	-
Growth Inhibition[b]	+	-	-	-	-

[a]Indigoidine production was rated by appearance of coloration of colonies following inoculation at 48 hrs (+), within 5 days (+/-), or not at all (-) during incubation.
[b]Growth inhibition of Aliivibrio fischeri was either (+) if a zone of clearing was present or (-) if there was no zone of clearing

.

Appendix: Figures

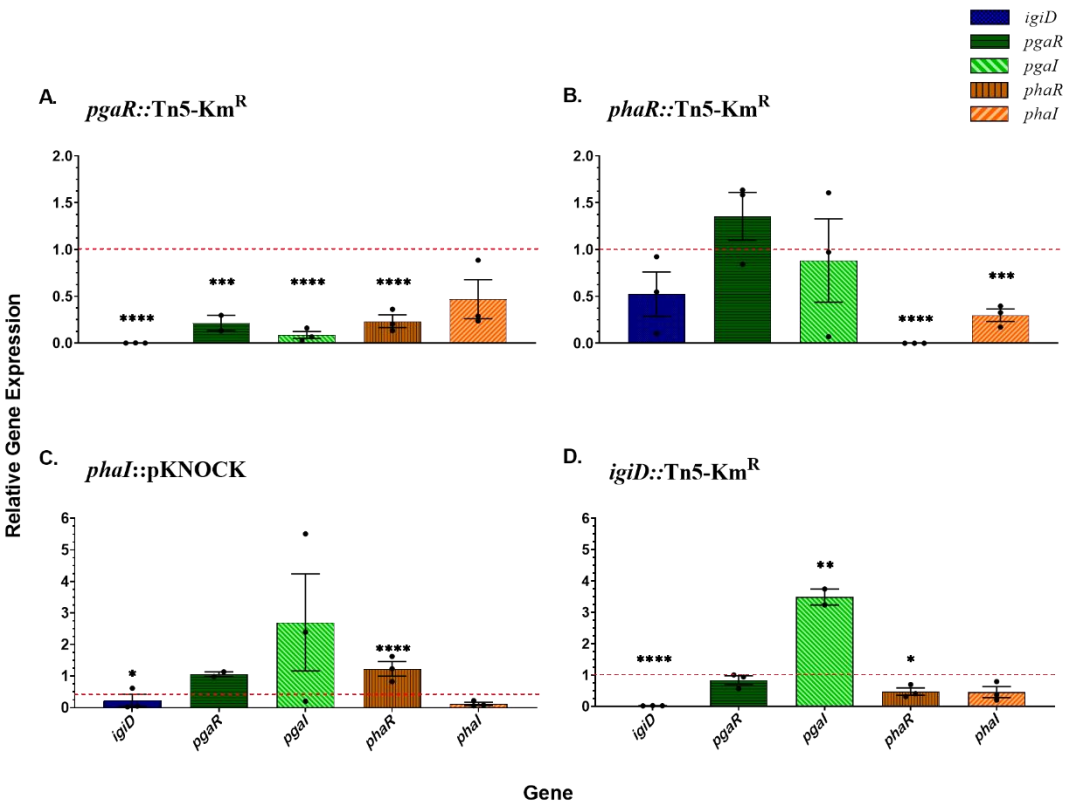

Figure 2.1 Gene expression of *luxRI* homologs and *igiD* synthase from agar grown cultures. Relative gene expression for *pgaR*::Tn5-KmR (A), *phaR*::Tn5-KmR (B), *phaI*::pKNOCK (C), *igiD*::Tn5-KmR (D). Gene expression was normalized to three housekeeping genes (*rpoC*, *alaS*, and *map*) and expressed relative to WT, set to 1. Each data point represents the average of three technical replicates and errors bars represent standard deviations between three biological replicates. Statistical significance was calculated using a two-way ANOVA ($p < 0.05$ [*], 0.01 [**], 0.001 [***], 0.0001 [****]).

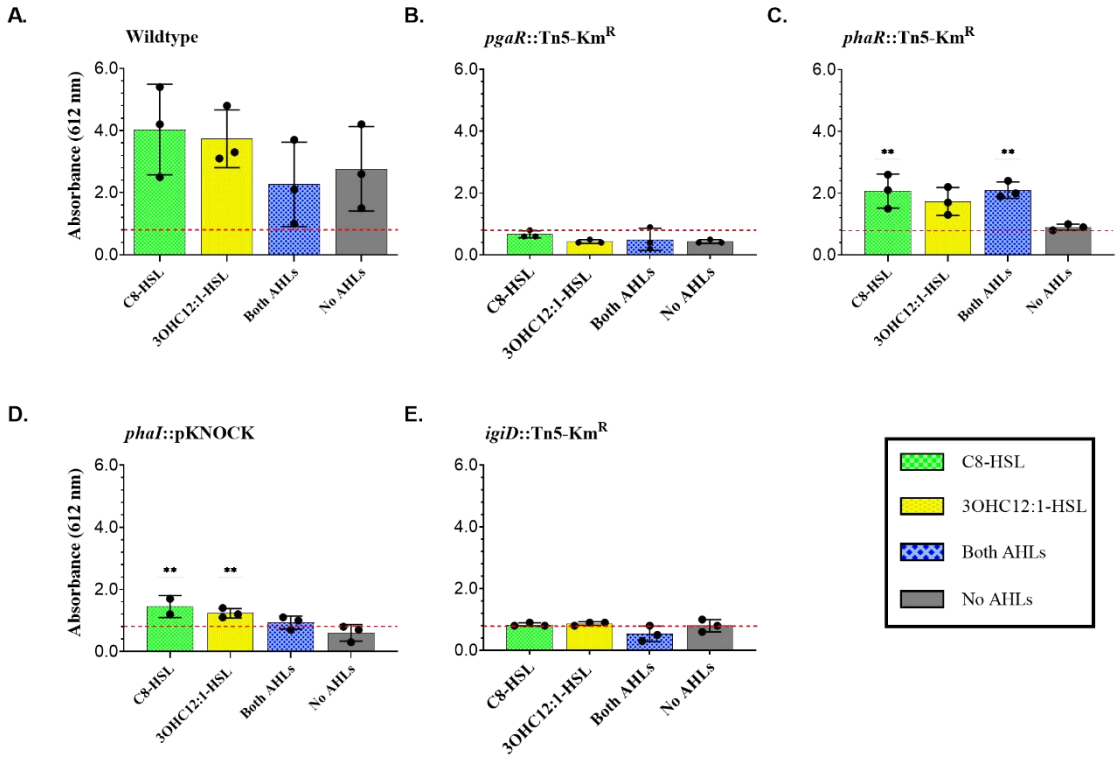

Figure 2.2 Indigoidine production in response to growth-phase dependent AHL exogenous addition. Indigoidine quantification in Y4I variants: WT (A), *pgaR*::Tn5-KM^R (B), *phaR*::Tn5-KM^R (C), *phaI*::pKNOCK (D), and *igiD*::Tn5-KM^R (E) following exogenous addition of AHLs, as indicated in the legend Indigoidine quantification was normalized to biomass and compared to no AHL control in the *igiD*::Tn5-KmR mutant (red dotted line). Error bars represent standard deviations from the mean of three biological replicates. Statistical significance was calculated by comparing AHL treatments to the no AHL control within strain genotypes. Asterisks represent statistical difference ($p < 0.01$).

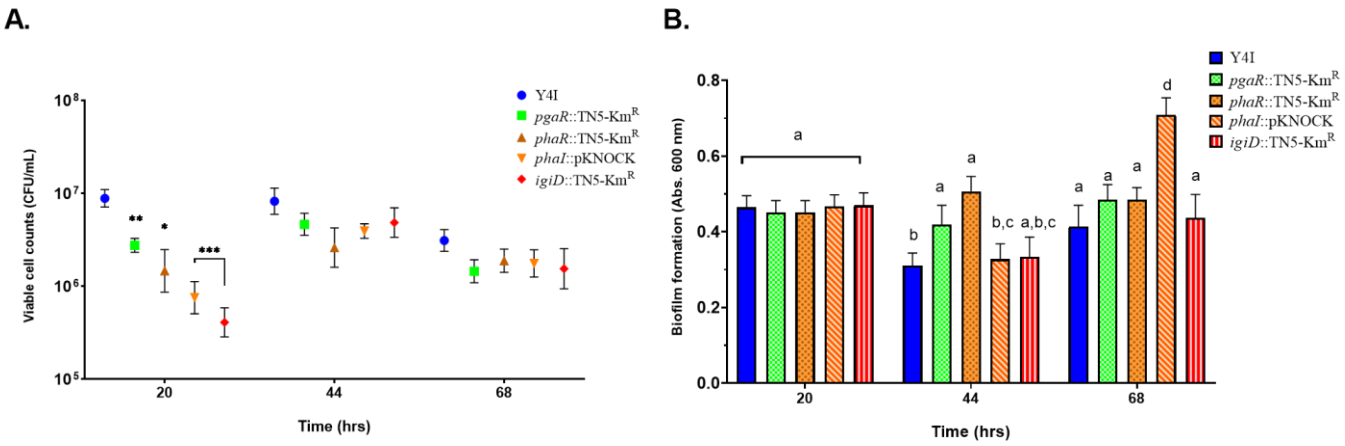

Figure 2.3 Surface Colonization and Biofilm production over time in Y4I mutants. Viable cell counts of surface attached cultures in Y4I variants (A). Each data point represents the average of three biological and three technical replicates. Data was normalized to cell abundance in liquid culture at the time of inoculation. Error bars represent the standard error of the mean of biological and technical triplicates. The asterisks denote statistical significance from WT at that time point ($p < 0.05$ [*], 0.01 [**], 0.001 [***]). Total biofilm of surface attached cultures in Y4I variants as determined by crystal violet assay (B). Data is representative of the mean of three biological and three technical replicates. Letters that are not shared represent significant difference ($p < 0.05$). Error bars represent the standard deviation from the mean.

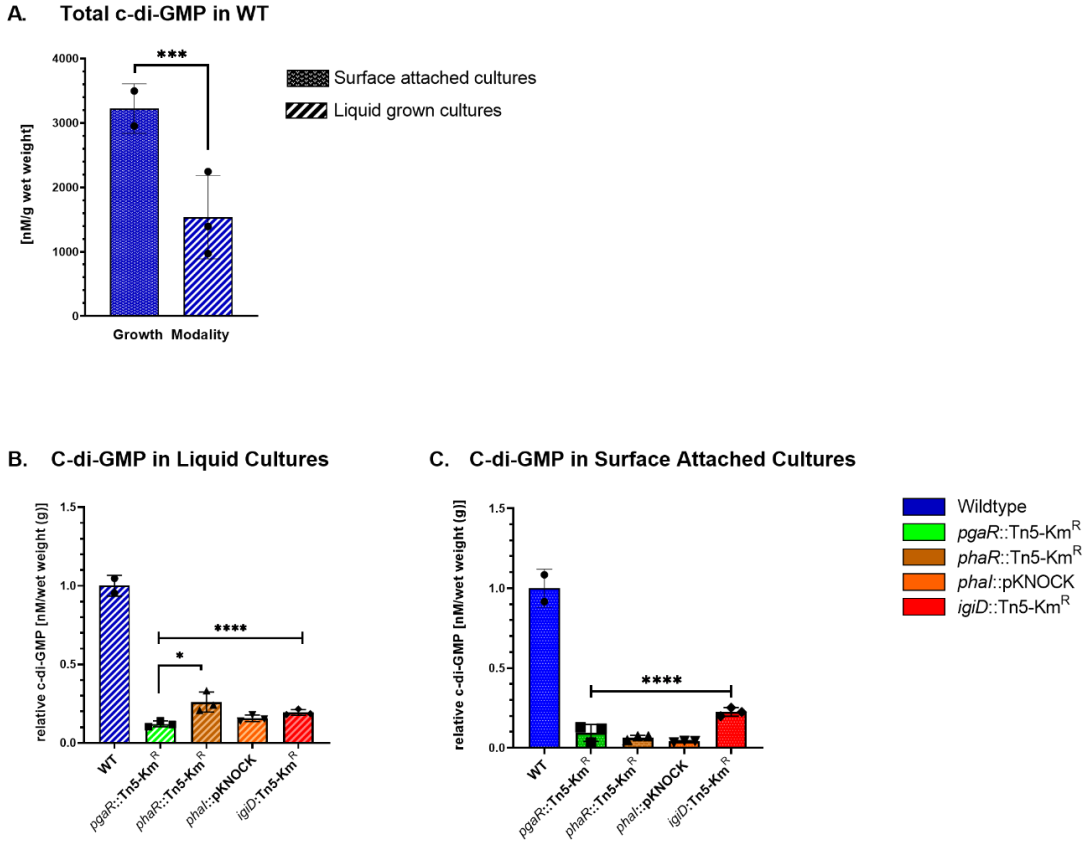

Figure 2.4 Cyclic-di-GMP concentrations in broth and agar grown cultures. A comparison of intracellular cyclic-di-GMP concentration in WT cultures grown on agar and in broth culture (A). Intracellular c-di-GMP concentration of Y4I variants grown on broth (B) and in agar culture (C) are shown. Each data point represents the average of three technical replicates. Error bars represent the standard deviation of the mean. Asterisks represent statistical significance (p < 0.05 [*], 0.001 [***], 0.0001 [****]).

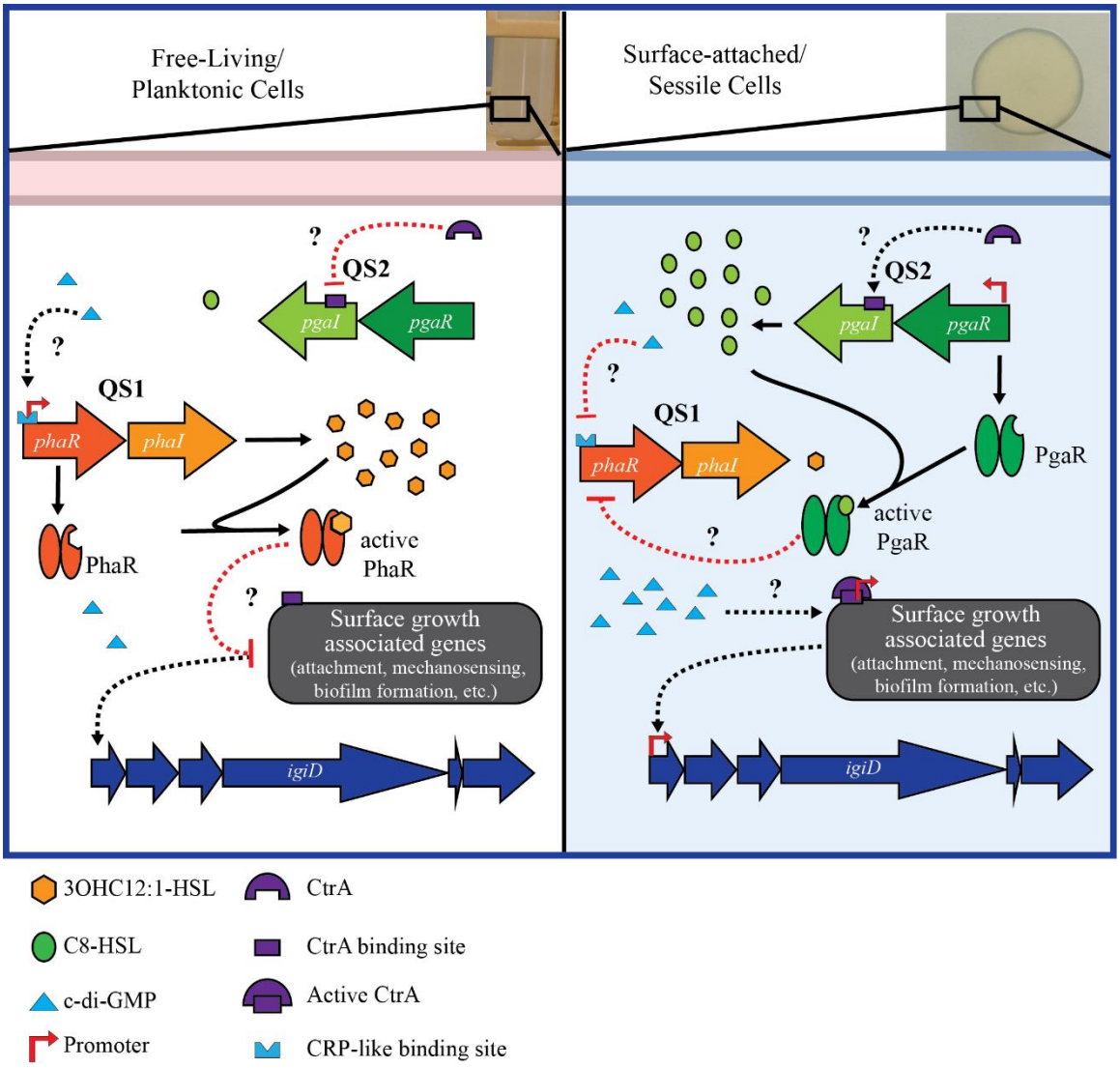

Figure 2.5 Working model of the regulatory network governing key physiologies in strain Y4I. Left panel shows genetic regulation during growth at low cell densities when Y4I is growing planktonically. During this growth modality, 3OHC12:1-HSL (QS1) concentrations are highest and we hypothesize that surface growth associated genes (e.g., mechanosensing, attachment, biofilm formation, flagella biosynthesis, and/or *ctrA* phosphorelay) are repressed, either directly or indirectly through QS1. Right panel shows genetic regulation during growth on a surface. It is predicted that when concentrations of C8-HSL are highest, QS2 represses expression of QS1, either directly or indirectly, allowing for the transcription of surface growth associated genes. Both c-di-GMP and CtrA are expected to play a role in activating surface-growth associated genes, though the specific mechanism of this regulation is currently unknown. Black lines are indicative of activation while red represents inhibition. Solid lines represent known pathways, while dotted lines are hypothesized.

Appendix: Supplemental Materials

Supplemental Table 2.1 Primers used in this study for gene expression analysis and construction of phaI mutant. Primer sets are listed together, sharing a prefix and designated with either "for" or "F" to indicate forward primer or "rev" or "R" to indicate reverse primer.

Primer Name	Sequence	TM	Product size	Source
map_for	GTG TTC CAC GCC CCG CCC AAC	70.4		Cude et al., 2012
map_rev	CCC GGC CGG TGA CAG GGT GAA	70.4	200bp	Cude et al., 2012
rpoC_for	CGG CGC TGA AGC GAT CCG TGA	68.4		Cude et al., 2012
rpoC_rev	CCG GAC GGT TGC CCG ATT CCA	68.4	200bp	Cude et al., 2012
alaS_for	GCT GTG GGC GGA GGG GCA ATG	70.4		Cude et al., 2012
alaS_rev	GCC GAT CGA ACC GCC GGT GAC	70.4	200bp	Cude et al., 2012
Y4I_3464_for	GGC AAG ATC CAG GGC ATA C	60.44		This study
Y4I_3464_rev	ATC AGG AAC GAC CGG TAC TC	59.02	302bp	This study
phaI_qPCR_for1	CAG CCT TGG CGC CTC GGA AA	66.6		Cude et al., 2015
phaI_qPCR_rev1	TGC AGC GGA GCG AAT TGC GA	68.6	216bp	Cude et al., 2015
pgaI_qPCR_for1	GGC GGC TCC ATG CGG TTT CT	66.6		Cude et al., 2015
pgaI_qPCR_rev1	CCT GCT GCG ATC CTG CCC TG	64.5	155bp	Cude et al., 2012
qPCR_igiD_for	GGT CAG AAA GGA CGC GTC GCG G	70.1		Cude et al., 2012
qPCR_igiD_rev	AGC GCG CGA TGC CGA GCT GAT C	70.1	229bp	Cude et al., 2012
pgaR_qPCR_for1	ATC AGG GGT CCG AAC GGC CA	66.6		This study
pgaR_qPCR_rev1	CGG CTG TAG CCG ATC GCC AG	68.6	227bp	This study
phaR_qPCR_for1	GGT GGG CTT TGA CGG GGT CG	68.6		This study
phaR_qPCR_rev1	AGC CGC TCC AGC TCC TTC CA	66.6	159bp	This study
phaI_F	CGC AAG CAG AAG CTG GTG GA	64.5		This study
phaI_R	ATA CCC GAA CCG CCT CAG CA	64.5	429bp	This study
pKNOCK_746	CAC TTA ACG GCT GAC ATG G	52.6		This study
pKNOCK_895	TTA ATT CGA CGC GTC CTC	50.0	149bp	This study

Supplemental Table 2.2 Position and nature of insertional mutations and location of qPCR primers.

Mutant designation	Gene disrupted and type of insertion	Length of wildtype gene (bp)	Location of insertion[a]	qPCR primer location[a,b]	length of insertion (bp)	Source
Y401BD4	*igiD*::Tn5-Km^R	3942	595	3288 (F) 3516 (R)	4080	Cude et al., 2012
Y411CE4	*pgaR*::Tn5-Km^R	720	269	354 (F) 580 (R)	4080	Cude et al., 2015
Y412AE6	*phaR*::Tn5-Km^R	636	45	90 (F) 248 (R)	4080	Cude et al., 2015
***phaI*::pKNOCK**	*phaI*::pKNOCK	666	268	829 (F) 1044 (R)	2400	This study

[a] Nucleotide position within the designated gene (bp)
[b](F) = position of start of forward primer and (R) = position of start of reverse primer

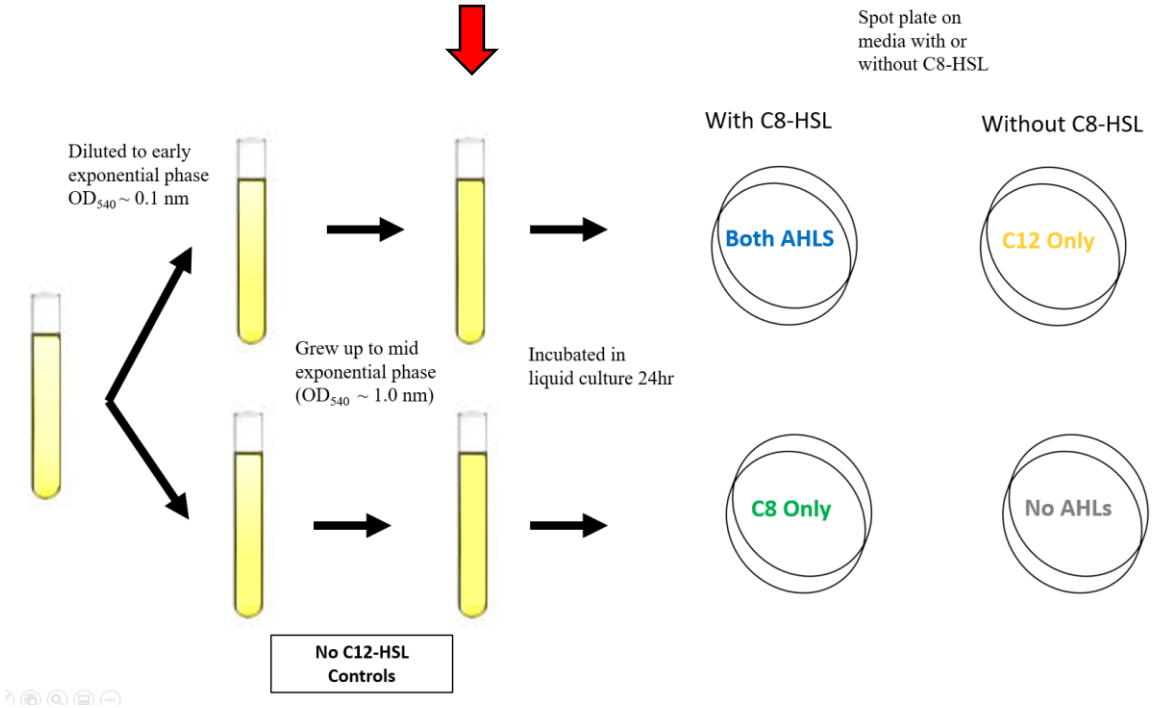

Supplemental Figure 2.1 Overview of methodology for AHL add back. Overnight cultures (3 biological and 3 technical) of Y4I and variants were split into duplicates (now 30 cultures) and diluted to early exponential phase (OD_{540} ~ 0.1 nm) and allowed to grow until they reached mid-exponential phase (OD_{540} ~ 1.0 nm). 3OHC12:1-HSL was added to one set of the duplicate cultures (red arrow). The other set of duplicate cultures became the C8-HSL alone treatment and the no AHL control. All cultures were allowed to continue growing until 24 hrs had been reached. All cultures were then spotted in 10 µL spots onto 10 mL YTSS agar plates with or without C8-HSL and incubated for 24 hrs. The resulting 4 conditions were then analyzed for their indigoidine production for each Y4I variant: both AHLs (blue), 3OHC12:1-HSL alone (yellow), C8-HSL alone (green), and no AHLs (gray).

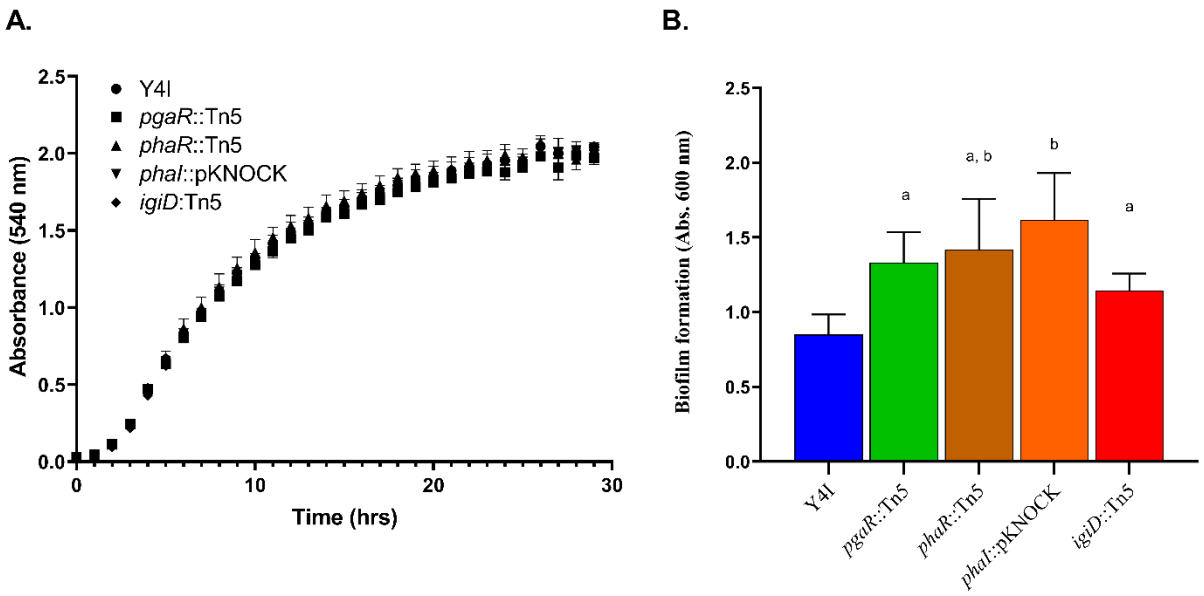

Supplemental Figure 2.2 Growth dynamics in liquid culture (A) and biofilm formation (B) in Y4I and mutants. For liquid cultures, data points are representative of the average of biological quadruplets. Biofilm formation was assessed by crystal violet assay at 24 hrs post inoculation. Data bars are representative of the average of two biological replicates containing technical septuplets. Error bars represent standard deviation from the mean and statistical significance was calculated using a one-way ANOVA.

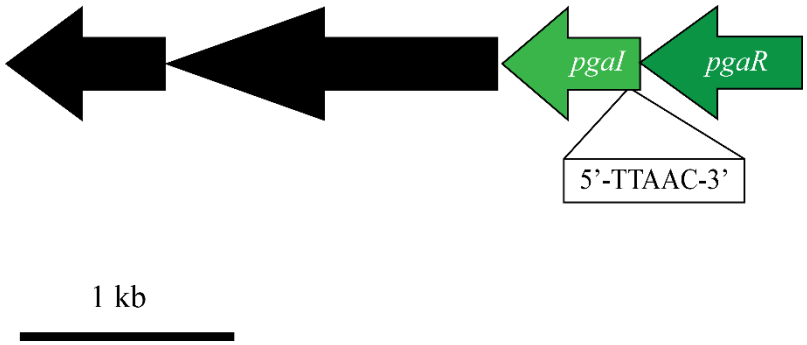

Supplemental Figure 2.3 Half CtrA binding site within pgaRI (green) operon. *pgaRI* (RBY4I_1689, RBY4I_3631) and *phaRI* (RBY4I_1027 and RBY4I_3464) genes were queried for CtrA binding motifs based on the approach outlined in Laub et al. 2000 . A CtrA half binding site within the *pgaRI* cassette was found (sequence shown below in box) starting at ~484 bp. Genes are represented by page arrows and shown to scale. Black arrows represents genes immediately downstream of QS2 (*pgaRI*).

Chapter 3 : SECONDARY METABOLITE PRODUCTION IN SYNTHETIC ROSEOBACTER COMMUNITIES ORCHESTRATES BIOFILM DYNAMICS

A version of this chapter was written by April C. Armes, Jillian L. Walton, and Alison Buchan and is intended to be submitted for publication.

A.C.A. and A. B. conceived and designed the experiments for surface attachment and biofilm formation assays. A.C.A. and J. L. W. conducted the experiments, carried out data analysis, generated figures, and wrote the manuscript. The manuscript was edited by A.C.A, J. L. W., and A. B.

I. Abstract

Within marine ecosystems, biofilms are critical to ecosystem functions contributing to global biogeochemical cycling, bioremediation, and biofouling. Biofilms are a consortium of microorganisms growing on a surface, suspended in a self-produced polymeric matrix. Due to their biological and physicochemical properties biofilms are ideal systems for studying microbial interactions, particularly those mediated by small diffusible molecules. The physical matrix and spatial arrangement of cells within biofilms facilitate microbial interactions, both cooperative and competitive in nature, between biofilm members. These interactions are often mediated by quorum sensing (QS), signaling systems that elicit population-level responses in a cell-density dependent manner, including the expression of secondary metabolites with antimicrobial activity. Despite the crucial role of secondary metabolites in biofilm dynamics, few studies have directly explored their contributions. Primary surface colonizers represent one area of interest regarding interactions within a biofilm. Members of the Roseobacter clade, a group of marine heterotrophic bacteria, are primary and aggressive surface colonizers. Clade members are excellent models to study community interactions given their diverse metabolic capabilities, numerous QS pathways, and abundance in coastal microbial assemblages. We utilized a five-member synthetic community of Roseobacters to address whether secondary metabolite production, mediated by QS, contributes to microbial community structure and dynamics by introducing QS mutants to a synthetic biofilm community grown in either complex or a defined media. Our findings indicate that a common marine QS signaling molecule, N-octanoyl-L-homoserine lactone (C8-HSL), influences community structure in a biofilm grown on a complex medium (i.e., tryptone and yeast extract). When given a less labile and more defined carbon source (i.e., *p*-coumaric acid) the relative abundance of the primary surface colonizer, Rhodobacterales strain Y4I is delayed while the underlying community interactions remain stable. For example, an inactivation of QS systems in Y4I, results in increased community cooperation while community competition is a consequence of antimicrobial production. Our results provide evidence that secondary metabolites are integral to biofilm community structure and dynamics in marine ecosystems.

II. Introduction

Microbial interactions play critical roles in defining microbial community structure and function. These microbial interactions span from more cooperative interactions, such as resistance to antimicrobials and co-metabolism (1–3), to more competitive interactions, such as production of inhibitory compounds and competition for resources (4–6). Many types of microbial interactions are mediated by small molecules that are not essential to primary metabolism but are produced to facilitate interactions between microbes and their biotic and abiotic environments (i.e., secondary metabolites [7]). Two common classes of secondary metabolites produced by microbes are signaling molecules and antimicrobial compounds. A well-known group of small, diffusible signaling molecules, the acylated homoserine lactones (AHLs), are common to many Proteobacteria where they are used to coordinate gene expression in a population density dependent manner (i.e., quorum sensing (QS [8]). Canonical AHL-mediated QS consists of a two-component system consisting of a transcriptional regulator (LuxR-type protein) and an AHL synthase (LuxI-type protein) that produces the diffusible ligand. When bound, these protein-ligand complexes can elicit global changes in gene expression (9). Common bacterial traits that are QS-regulated include, but are not limited to: bioluminescence, pathogenicity, biofilm formation, and antimicrobial production (10–13). Antimicrobials are thought to contribute to microbial interactions principally through inhibition of the growth of competitors. However, for some microbes, these compounds may themselves function as inter-microbial signals at low concentrations (14). Thus, these two classes of molecules can have overlapping roles and are crucial to competitive and cooperative microbial interactions.

In many environments, diverse microorganisms are enclosed in biofilms where they are in close physical association with one another and encased in a self-produced polymeric matrix. The biological and physicochemical properties of biofilms make them ideal systems to study microbial interactions, especially those that are mediated by diffusible small molecules. In addition, biofilms play critical roles in ecosystem functioning, where they mediate transformations key to biogeochemical cycling (15), bioremediation (16), and biofouling (17). In turn, biofilm-associated microorganisms are afforded some degree of protection by the biofilm matrix from external environmental stressors, predators, toxins, and antibiotics (18). Secondary metabolites commonly have enhanced biosynthesis in biofilms, leading to higher concentrations of these compounds in the local environment and subsequently influencing microbial interactions along the spectrum from cooperation to competition (19).

Current understanding of QS-mediated microbial interactions within biofilms is principally based on co-culture and natural assemblages (20, 21). While valuable, co-culture studies can be limited by an over-simplification of microbial interactions. On the other hand, mesocosm experiments using complex natural communities introduces a wide range of variables to consider when trying to tease apart microbial interactions (22–24). Synthetic intentional communities provide an opportunity to limit community complexity while still allowing for a higher order level of interactions beyond pairwise interactions. In addition, synthetic communities have been used recently in surface colonization and biofilm studies to mimic interactions found in natural ecosystems (25–27). Despite the recent emergence of multispecies-based biofilm studies, our knowledge of microbial interactions within natural biofilm communities is still relatively incomplete, specifically those cooperative and competitive interactions influenced by QS. A critical aspect to understanding these QS-linked interactions within multispecies biofilm communities is to evaluate the fitness, physiological, and ecological aspects between individual species and a multispecies biofilm consortium. To address this knowledge gap, we systematically evaluated the contribution of

QS using a series of bacterial mutants unable to produce secondary metabolites in a low diversity and defined synthetic community to investigate cooperation and competition within a biofilm.

Members of the heterotrophic clade of bacteria, known as the Roseobacter clade, comprise up to 20% of the microbial communities in marine ecosystems, possess a large genetic repertoire, and demonstrate high metabolic diversity. As a result of their vast metabolic capabilities, Roseobacters are adept at transforming phenolic compounds and play a role in carbon and sulfur cycling (28, 29). In marine ecosystems Roseobacters are important primary surface colonizers, promoting surface colonization and biofilm formation of other marine bacteria through the production of secondary metabolites (30). In addition to the colonization role of secondary metabolites, growth substrate also has been reported to play a role in defining Roseobacter synthetic communities (26). Due to their predilection to form a biofilm on a variety of surfaces and robust secondary metabolite production, members of the Roseobacter clade are ideal model organisms for examining the molecular mechanisms that mediate the cooperative and competitive microbial interactions within biofilm communities.

II. Methods and Materials

Synthetic community bacterial strains, growth conditions, and maintenance

Four of the five strains used to assemble the synthetic communities in this study were previously isolated from southeastern United States estuaries or coastal waters (Rhodobacterales strain Y4I, *Sagittula stellata* sp. E-37, *Citreicella* sp. SE45, and *Sulfitobacter* sp. EE-36). The final strain, *Roseovarius nubinhibens* ISM, was previously isolated from the Caribbean Sea (31). Previously established Y4I mutants: *igiD*::Tn5-Km^R, *pgaR*::Tn5-Km^R, *phaR*::Tn5-Km^R, and *clpA*::Tn5-Km^R were generated using a mini Tn5 transposon system (4, 32). The *phaI*::pKNOCK mutant was previously generated using targeted insertional mutagenesis (33). All Y4I mutant variants encode a chromosomally located kanamycin resistance gene.

For routine maintenance, all strains were maintained on YTSS agar [per liter: 15 g Instant Ocean (Thermo Fisher Scientific), 15 g agar (Thermo Fisher Scientific), 4 g tryptone, 2.5 g yeast extract]. Y4I strains were routinely passaged in 20% YTSS (per liter: 15 g Instant Ocean, 0.8 g tryptone, 0.5 g yeast extract) to reduce flocking in these strains. Each strain was passaged onto basal medium (BM - per liter 8.7 mM KCl, 8.7 mM CaCl2, 43.5 mM MgSO4, and 174 mM NaCl with 225 uM K2HPO4, 13.35 mM NH4Cl, 71 mM Tris-HCl [pH 7.5], 68 uM Fe-EDTA, trace metals [7.8492 mM nitriloacetic acid, 0.5325 mM MnSO4∗H2O, 0.4203 mM CoCl2 ∗6H2O, 0.3478 mM ZnSO4 ∗7H2O, 0.0376 mM CuSO4, 0.1052 mM NiCl2 ∗6H20, 1.1565 mM Na2SeO3, 0.4134 mM Na2MoO4∗2H2O, 0.3259 mM Na2WO4∗2H2O, 0.2463 mM Na2SiO3∗9H2O] and trace vitamins [0.0020 % vitamin H (Biotin), 0.0020 % folic acid, 0.0100 % pyridoxine-HCl (B6), 0.0050 % riboflavin (B2), 0.0050% thiamine (B1), 0.0050 % nicotinic acid, 0.0050 % pantothenic acid (B5), 0.0001% cyanocobalamin (B12), 0.0050% p-aminobenzoic acid]) containing either 10 mM sodium acetate or 2 mM p-hydroxybenzoic acid (POB). All strains were incubated at 30°C in the dark unless otherwise noted.

Surface attachment to glass beads

Surface attachment to glass beads was assessed as previously described by Cude *et al* (2012). Briefly, sterilized 4 mm glass beads (Pyrex, Corning Incorporated Corning, NY) in a 96-well polystyrene plate (Costar, Corning Incorporated Corning, NY) were inoculated with the following strains in monoculture: E-37, SE45, EE-36, ISM, wildtype Y4I, *igiD*::Tn5-Km^R, *pgaR*::Tn5-Km^R, *phaR*::Tn5-Km^R, and *phaI*::pKNOCK in triplicate. Cells were allowed to

attach to glass beads for 12 hrs, 24 hrs, and 48 hrs. Following incubation, glass beads were extracted from wells and cells were dislodged from beads as previously described (4, 33). Following extraction from glass beads, cells were serially diluted and plated onto YTSS (1.5 % agar) and incubated at 25°C.

Viable cell counts and total biomass on synthetic community biofilms

All experiments assessed interactive effects of QS by comparing viable cell density or total biomass in a mixed species community containing different Y4I variants using a complex medium (20 % YTSS) or a defined medium containing 2 mM coumarate as the sole carbon source. Five different synthetic community mixes were assembled. Each synthetic community consisted of E-37, SE45, EE-36, ISM and one of the following Y4I variants: wildtype Y4I, *pgaR*::Tn5-Km^R, *phaR*::Tn5-Km^R, *phaI*::pKNOCK, *igiD*::Tn5-Km^R. Synthetic mixed communities were seeded at approximately equal densities of ~1 x 10^5 cells mL^{-1}.

To assess community structure within biofilms, surface attachment assays for synthetic biofilm communities were performed as described above. Each well was seeded with ~1 x 10^5 cells mL^{-1} and the inoculated plate was incubated at 30°C. A duplicate of each plate was made to assess total biomass described below. All cultures were inoculated in biological and technical triplets. Viable cells were extracted, vortexed, and serially diluted at each time point. All viable cell counts were plated onto YTSS agar and allowed to incubate at 25°C until colony morphology was discernible (~5 days). Colony morphology of each strain was readily identifiable except for Y4I mutant variants, which lacked the blue pigmentation diagnostic of the wildtype strain (4, 26, 32, 33). Thus, all mixed cultures containing Y4I mutant variants were also plated onto YTSS containing kanamycin (50 µg/mL) as a control to differentiate between Y4I variants from other community members.

Total biomass on biofilm-grown cultures was assessed by performing a crystal violet stain on glass beads as previously described (33). Briefly, liquid was aspirated out of wells. Glass beads were washed with a 1.5 % sea salt solution (Instant Ocean) to remove loosely attached cells. Glass beads were extracted using a vacuum apparatus and moved to a clean 96-well plate. Cells attached to glass beads were stained using a 2% crystal violet solution and solubilized with 95 % EtOH. Absorbance was read at 600 nm using a microplate reader (Bio Tek Instruments, Inc., Synergy HT Multi-Mode Microplate Reader, SN 270212).

Complex Growth Medium (20 % YTSS)

Prior to inoculating the 96-well plate, all bacterial strains were grown individually in liquid YTSS in biological triplicates. Overnight cultures were diluted 1:10 in fresh YTSS and allowed to grow until mid-exponential growth was reached (~3 hrs). For each culture, cells were harvested in triplicate by transferring 1 mL culture to 1.5 mL centrifuge tube and spun at 8000 rpm for 10 min. The supernatant was withdrawn and cells were resuspended in fresh YTSS. All cultures were diluted to ~1 x 10^6 cells mL^{-1}. Technical replicates were used to establish controls for mono- and synthetic mixed cultures. Briefly, 1 mL of each culture was combined to establish a master mix of ~5 x 10^6 cells mL^{-1} mixed cultures containing: E-37, SE45, EE-36, ISM, and a Y4I variant. Synthetic mix cultures were then diluted to 1 x 10^6 cells mL^{-1} and used to inoculate 96-well plates at a final inoculum of ~1 x 10^5 cells mL^{-1}. Final dilutions were plated to assess cell abundance of mixed cultures at time of inoculation. Monoculture controls (~10^5 cell mL^{-1}) were included in both viable cell abundance and total biomass assays. Six replicates of each plate were made to assay viable cell abundance and total biomass over time on glass beads.

Following inoculation of 96-well plates, each plate (in duplicate) was wrapped with dampened cellulose fiber sheets, stored in a sealing high-density polyethylene (HDPE) bag,

and incubated at 30°C. At 20 (day 1), 44 (day 2), and 68 (day 3) hrs, cells were extracted from beads of duplicate plates. Viable cells and total biomass were assessed as described above.

Defined Growth Medium (Coumarate)

For defined medium, the experimental design was set up as described above with the following exceptions: (i) overnight cultures were inoculated into 1 part YTSS and 9 parts BM and allowed to reach mid-exponential growth (~ 12 hrs). (ii) Liquid cultures (1 mL) were harvested and washed with BM. (iii) All cultures were primed by inoculation into BM containing 2 mM POB and allowed to grow overnight at 30°C. POB cultures (10 mL) were spun down and washed with BM to remove any residual carbon. BM containing coumarate (2 mM) was inoculated with 0.01 – 0.1 mL of cultures to achieve an inoculum of 1 x 10^6 cells mL^{-1}. (iv) Monoculture controls were included for total biomass assays. (v) At 24 hrs (day 1), 96 hrs (day 4), 216 hrs (day 9), and 336 hrs (day 14), cell abundance and total biomass was assessed from duplicate plates.

Inhibition Assays

A factorial growth inhibition assay using synthetic community members was utilized to determine antagonistic interactions among community members. Briefly, liquid cultures of community members and Y4I variants were grown overnight (30°C, shaking). Overnight cultures were diluted 10-fold and each of the five strains were spread evenly onto individual YTSS agar (1.5%) plates. Each strain as well as Y4I variants were grown to mid-exponential phase and then spotted (10 ul) on top of the spread plates. Y4I variants included an indigoidine null mutant (*igiD*::Tn5-Km^R) and an indigoidine hyper-producing mutant (*clpA*::Tn5-Km^R). QS mutants *pgaR*::Tn5-Km^R, *phaR*::Tn5-Km^R, and *phaI*::pKNOCK were not included in inhibition assays as they have been previously demonstrated to lack inhibitory activity (4, 32, 33). Growth inhibition assays were incubated at 30°C. Zones of clearing surrounding inhibitor organisms were assessed 24 hrs post inoculation.

AHL Extraction and Detection

To assess quorum sensing cross-talk between community members we extracted identified putative AHLs produced by synthetic community members along with two Y4I variants: wildtype Y4I and *phaI*::pKNOCK. AHL extractions on YTSS from *pgaR*::TN5-Km^R and *phaR*::TN5-Km^R mutants have been previously published (4). AHLs were extracted as described in Cude 2015. Briefly, mid-exponential phase cultures in triplicate were spot plated onto YTSS agar in a 60 mm petri dish containing a 0.22 uM PES filter and incubated at 30°C for 24 hrs. Filters were aseptically removed and weighed. Cell biomass from filters was extracted and used to estimate microbial abundance. YTSS agar was removed from petri dishes, finely minced, and dissolved in 100 mL ethyl acetate for 3 hrs. Liquid layer was decanted from residual solid layer and vacuum filtered through a silica medium. Extracted AHLs were concentrated in vacuo to produce an oil. This oil was then resuspended in 300 uL acidified ethyl acetate and transferred to an autosampler vial. Samples were stored at -20 °C until analysis. AHLs were detected using high-performance liquid chromatography–tandem mass spectrometry (HPLC-MS/MS) at the Biological and Small Molecule Mass Spectrometry Facility at the University of Tennessee.

Data Analysis

Viable cell counts were analyzed and visualized using RStudio v1.4.1106. All viable cell count data were normalized to the mean relative abundance within replicates. Area plots were constructed based on mean relative abundance of the strains in each mix over their respective time points for each media type. Beta diversity analysis was performed using the bcdist() function in the ecodist package (34) for each time point for the complex medium and defined medium. The adonis() function in the vegan package (35) was used to conduct a permutational multivariate analysis of variance (PERMANOVA) on the paired time points and on the aggregated time points for both carbon sources. Alpha diversity was calculated within each time point using the Shannon Diversity Index in the vegan package (36, 37).

Surface attachment assays and total biomass via crystal violet assays were analyzed and visualized using GraphPad Prism v9.0.0 (GraphPad Software, San Diego, California USA, www.graphpad.com). Statistical significance was calculated using a Two-Way analysis of variance (ANOVA). Variability of differences was corrected using Geisser-Greenhouse correction. Multiple comparisons were assessed using Dunnet's multiple comparisons for surface attachment assays and Tukey's HSD (honestly significant difference) for crystal violet assays (**Supplemental Table 3.1-3.3**).

III. Results

To evaluate the impact of secondary metabolite production, such as AHLs and antimicrobials on microbial interactions in biofilms we conducted synthetic community experiments using a five-member Roseobacter community. The selected strains (E-37, Y4I, ISM, EE-36, and SE45) are representatives of those found in high abundance in marine environments, where they have been reported to be metabolically active (38, 39). In addition, these strains have been extensively studied in their ability to degrade plant-derived aromatic compounds and each possess genes found in the protocatechuate pathway, responsible for degrading coumarate (29, 40–42). Finally, these strains have previously been used in a synthetic community study (26). As secondary metabolite production is intrinsically linked with central metabolism, we also considered the influence of growth medium (i.e., complex vs. defined). For these community studies, we quantified growth inhibition, putative AHL production, surface colonization, as well as biofilm composition and formation. We also assessed cooperation and competition. Here, we improve upon the previous definition of biofilm community cooperation and competition presented by Ren et al (2015) and characterized community cooperation as an increase in biofilm formation compared to the best biofilm producer in monoculture without loss of total cell viability in the community. Community competition is defined as a decrease in biofilm formation compared to the worst biofilm producer in monoculture or a decrease in viability of the mixed community (25).

Secondary metabolites reveal interactions between synthetic biofilm members. Previous studies have reported both QS systems and biosynthetic pathways for antimicrobial production (e.g., PKS and NRPS) are prevalent in Roseobacter genomes (4, 43, 44). All five strains used in this study possess at least one QS component. Three of the five strains (E-37, SE45, Y4I) contain one or more canonical *luxRI* paired QS system(s). Additionally, these strains each harbor an unpaired (i.e., orphaned or solo) LuxR homolog. In contrast, two members (ISM and EE-36) possess only orphaned LuxR and LuxI homologs (**Table 3.1**). Pairwise comparisons between synthetic community members LuxI homologs to PgaI and PhaI in Y4I revealed that E-37 and SE45 possess more than 50 % amino acid identity to PgaI. Both EE-36 and ISM shared more than 25 % amino acid identity with PhaI in Y4I. High protein similarity in AHL synthases suggests the synthesis of AHLs with similar structures.

It has previously been demonstrated that Y4I possesses two QS systems (*pgaRI* and *phaRI*) which coordinately regulate the production of the blue pigmented antimicrobial indigoidine, encoded by a non-ribosomal polypeptide synthase (NRPS), termed *igiD* (32). NRPS-like genes encode secondary metabolites such as toxins, antimicrobials, and pigments (45). Two other community members have been reported to possess NRPS-like genes: E-37 and ISM (40), but neither these genes nor their products have been characterized. Both SSE37_17955 and ISM_16730 share more than 90 % sequence identity to LLM class flavin-dependent oxidoreductases in more closely related organisms (i.e., organisms in their respective genera) and are distinct from *igiD* in Y4I. ISM produces a dark orange pigment while E-37 does not produce pigmentation. The gene(s) responsible for pigmentation in ISM have yet to be identified. Whether the NRPS genes found in E-37 and ISM confer antimicrobial properties is currently unknown.

In order to determine whether secondary metabolite production among individual community members could inhibit the growth of community residents, we performed a pairwise assessment of interactions between the five synthetic community members using a fully factorial growth inhibition assay. Only one strain, Rhodobacterales strain Y4I, was able to inhibit the growth of any of the other strains (2 of 4; **Table 3.2**). Using mutants that are either abolished in pigment production (*igiD*::Tn5-Km^R) or hyper-pigmented (*clpA*::Tn5-Km^R), the inhibition of strains EE-36 and E-37 was strictly correlated with indigoidine production (**Table 3.2**), indicating this compound could be an important community determinant in this synthetic community. Previous studies demonstrate the competitive nature of Y4I in community members in both co-culture and synthetic community studies likely as a result of indigoidine production (4, 26, 32, 33). Given that competition and surface attachment has been linked to both QS systems and indigoidine null mutants in Y4I we used mutant strains harboring disruption in these pathways to assess the impact of secondary metabolite on biofilm community composition and dynamics.

A necessary first step to predicting community dynamics was to assess the potential for QS cross-talk. QS cross-talk, that is the ability for noncognate AHLs to bind to LuxR homologs in differing organisms, has been modeled to contribute to competition or cooperation in diverse microorganisms (46). Therefore, we evaluated whether synthetic community members were able to produce similar AHLs facilitating potential QS cross-talk between community members. We examined each synthetic community member along with wildtype Y4I and the *phaI* variant for the ability to produce overlapping AHLs: N-octanoyl-L-homoserine lactone (C8-HSL) and the N-3-oxo-dodecenoyl-homoserine lactone isomer, 3OHC12:1-HSL. Previous studies demonstrated that *pgaR*::TN5-Km^R and *phaR*::TN5-Km^R are impaired in their ability to produce their cognate AHLs C8-HSL and 3OHC12:1-HSL, respectively (32). As a preliminary quantification for AHL production, we performed high-performance liquid chromatography–tandem mass spectrometry (HPLC-MS/MS) as previously described (32, 47, 48). HPLC-MS/MS revealed that community members produced AHLs with varying lengths of carbon in acyl chains. Specifically, we detected AHLs with masses corresponding to N-3-oxo-propionyl-L-homoserine lactone (3OHC3-HSL), N-pentanoyl-L-Homoserine lactone (C5-HSL), C8-HSL, N-3-hydroxydecanoyl-L-Homoserine lactone (3OHC10-HSL), N-dodecanoyl-L-homoserine lactone (C12-HSL), and 3OHC12:1-HSL (Y4I only). In almost all cases, Y4I produced a higher concentration of AHLs compared to community members. The exceptions were C5-HSL and C12-HSL, where peak areas of these AHLs were relatively equal in all community members. Thus, it is likely that the predominant putative AHLs produced by synthetic community members, excluding Y4I, are C5-HSL and C12-HSL (**Table 3.1**).

Y4I is an aggressive surface colonizer compared to other community members. We assessed surface attachment of the five individual synthetic community members in monoculture as well as the Y4I QS and indigoidine variants at 12, 24, and 48 hours post inoculation. With the exception of Y4I, only 0.03 – 4 % of the initial inoculum (~ 10^8 cells mL^{-1}) was present on glass beads after 12 hrs. For Y4I, 97 % of the initial inoculum adhered to glass beads after 12 hrs. These results demonstrate that other community members experience a lag in attachment to glass beads compared to Y4I. At 24 and 48 hrs, all strains increased in surface-attached viable cells. However, viable cell abundance of Y4I attached to a glass surface was significantly greater than all community members at 24 hrs ($p < 0.05$). Viable cell counts of Y4I remain significantly higher than community members at 48 hrs ($p < 0.05$) except for EE-36 (**Figure 3.1**). Attached viable cell abundance among Y4I variants were comparable (**Supplementary Figure 3.1**).

***Secondary metabolites influence biofilm composition*.** We next assessed whether QS or antimicrobial production influenced microbial biofilm community structure (composition) and dynamics (cooperation or competition) in the five-member synthetic Roseobacter communities. Each synthetic community contained one of the following Y4I variants: wildtype, *pgaR*::Tn5-Km^R, *phaR*::Tn5-Km^R, *phaI*::pKNOCK, and *igiD*::Tn5-Km^R. Both the *pgaR* and *phaR* variants are unable to sense their cognate AHLs, C8-HSL and 3OHC12:1-HSL respectively. Additionally, the *pgaR* mutant is unable to produce the indigoidine, while the *phaR* variant expresses delayed and reduced amounts of indigoidine. To eliminate this leaky phenotype, we previously generated a mutant in the corresponding AHL synthase gene, *phaI*. This mutant is unable to produce 3OHC12:1-HSL, but transcriptional regulators PhaR and PgaR remain functional. Thus, the *phaI* variant is able to sense AHLs corresponding to the *phaRI* and *pgaRI* QS systems. The indigoidine biosynthesis mutant, *igiD*::Tn5-Km^R, is unable to produce indigoidine but expresses WT levels of both QS systems (33). Due to the nature of these variants, we can assess the discrete and compounded impact of QS systems and antimicrobial production.

Viable cellular abundances for each synthetic community were assessed and relative abundance of each community member over time was determined. Across all communities the relative abundance of each strain remained moderately stable. However, composite community viable cell abundance varied over time due to the presence of Y4I variants within synthetic communities. For example, synthetic communities harboring either wildtype Y4I or the *phaR* variant stabilized after 1 day, whereas total viable cells in synthetic communities containing an indigoidine null mutant decreased in viability on day 2. In contrast, communities possessing the *pgaR* mutant continually increased in viability over time. Synthetic communities including the *phaI* variant initially decreased in viability but rebounded on day 3. Despite the modality of community dynamics within each synthetic community, biofilm communities within the complex medium were characterized by an overwhelming dominance of Y4I regardless of variant, comprising 57-89% of the community (**Figure 3.2A**).

We used a defined medium containing coumarate to: (i) decrease the competitive advantage of Y4I and (ii) determine if carbon source affected community interactions. When providing a growth disadvantage using the phenolic compound, coumarate, as the sole carbon source all Y4I variants displayed an initial decrease in viability in synthetic communities (**Figure 3.2B**). This result is consistent with previous findings and posited to be a result of toxic waste build-up due to coumarate metabolism (26). In fact, Y4I variants demonstrate a loss of viability compared to no carbon controls in liquid monocultures when grown on coumarate (**Supplemental Figure 3.2**). However, Y4I variants within synthetic community biofilms increased in the presence of coumarate. This increase in viable cells was comparable to no carbon controls (**Supplementary Figure 3.3**). Furthermore, all Y4I

variants dominated the community by the end of the experiment in the defined medium condition. The synthetic community containing the indigoidine null mutant experienced a lag in relative abundance before rising to dominance. Similar to the trends observed in a complex medium, synthetic communities harboring wildtype Y4I and the *phaR* variant stabilized on day 9, while the synthetic community possessing the *pgaR* mutant continued to increase in viability. At day 14, communities containing the *phaI* variant appeared to stabilize. From day 1 to day 14, the dominant community member in defined medium biofilms switched from SE45 (75-87% on day 1) to Y4I (61-87% on day 14), regardless of Y4I variant included (**Figure 3.2B**).

To investigate the diversity and treatment effects on community structure, we performed beta diversity analysis, alpha diversity analysis, and PERMANOVA (**Supplemental Tables 3.4-3.8**). The community structures of each synthetic community from day 0 to day1 are dissimilar between growth substrates (i. e., complex and defined media) but became more similar at later time points (**Figure 3.3**). Across all time points the structures of each community were significantly different based on growth substrate ($p < 0.05$, **Supplemental Tables 3.4-3.8**). As expected, synthetic communities are not significantly different at day 0 (**Figure 3.3**, $p < 0.05$). Additionally, the structures of synthetic communities on day 1 were not only significantly different based on growth substrate but also which Y4I variant was included in the synthetic community ($p < 0.05$, **Supplementary Table 3.6**). Each time point also was significantly different from other time points within and between media types ($p < 0.05$, **Supplemental Tables 3.4-3.8**). The alpha diversity of each synthetic community drops from day 0 to day 1, corresponding to a drop in evenness of the community structure (**Supplemental Figure 3.4**).

Secondary metabolites influence biofilm interactions. Because viable cell abundance alone cannot fully explain the interactions within mixed species communities, we assessed total biofilm production of our five-member synthetic communities across both growth substrates. To determine interactions within mixed communities, biofilm production was measured in both monocultures and synthetic communities using a beaded crystal violet assay where synthetic communities were compared to the best and worst biofilm producers in monoculture (**Figures 3.4, 3.5**).

When grown on a complex medium, biofilm production was initially similar among mono- and mixed cultures, except for EE-36. In this medium, EE-36 produced the most biofilm during each sampling effort. The worst biofilm producer in monoculture switched from ISM on day 1 to Y4I on days 2 and 3 (**Figure 3.4A-C**). Biofilm production in synthetic communities increased over time, with synthetic communities harboring the *phaI*::pKNOCK mutant showing the greatest increase in biofilm production over the course of the experiment (**Figure 3.4B,C**). Biofilm formation in all synthetic communities increased over time compared to their Y4I variant monoculture counterparts (**Supplementary Figure 3.5**), suggesting biofilm communities confer a growth advantage in the presence of readily available nutrients, even for social cheaters (i. e., QS mutants).

Similar to biofilm production observed on day 1 in the presence of a complex medium, biofilm production in all mono- and mixed cultures were comparable with the exception of E-37 in a defined medium containing a less labile carbon source (coumarate). Initially, E-37 produced the worst biofilm in monoculture (**Figure 3.5A**). However, the worst biofilm producer switched between ISM and Y4I variants (wildtype and *phaR*::Tn5-Km^R) at later time points (**Figure 3.5B-D**). Y4I variants produced the most and least biofilm throughout this experiment. On day 1 and day 4 wildtype produced the most biofilm, and the *phaI* variant produced the most biofilm on day 14 (**Figure 3.5A,C,D**). On day 9 and day 14, the *phaR* variant and Y4I produced the worst biofilms, respectively (**Figure 3.5C,D**). Synthetic

communities harboring a *pgaR* variant produced nearly 3% more biofilm than the best biofilm producer in monoculture on day 4, whereas communities containing the *igiD* variant produced almost 5% less biofilm than the worst biofilm former in monoculture on day 14 (**Figure 3.5B,D**). Synthetic communities harboring Y4I variants produced similar amounts of biofilm compared to their monoculture counterparts, with the following exceptions: at day 4 synthetic communities containing the *pgaR* variant had significantly ($p < 0.05$) more biofilm production compared to its monoculture counterpart (**Figure 3.5B**). Conversely, the synthetic community including the *igiD* variant showed a decrease in biofilm formation compared to its monoculture counterpart at day 14 (**Supplementary Figure 3.6**). In general, synthetic communities demonstrated a similar modality in biofilm production compared to their monoculture counterparts as either an increase in biofilm production over time or variations of cyclic increases and decreases in biofilm formation.

IV. Discussion

Here we assessed the effect of secondary metabolite production and growth substrate on community dynamics and composition. It has been hypothesized that competitive interactions shape community structure while cooperative interactions stabilize it, thereby affecting the overall function and dynamic of the biofilm (49). Community cooperation is most evident within synthetic communities in defined medium harboring the *pgaR* variant as both biofilm production and total viable cells continue to increase with time in the presence of both growth substrates (**Figures 3.6**). The mutant variant in this synthetic community is impaired in both QS pathways and is unable to produce indigoidine (32, 33). Thus, a community containing a Y4I mutant impaired in both QS pathways and indigoidine production (i.e., *pgaR*::Tn5-Km^R) contributes to cooperation among other community members under limited nutrient conditions. Given access to more nutrients (i.e., complex medium), fewer competitive interactions were observed (**Supplemental Figure 3.8**). This finding is supported by synthetic soil communities where biofilms evolve to decrease negative interactions and increase co-metabolism between biofilm members (25), but in this case rather than evolving, mutant variants were constructed. Further evidence of cooperation is demonstrated by communities containing the *phaI* variant. Cooperation within this synthetic community is exhibited by continual increase in biofilm formation and the stability of community member abundance over time (**Figures 3.2B, 3.5**). The *phaI* variant is also impaired in indigoidine production as well as AHL synthesis for its cognate AHL (33). Inclusion of this mutant in synthetic communities allowed us to explore the possibility of QS cross-talk between related species.

Possible evidence for QS cross-talk within these mixed communities is evident within the synthetic community harboring the *phaI* variant. This mutant variant is unable to produce 3OHC12:1-HSL but is able to sense both AHLs predominantly produced by Y4I (C8-HSL and 3OHC12:1-HSL, [33]). However, AHL detection using HPLC-MS/MS indicates all community members putatively produce AHLs with masses corresponding to C12-HSL (**Table 3.1**). HPLC-MS is commonly used to identify AHLs in marine bacteria, however these techniques required the use of an internal standard to identify AHLs. The HPLC-MC/MC detection method used here was developed to eliminate the need for internal standards (47). We recognize the inclusion of nuclear magnetic resonance (NMR) data to determine the molecular structure of the AHLs produced by community members would bolster these results. Even though preliminary AHL data indicates that community strains do not share strong evidence for overlapping AHLs, it is still possible that QS cross-talk may be occurring given the promiscuous nature of LuxR homologs binding to non-cognate AHLs. It is plausible the QS systems in Y4I is able to recognize the AHLs produced by community members with similar masses and acyl-chains length (e.g., C12-HSL). Some excellent reviews have discussed the promiscuity of AHL ligand binding with non-cognate LuxR-like regulatory

proteins (50–52). Given that the *phaRI* pathway in Y4I is likely involved in regulating biofilm formation (33), the putative cross-talk between biofilm community members presented here may aid in the increased biofilm formation observed in this synthetic community. This type of QS cross-talk has been demonstrated in host-microbe models. For example, in plant-associated biofilms presumed cross-talk among rhizosphere bacteria lead to the enhanced synthesis of secondary metabolites compared to non-adherent soil community counterparts resulting in an increase of biofilm formation (19).

Competition within synthetic biofilms seems prevalent in synthetic communities harboring either wildtype Y4I or the *phaR* , or *igiD* variants (**Figure 3.6**). Unlike the other Y4I variants, wildtype and the *phaR* mutant are both able to produce indigoidine, though to varying degrees (32). Growth inhibition assays showed that the blue-pigmented secondary metabolite, indigoidine, inhibits the growth of several members within these synthetic communities (**Table 3.2**) indicating that the antimicrobial may play a role in dictating biofilm community structure. Furthermore, indigoidine has been reported to inhibit the growth of multiple marine microorganisms (4). Conversely, the *igiD* variant is unable to produce indigoidine but still exhibits competition within the synthetic community. These competitive interactions reveal that antimicrobial production may not be the only secondary metabolite responsible for competition in these communities. This finding indicates the need for further investigation into secondary metabolites that elicit competitive interaction Our results support previous findings that the majority of species interactions may be competitive in natural environments (53, 54).

Recently, Roseobacter community composition has been shown to be impacted by primary growth substrates (26). Additionally, a recent study demonstrated that nutrient availability and concentration impacts microbial community interactions, specifically growth inhibition (55). Here we show that synthetic community structures stabilize in a similar manner independent of the growth substrate. However, community dynamics vary due to the type of Y4I variant present in the community, resulting in significantly different structuring in each of the synthetic communities at day 1 (**Supplementary Table 3.6**). Moreover, each media type significantly impacted community structure at day 1 and the following timepoints. Interestingly, the Y4I variants experienced growth inhibition in liquid monoculture in the presence of coumarate, but when added to a mixed community, they dominate the community. The deviation in growth dynamics between liquid monocultures and multispecies biofilms across all Y4I variants can be explained by two possibilities: (i) evidence for co-metabolism and (ii) biofilm-mediated defense again harmful substrates. Both SE45 and E-37 have previously been reported to use coumarate as a sole carbon source. A by-product of coumarate metabolism is *p*-hydroxybenzoate (POB) which all community members can degrade through the protocatechuate pathway (26, 40). The degradation of coumarate into exudate metabolites, such as POB, may explain why we see a delayed increase in Y4I variants in biofilm communities in the presence of this compound. Alternatively, coumarate is posited to be toxic at high concentrations (>5 mM- [26]). It is possible that in the presence of a multispecies biofilm Y4I is protected against the inhibitory action of these metabolites. Previous reports support the protective nature of biofilms against toxic compounds resulting in increased bacterial stress tolerance (56).

The observations presented here provide a direct link between secondary metabolite production in the form of AHLs and antimicrobials on biofilm community structure and dynamics. As AHLs and antimicrobial production are commonly associated with many mixed species biofilms, this work may be applied to both environmental and host-pathogen biofilms. Our results support that primary surface colonizers, such as those in the Roseobacter clade, influence community interactions through their diverse metabolic capabilities regardless of nutrient source provided. Whereas nutrient conditions in marine

ecosystems may fluctuate, community interactions may well be steady. To our knowledge, this work lays the foundation for understanding how cell-to-cell communication, in the form of quorum sensing, influences cooperative and competitive social behaviors within microbial biofilm communities in marine ecosystems.

References

1. Burmølle M, Webb JS, Rao D, Hansen LH, Sørensen SJ, Kjelleberg S. 2006. Enhanced Biofilm Formation and Increased Resistance to Antimicrobial Agents and Bacterial Invasion Are Caused by Synergistic Interactions in Multispecies Biofilms. Appl Environ Microbiol 72:3916–3923.
2. Leriche V, Briandet R, Carpentier B. 2003. Ecology of mixed biofilms subjected daily to a chlorinated alkaline solution: spatial distribution of bacterial species suggests a protective effect of one species to another. Environ Microbiol 5:64–71.
3. Pande S, Kaftan F, Lang S, Svatoš A, Germerodt S, Kost C. 2015. Privatization of cooperative benefits stabilizes mutualistic cross-feeding interactions in spatially structured environments. ISME J 2015 106 10:1413–1423.
4. Cude WN, Mooney J, Tavanaei AA, Hadden MK, Frank AM, Gulvik CA, May AL, Buchan A. 2012. Production of the antimicrobial secondary metabolite indigoidine contributes to competitive surface colonization by the marine roseobacter *Phaeobacter sp.* strain Y4I. Appl Environ Microbiol 78:4771–4780.
5. Rao D, Webb JS, Kjelleberg S. 2005. Competitive Interactions in Mixed-Species Biofilms Containing the Marine Bacterium *Pseudoalteromonas tunicata*. Appl Environ Microbiol 71:1729–1736.
6. Guittar J, Koffel T, Shade A, Klausmeier CA, Litchman E. 2021. Resource Competition and Host Feedbacks Underlie Regime Shifts in Gut Microbiota. Am Nat 198:1–12.
7. Miller MB, Bassler BL. 2001. Quorum Sensing in Bacteria. Annu Rev Microbiol 55:165–99.
8. Case RJ, Labbate M, Kjelleberg S. 2008. AHL-driven quorum-sensing circuits: their frequency and function among the Proteobacteria. ISME J 2008 24.
9. Fuqua C, Parsek MR, Greenberg EP. 2001. Regulation of Gene Expression by Cell-to-Cell Communication: Acyl-Homoserine Lactone Quorum Sensing. Annu Rev Genet 35:439–468.
10. Lyell NL, Stabb E V. 2013. Symbiotic characterization of *Vibrio fischeri* ES114 mutants that display enhanced luminescence in culture. Appl Environ Microbiol 79:2480–2483.
11. Pusic P, Sonnleitner E, Bläsi U. 2021. Specific and Global RNA Regulators in *Pseudomonas aeruginosa*. Int J Mol Sci 22.
12. Su Y, Tang K, Liu J, Wang Y, Zheng Y, Zhang X-H. 2019. Quorum Sensing System of *Ruegeria mobilis* Rm01 Controls Lipase and Biofilm Formation. Front Microbiol 9:3304.
13. Duerkop BA, Varga J, Chandler JR, Peterson SB, Herman JP, Churchill MEA, Parsek MR, Nierman WC, Greenberg EP. 2009. Quorum-Sensing Control of Antibiotic Synthesis in *Burkholderia thailandensis*. J Bacteriol 191:3909–3918.
14. Beyersmann PG, Tomasch JJ, Son K, Stocker R, Göker M, Wagner-Döbler I, Simon M, Brinkhoff T. 2017. Dual function of tropodithietic acid as antibiotic and signaling molecule in global gene regulation of the probiotic bacterium *Phaeobacter inhibens*. Sci Rep 7:730.
15. Decho AW, Visscher PT, Ferry J, Kawaguchi T, He L, Przekop KM, Norman RS, Reid RP. 2009. Autoinducers extracted from microbial mats reveal a surprising diversity of *N* -acylhomoserine lactones (AHLs) and abundance changes that may relate to diel pH. Environ Microbiol 11:409–420.
16. Yoshida S, Ogawa N, Fujii T, Tsushima S. 2009. Enhanced biofilm formation and 3-chlorobenzoate degrading activity by the bacterial consortium of *Burkholderia* sp. NK8 and *Pseudomonas aeruginosa* PAO1. J Appl Microbiol 106:790–800.
17. Adnan M, Alshammari E, Patel M, Ashraf SA, Khan S, Hadi S. 2018. Significance and potential of marine microbial natural bioactive compounds against biofilms/biofouling: necessity for green chemistry. PeerJ 6:e5049.

18. Dang H, Lovell CR. 2016. Microbial Surface Colonization and Biofilm Development in Marine Environments. Microbiol Mol Biol Rev 80:91–138.
19. Rieusset L, Rey M, Muller D, Vacheron J, Gerin F, Dubost A, Comte G, Prigent-Combaret C. 2020. Secondary metabolites from plant-associated *Pseudomonas* are overproduced in biofilm. Microb Biotechnol 13:1562–1580.
20. Chandler JR, Heilmann S, Mittler JE, Greenberg EP. 2012. Acyl-homoserine lactone-dependent eavesdropping promotes competition in a laboratory co-culture model. ISME J 2012 612 6:2219–2228.
21. Dobretsov S, Teplitski M, Bayer M, Gunasekera S, Proksch P, Paul VJ. 2011. Inhibition of marine biofouling by bacterial quorum sensing inhibitors. 8:893-905.
22. Smalley NE, An D, Parsek MR, Chandler JR, Dandekar AA. 2015. Quorum sensing protects *Pseudomonas aeruginosa* against cheating by other species in a laboratory coculture model. J Bacteriol 197:3154–3159.
23. Smith AC, Rice A, Sutton B, Gabrilska R, Wessel AK, Whiteley M, Rumbaugh KP. 2017. Albumin inhibits *Pseudomonas aeruginosa* quorum sensing and alters polymicrobial interactions. Infect Immun 85:9.
24. Agogué H, Mallet C, Orvain F, De Crignis M, Mornet F, Dupuy C. 2014. Bacterial dynamics in a microphytobenthic biofilm: A tidal mesocosm approach. J Sea Res 92:36–45.
25. Ren D, Madsen JS, Sørensen SJ, Burmølle M. 2015. High prevalence of biofilm synergy among bacterial soil isolates in cocultures indicates bacterial interspecific cooperation. ISME J 9:81–89.
26. Quigley LNM, Edwards A, Steen AD, Buchan A, Fagervold SK. 2019. Characterization of the Interactive Effects of Labile and Recalcitrant Organic Matter on Microbial Growth and Metabolism. Front Microbiol 10:1–15.
27. de Souza RSC, Armanhi JSL, Arruda P. 2020. From Microbiome to Traits: Designing Synthetic Microbial Communities for Improved Crop Resiliency. Front Plant Sci 0:1179.
28. Wagner-Döbler I, Biebl H. 2006. Environmental biology of the marine Roseobacter lineage. Annu Rev Microbiol 60:255–280.
29. Buchan A, González JM, Chua MJ. 2019. Aerobic Hydrocarbon-Degrading Alphaproteobacteria: Rhodobacteraceae (Roseobacter), p. 93–104. *In* Taxonomy, Genomics and Ecophysiology of Hydrocarbon-Degrading Microbes. Springer International Publishing.
30. Kviatkovski I, Minz D. 2015. A member of the Rhodobacteraceae promotes initial biofilm formation via the secretion of extracellular factor(s). Aquat Microb Ecol 75:155–167.
31. González JM, Covert JS, Whitman WB, Henriksen JR, Mayer F, Scharf B, Schmitt R, Buchan A, Fuhrman JA, Kiene RP, Moran MA. 2003. *Silicibacter pomeroyi* sp. nov. and *Roseovarius nubinhibens* sp. nov., dimethylsulfoniopropionate-demethylating bacteria from marine environments. Int J Syst Evol Microbiol 53:1261–1269.
32. Cude WN, Prevatte CW, Hadden MK, May AL, Smith RT, Swain CL, Campagna SR, Buchan A. 2015. *Phaeobacter sp.* strain Y4I utilizes two separate cell-to-cell communication systems to regulate production of the antimicrobial indigoidine. Appl Environ Microbiol 81:1417–1425.
33. Armes AC, Buchan A. 2021. Cyclic di-GMP Is Integrated Into a Hierarchal Quorum Sensing Network Regulating Antimicrobial Production and Biofilm Formation in Roseobacter Clade Member Rhodobacterales Strain Y4I. Front Mar Sci 8:1–12.
34. Goslee SC, Urban DL. 2007. The ecodist Package for Dissimilarity-based Analysis of Ecological Data. J Stat Softw 22:1–19.
35. Jari Oksanen, Roeland Kindt, Solymos M, Henry H. Stevens, Helene Wagner. 2008. The vegan Package. 1.15-1.
36. Fisher RA, Corbet AS, Williams CB. 1943. The Relation Between the Number of

Species and the Number of Individuals in a Random Sample of an Animal Population. J Anim Ecol 12:42.
37. Hurlbert SH. 1971. The Nonconcept of Species Diversity: A Critique and Alternative Parameters. Ecology 52:577–586.
38. Buchan A, González JM, Moran MA. 2005. Overview of the marine *Roseobacter* lineage. Appl Environ Microbiol 71:5665–5677.
39. Bakenhus I, Dlugosch L, Billerbeck S, Giebel H-A, Milke F, Simon M. 2017. Composition of Total and Cell-Proliferating Bacterioplankton Community in Early Summer in the North Sea – Roseobacters Are the Most Active Component. Front Microbiol 0:1771.
40. Newton RJ, Griffin LE, Bowles KM, Meile C, Gifford S, Givens CE, Howard EC, King E, Oakley CA, Reisch CR, Rinta-Kanto JM, Sharma S, Sun S, Varaljay V, Vila-Costa M, Westrich JR, Moran MA. 2010. Genome characteristics of a generalist marine bacterial lineage. ISME J 4:784–798.
41. Buchan A, Neidle EL, Moran MA. 2004. Diverse Organization of Genes of the *B*-Ketoadipate Pathway in Members of the Marine Roseobacter Lineage. Appl Environ Microbiol 70:1658–68.
42. Frank AM, Chua MJ, Gulvik CA, Buchan A. 2018. Functional Redundancy in the Hydroxycinnamate Catabolism Pathways of the Salt Marsh Bacterium *Sagittula stellata* E-37. Appl Environ Microbiol 84.
43. Slightom RN, Buchan A. 2009. Surface colonization by marine roseobacters: integrating genotype and phenotype. Appl Environ Microbiol 75:6027–37.
44. Newton RJ, Griffin LE, Bowles KM, Meile C, Gifford S, Givens CE, Howard EC, King E, Oakley CA, Reisch CR, Rinta-Kanto JM, Sharma S, Sun S, Varaljay V, Vila-Costa M, Westrich JR, Moran MA. 2010. Genome characteristics of a generalist marine bacterial lineage. ISME J 2010 46 4:784–798.
45. Maglangit F, Yu Y, Deng H. 2021. Bacterial pathogens: threat or treat (a review on bioactive natural products from bacterial pathogens). Nat Prod Rep 38:782–821.
46. Valente RS, Nadal-Jimenez P, Carvalho AFP, Vieira FJD, Xavier KB. 2017. Signal Integration in Quorum Sensing Enables Cross-Species Induction of Virulence in *Pectobacterium wasabiae*. MBio 8.
47. May AL, Eisenhauer ME, Coulston KS, Campagna SR. 2012. Detection and quantitation of bacterial acylhomoserine lactone quorum sensing molecules via liquid chromatography-isotope dilution tandem mass spectrometry. Anal Chem 84:1243–1252.
48. Zimmer BL, May AL, Bhedi CD, Dearth SP, Prevatte CW, Pratte Z, Campagna SR, Richardson LL. 2014. Quorum sensing signal production and microbial interactions in a polymicrobial disease of corals and the coral surface mucopolysaccharide layer. PLoS One 9.
49. Liu W, Røder HL, Madsen JS, Bjarnsholt T, Sørensen SJ, Burmølle M. 2016. Interspecific Bacterial Interactions are Reflected in Multispecies Biofilm Spatial Organization. Front Microbiol 0:1366.
50. Lazdunski AM, Ventre I, Sturgis JN. 2004. Regulatory circuits and communication in gram-negative bacteria. Nat Rev Microbiol 2:581–592.
51. Galloway WRJD, Hodgkinson JT, Bowden SD, Welch M, Spring DR. 2010. Quorum Sensing in Gram-Negative Bacteria: Small-Molecule Modulation of AHL and AI-2 Quorum Sensing Pathways. Chem Rev 111:28–67.
52. Hawver LA, Jung SA, Ng W-L. 2016. Specificity and complexity in bacterial quorum-sensing systems. FEMS Microbiol Rev 40:738–52.
53. Leigh J, Fitter AH, Hodge A. 2011. Growth and symbiotic effectiveness of an arbuscular mycorrhizal fungus in organic matter in competition with soil bacteria. FEMS Microbiol Ecol 76:428–438.
54. Foster KR, Bell T. 2012. Competition, Not Cooperation, Dominates Interactions among

Culturable Microbial Species. Curr Biol 22:1845–1850.
55. Ratzke C, Barrere J, Gore J. 2020. Strength of species interactions determines biodiversity and stability in microbial communities. Nat Ecol Evol 4:376–383.
56. Lee KWK, Periasamy S, Mukherjee M, Xie C, Kjelleberg S, Rice SA. 2013. Biofilm development and enhanced stress resistance of a model, mixed-species community biofilm. ISME J 2014 84 8:894–907.

Appendix: Tables

Table 3.1. Table of community members, their *luxRI* homologous genetic loci, and putative AHLs produced by community members.

Species	LuxR gene locus	LuxI gene locus	Predominant AHLs (putative)
Sagittula stellata E-37	SSE37_11169[ac]	SSE37_11164[ac]	C_5-HSL; C_{12}-HSL; $3OHC_{10}$-HSL
	SSE37_06082[bc]		
Sulfitobacter sp. EE-36		EE36_01635[bc]	C_5-HSL; C_{12}-HSL
	EE36_03628[bc]		
Roseovarius nubinhibens ISM		ISM_03755[bc]	C_5-HSL; C_{12}-HSL; $3OHC_{10}$-HSL
	ISM_09921[bc]		
	ISM_15650[bc]		
Citreicella sp. SE45	CSE45_4055[ac]	CSE45_4054[ac]	C_5-HSL; C_{12}-HSL
	CSE45_1818[bc]		
Rhodobacterales strain Y4I	RBY4I_1689[ac]	RBY4I_3631[ac]	C_8-HSL[d]
	RBY4I_1027[ac]	RBY4I_3464[ac]	$3OHC_{12:1}$-HSL[d]
	RBY4I_896[bc]		

[a] Paired QS system, [b] Solo *luxR/luxI* (gray), [c]Cude et al., 2013, [d]Cude et. al 2015

Table 3.2. Factorial growth inhibition of synthetic community members.

	Inhibitor Organism						
Lawn	Y4I	†*clpA*::Tn5-Km^R	‡*igiD*::Tn5-Km^R	E-37	EE-36	ISM	SE45
Y4I	X	X	X	-	-	-	-
E-37	+	+	-	X	-	-	-
EE-36	+	+	-	-	X	-	-
ISM	+/-	-	-	-	-	X	-
SE45	-	-	-	-	-	-	X

(+) growth inhibition, (+/-) inconsistent growth inhibition, (-) no growth inhibition, (X) not tested;
†hyperpigmented Y4I variant, ‡indigoidine null Y4I variant

Appendix: Figures

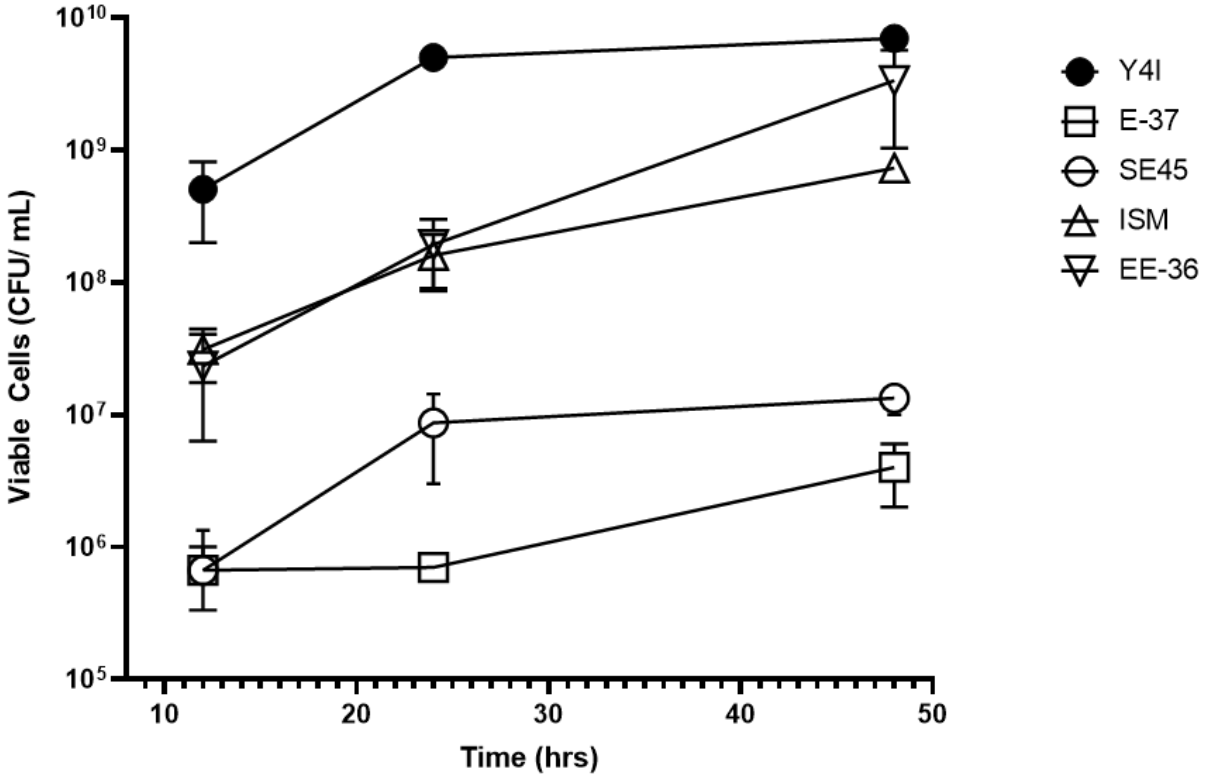

Figure 3.1. Surface colonization of Roseobacter strains to glass beads in a complex medium over 48 hrs. Viable cell abundance of five Roseobacter strains: Y4I (closed circles), E-37 (open squares), SE45 (open circles), ISM (open upward triangles), and EE-36 (open downward triangles). Cellular abundance at 0 hrs represents CFU/mL from liquid inoculum culture (seeding density ~ 10^8 cells mL^{-1}). Each data point represents the average of three biological replicates. Error bars represent the standard error of the mean. All cultures were statistically significant from Y4I at 24 hrs and 48 hrs except for EE36 which was only significantly different at 24 hrs (p <0.05). Y4I variants (not shown) were not significantly different from WT Y4I (**Supplemental Figure 3.1**). Two-way ANOVA for all strains used in this assay can be found in **Supplemental Table 3.3**.

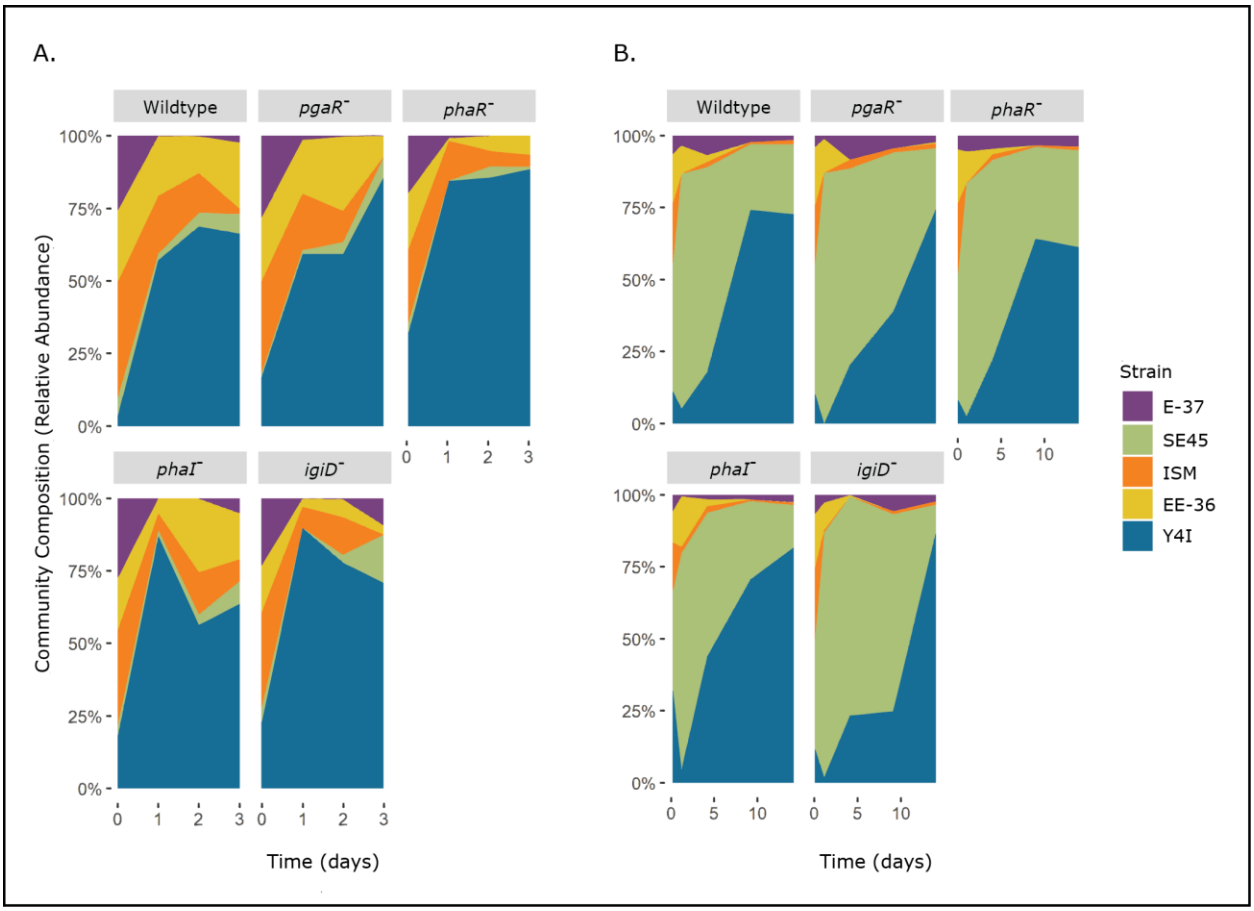

Figure 3.2. Relative abundance of community members over time of biofilms grown in a complex medium (A) and defined medium (B). Each synthetic community is designated by the Y4I variant included (gray boxes): Wild type Y4I, *pgaR*::Tn5-Km^{R} (*pgaR*$^{-}$), *phaR*::Tn5-Km^{R} (*phaR*$^{-}$), *phaI*::pKNOCK (*phaI*$^{-}$), *igiD*::Tn5-Km^{R} (*igiD*$^{-}$). Relative abundance was calculated from the mean CFU mL^{-1}count of at least six replicates for each strain within each mix and the total CFU mL^{-1}for each mix. Individual strains are color-coded in each mixture according to the key.

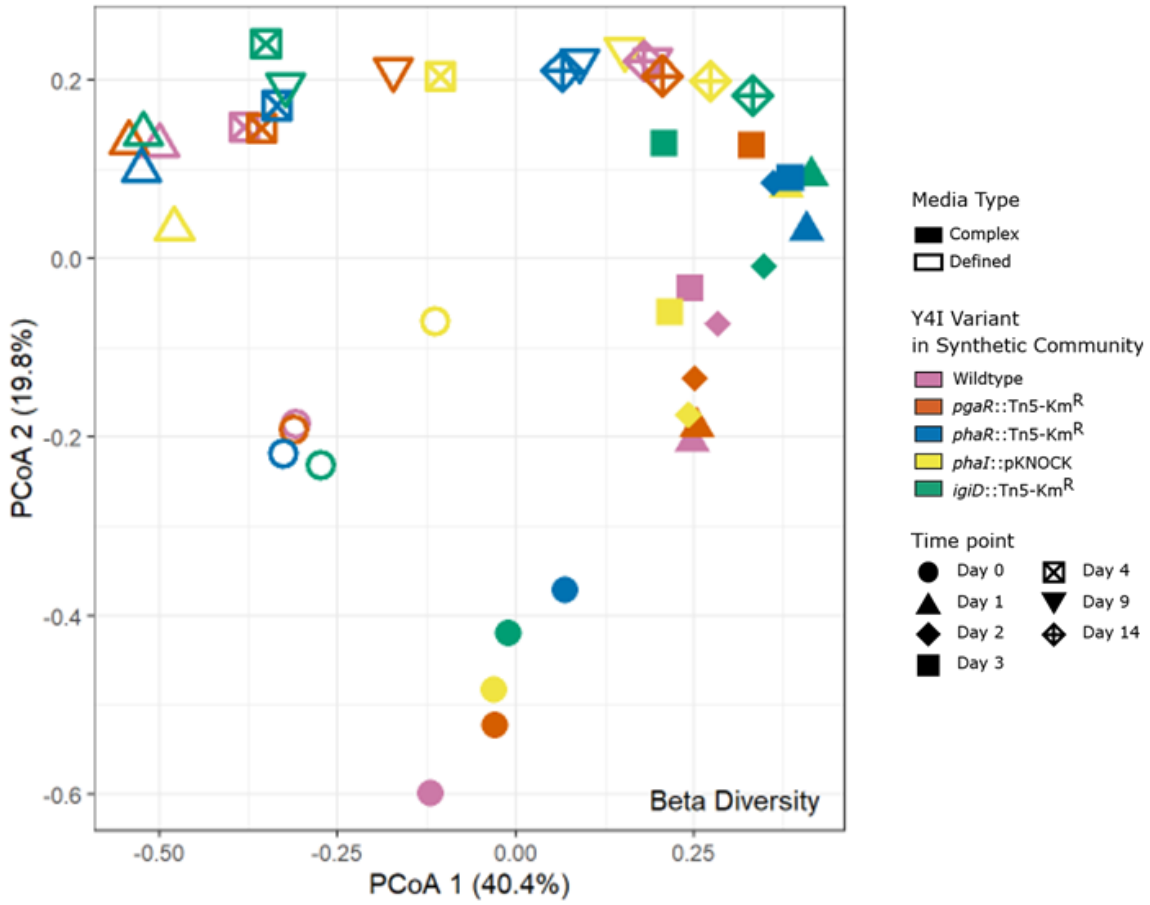

Figure 3.3. PCoA plot using Bray Curtis Dissimilarity Index to determine beta diversity between each carbon source, mixed community, and time point. Media type is denoted by closed (complex medium) and open shapes (defined medium), synthetic community harboring Y4I variants are differentiated by color, and time point is denoted by shape.

Figure 3.4 Biofilm production of monoculture community members and five-member synthetic communities in complex medium over time (A-C). Synthetic communities are designated by the Y4I variant in each community [Wild type Y4I, *pgaR*::Tn5-Km^R (*pgaR*$^-$), *phaR*::Tn5-Km^R (*phaR*$^-$), *phaI*::pKNOCK (*phaI*$^-$), *igiD*::Tn5-Km^R (*igiD*$^-$)]. Each data point (black dots) was collected by quantifying biomass production using a standard crystal violet assay. Error bars represent the standard error of the mean of three biological replicates and three technical replicates. Gray dotted line represents biomass production of the best biofilm former in monoculture, red dotted line indicates biomass production of the worst biofilm former in monoculture at that time point. Biologically relevant statistical significances are depicted ($p < 0.05$ [*], 0.01 [**], 0.001 [***]). For full statistical results see Supplemental Table 1.

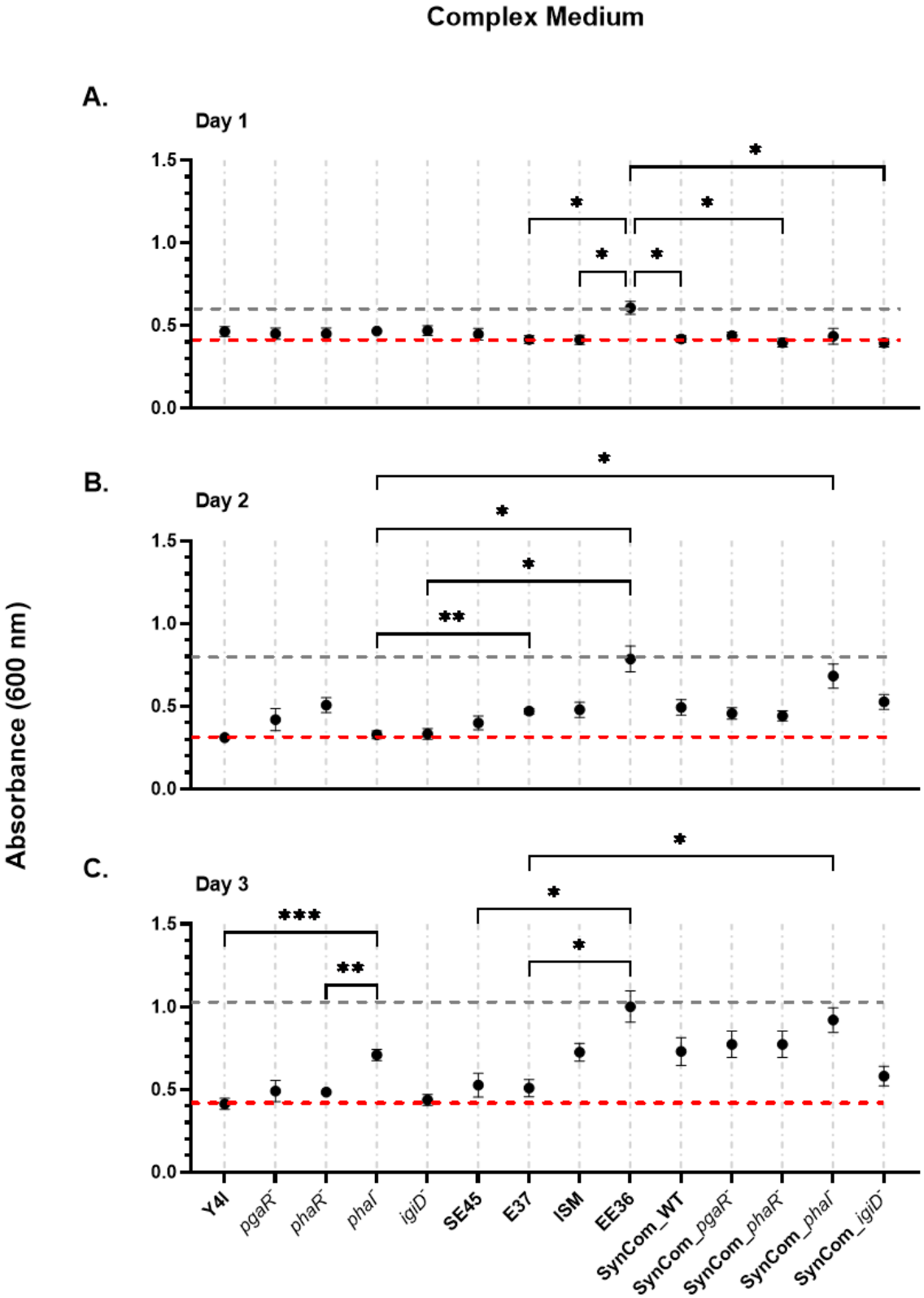
Complex Medium
A.
Day 1
B.
Day 2
C.
Day 3
Absorbance (600 nm)
1.5
1.0
0.5
0.0
*
**
***
Y4I
pgaR⁻
phaR⁻
phaI⁻
igiD⁻
SE45
E37
ISM
EE36
SynCom_WT
SynCom_pgaR⁻
SynCom_phaR⁻
SynCom_phaI⁻
SynCom_igiD⁻
Cultures

Figure 3.5 Biofilm production of monoculture community members and five-member synthetic communities in defined medium over time (A-D). Synthetic communities are designated by the Y4I variant in each [Wild type Y4I, *pgaR*::Tn5-Km^R (*pgaR*$^-$), *phaR*::Tn5-Km^R (*phaR*$^-$), *phaI*::pKNOCK (*phaI*$^-$), *igiD*::Tn5-Km^R (*igiD*$^-$)]. Each data point (black dots) was collected by quantifying biomass production using a standard crystal violet assay for at least 6 replicates for mixed and monocultures. Error bars represent the standard error of the mean. Gray dotted line represents biomass production of the best biofilm former in monoculture, red dotted line indicates biomass production of the worst biofilm former in monoculture at that time point. Asterisks represent statistical significance between cultures ($p < 0.05$ [*], 0.01 [**]). ANOVA table of significance can be found in Supplemental Table 2.

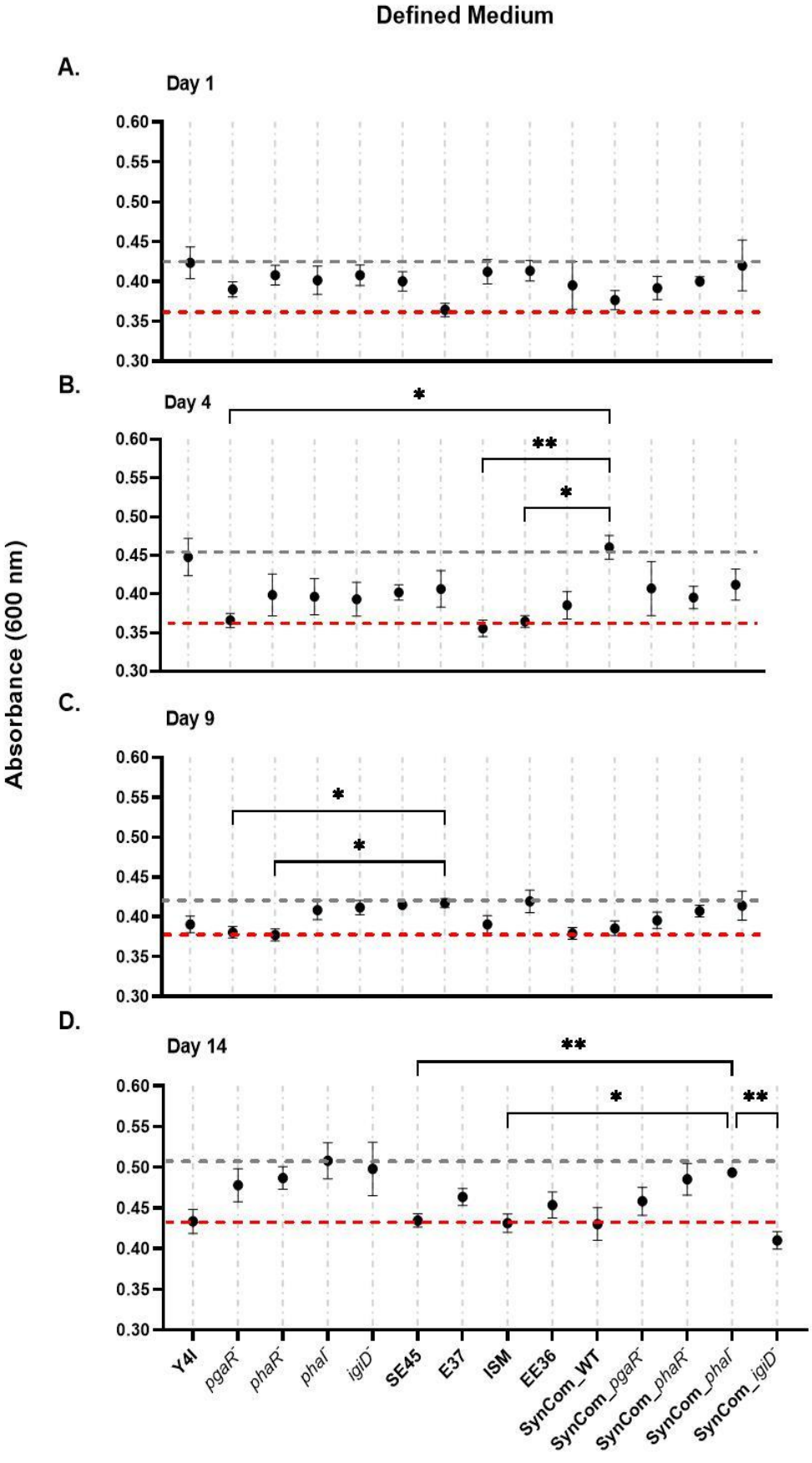
Defined Medium
A.
Day 1
B.
Day 4
C.
Day 9
D.
Day 14
Absorbance (600 nm)
0.60
0.55
0.50
0.45
0.40
0.35
0.30
*
**
*
*
*
**
*
**
Y4I
pgaR⁻
phaR⁻
phaI⁻
igiD⁻
SE45
E37
ISM
EE36
SynCom_WT
SynCom_pgaR⁻
SynCom_phaR⁻
SynCom_phaI⁻
SynCom_igiD⁻
Cultures

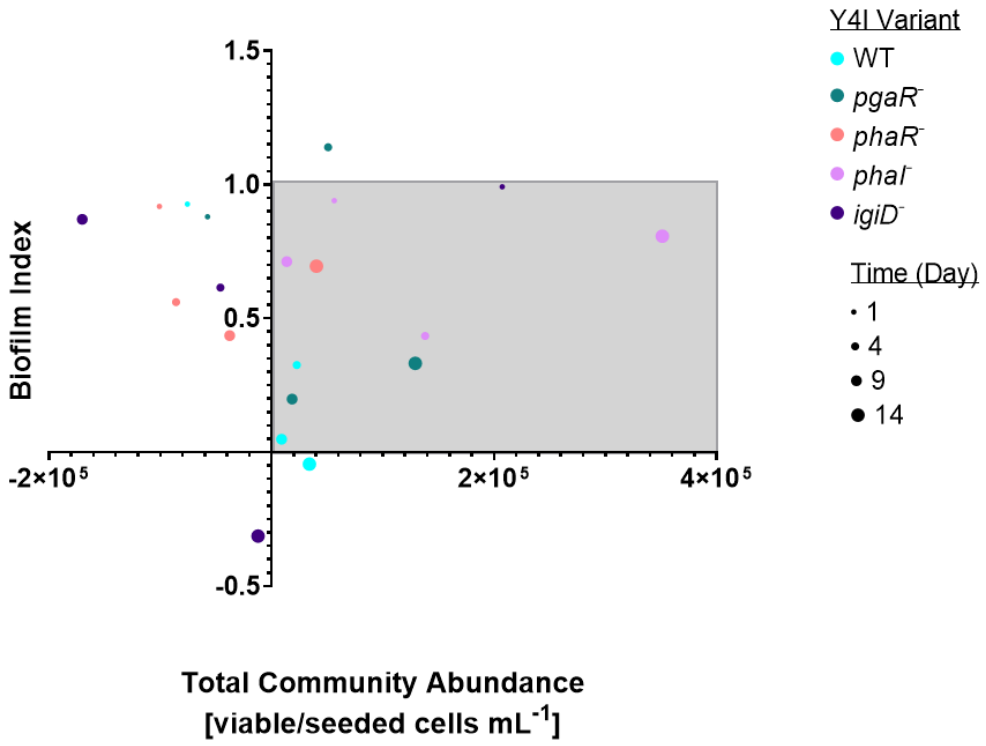

Figure 3.6 Biofilm production index of synthetic communities harboring Y4I variants in defined medium over time. Y4I variants within communities are color coded according to the legend and time point at which data was extracted varies by size of dots. Each data point represents the average of at least 6 replicates. Communities outside of gray box indicate greatest evidence for community cooperation or competition depending on Y4I variant included over time.

Appendix: Supplemental Materials

Supplemental Table 3.1 Two-way ANOVA Table for crystal violet assay performed for biofilm formation in complex medium (20% YTSS) by day.

Tukey's multiple comparisons test	**Mean Diff.**	**95.00% CI of diff.**	**Adjusted P Value**	**Mean 1**	**Mean 2**	**SE of diff.**	**N1**	**N2**	**q**	**DF**
Day 1										
E37 vs. EE36	-0.1922	-0.3796 to -0.004875	0.042	0.4156	0.6078	0.04684	9	9	5.804	13.72
ISM vs. EE36	-0.1933	-0.3847 to -0.001955	0.0466	0.4144	0.6078	0.04828	9	9	5.664	14.47
EE36 vs. SynComm_Y4I	0.1889	0.007154 to 0.3706	0.0389	0.6078	0.4189	0.04442	9	9	6.013	12.13
EE36 vs. SynComm_phaR	0.2111	0.02332 to 0.3989	0.0215	0.6078	0.3967	0.04701	9	9	6.351	13.81
EE36 vs. SynComm_igiD	0.2122	0.02550 to 0.3989	0.0199	0.6078	0.3956	0.0466	9	9	6.44	13.58
Day 2										
Y4I vs. E37	-0.16	-0.2667 to -0.05333	0.0015	0.31	0.47	0.02713	9	9	8.342	15.22
Y4I vs. EE36	-0.476	-0.8606 to -0.09151	0.0166	0.31	0.786	0.08122	9	7	8.288	6.885
Y4I vs. SynComm_phaI	-0.3726	-0.7144 to -0.03087	0.031	0.31	0.6826	0.07614	9	8	6.921	8.181
Y4I vs. SynComm_igiD	-0.2164	-0.4262 to -0.006622	0.0415	0.31	0.5264	0.04932	9	8	6.205	10.09

Supplemental Table 3.1 Continued

Tukey's multiple comparisons test	**Mean Diff.**	**95.00% CI of diff.**	**Adjusted P Value**	**Mean 1**	**Mean 2**	**SE of diff.**	**N1**	**N2**	**q**	**DF**
phaI::pKNOCK vs. E37	-0.1422	-0.2550 to -0.02941	0.0081	0.3278	0.47	0.02852	9	9	7.052	14.68
phaI::pKNOCK vs. EE36	-0.4583	-0.8422 to -0.07428	0.02	0.3278	0.786	0.0817	9	7	7.932	7.038
phaI::pKNOCK vs. SynComm_phaI	-0.3549	-0.6966 to -0.01314	0.0407	0.3278	0.6826	0.07665	9	8	6.547	8.382
igiD::TN5-KmR vs. EE36	-0.4527	-0.8352 to -0.07015	0.0194	0.3333	0.786	0.08487	9	7	7.544	8.06
igiD::TN5-KmR vs. SynComm_igiD	-0.3493	-0.6928 to -0.005849	0.0453	0.3333	0.6826	0.08001	9	8	6.174	9.707
SE45 vs. EE36	-0.386	-0.7708 to -0.001222	0.0491	0.4	0.786	0.0886	9	7	6.162	9.255
Day 3										
Y4I vs. phaI::pKNOCK	-0.2956	-0.4814 to -0.1097	0.0007	0.4133	0.7089	0.04763	9	9	8.776	15.98
Y4I vs. ISM	-0.3122	-0.5643 to -0.06010	0.0101	0.4133	0.7256	0.06276	9	9	7.036	13.38
Y4I vs. EE36	-0.5878	-1.014 to -0.1620	0.0058	0.4133	1.001	0.09978	9	9	8.331	9.952
Y4I vs. SynComm_phaI	-0.5067	-0.8480 to -0.1653	0.0028	0.4133	0.92	0.08183	9	9	8.756	11.02

Supplemental Table 3.1 Continued

Tukey's multiple comparisons test	**Mean Diff.**	**95.00% CI of diff.**	**Adjusted P Value**	**Mean 1**	**Mean 2**	**SE of diff.**	**N1**	**N2**	**q**	**DF**
pgaR::TN5-KmR vs. EE36	-0.5108	-0.9654 to -0.05628	0.0216	0.4903	1.001	0.1136	8	9	6.357	13.72
pgaR::TN5-KmR vs. SynComm_phaI	-0.4297	-0.8175 to -0.04190	0.0235	0.4903	0.92	0.09826	8	9	6.185	14.87
phaR::TN5-KmR vs. phaI::pKNOCK	-0.2244	-0.3820 to -0.06691	0.0036	0.4844	0.7089	0.03831	9	9	8.285	11.82
phaR::TN5-KmR vs. ISM	-0.2411	-0.4819 to -0.0003386	0.0496	0.4844	0.7256	0.05602	9	9	6.087	9.656
phaR::TN5-KmR vs. EE36	-0.5167	-0.9411 to -0.09222	0.0158	0.4844	1.001	0.09568	9	9	7.636	8.536
phaR::TN5-KmR vs. SynComm_phaI	-0.4356	-0.7729 to -0.09816	0.0105	0.4844	0.92	0.07679	9	9	8.022	8.847
phaI::pKNOCK vs. igiD::TN5-KmR	0.2722	0.08707 to 0.4574	0.0017	0.7089	0.4367	0.04743	9	9	8.117	15.97
igiD::TN5-KmR vs. ISM	-0.2889	-0.5406 to -0.03714	0.0186	0.4367	0.7256	0.06261	9	9	6.525	13.31
igiD::TN5-KmR vs. EE36	-0.5644	-0.9901 to -0.1387	0.0078	0.4367	1.001	0.09969	9	9	8.008	9.92
igiD::TN5-KmR vs. SynComm_phaI	-0.4833	-0.8245 to -0.1422	0.0041	0.4367	0.92	0.08172	9	9	8.364	10.97

Supplemental Table 3.1 Continued

Tukey's multiple comparisons test	**Mean Diff.**	**95.00% CI of diff.**	**Adjusted P Value**	**Mean 1**	**Mean 2**	**SE of diff.**	**N1**	**N2**	**q**	**DF**
SE45 vs. EE36	-0.4744	-0.9414 to -0.007484	0.0447	0.5267	1.001	0.1184	9	9	5.665	14.96
E37 vs. EE36	-0.4922	-0.9293 to -0.05515	0.0221	0.5089	1.001	0.1073	9	9	6.488	12.4
E37 vs. SynComm_phaI	-0.4111	-0.7724 to -0.04982	0.0194	0.5089	0.92	0.09085	9	9	6.4	14.19

Supplemental Table 3.2 Two-way ANOVA Table for crystal violet assay performed for biofilm formation in defined medium (coumarate) by day.

Tukey's multiple comparisons test	**Mean Diff.**	**95.00% CI of diff.**	**Adjusted P Value**	**Mean 1**	**Mean 2**	**SE of diff.**	**N1**	**N2**	**q**	**DF**
D4										
pgaR::Tn5-Km^R vs. SynComm_pgaR	-0.09458	-0.1742 to -0.01500	0.0185	0.3658	0.4603	0.01783	8	6	7.501	8.353
ISM vs. SynComm_pgaR	-0.105	-0.1855 to -0.02446	0.0091	0.3553	0.4603	0.01871	9	6	7.937	9.592
EE36 vs. SynComm_pgaR	-0.09583	-0.1750 to -0.01665	0.018	0.3645	0.4603	0.0171	8	6	7.926	7.367
D9										
pgaR::Tn5-Km^R vs. E37	-0.03667	-0.07252 to -0.0008163	0.0427	0.3805	0.4171	0.009063	9	8	5.721	14.67
phaR::Tn5-Km^R vs. E37	-0.04	-0.07816 to -0.001835	0.0364	0.3771	0.4171	0.009449	8	8	5.987	12.98
D14										
phaR::Tn5-Km^R vs. MixE	0.07667	0.005380 to 0.1480	0.0304	0.4867	0.41	0.01765	9	6	6.142	13
SE45 vs. SynComm_phaI	-0.05889	-0.09902 to -0.01876	0.0024	0.4344	0.4933	0.009904	9	6	8.409	12.75

Supplemental Table 3.2 Continued

Tukey's multiple comparisons test	**Mean Diff.**	**95.00% CI of diff.**	**Adjusted P Value**	**Mean 1**	**Mean 2**	**SE of diff.**	**N1**	**N2**	**q**	**DF**
ISM vs. SynComm_phaI	-0.06222	-0.1142 to -0.01020	0.0148	0.4311	0.4933	0.01254	9	6	7.015	11.33
SynComm_phaI vs. SynComm_igiD	0.08333	0.02655 to 0.1401	0.0057	0.4933	0.41	0.01229	6	6	9.587	7.429

Supplemental Table 3.3 Two-way ANOVA Table for surface attachment assays performed over 48 hrs in complex medium (20% YTSS) by hour.

Dunnett's multiple comparisons test	**Mean Diff.**	**95.00% CI of diff.**	**Adjusted P Value**	**Mean 1**	**Mean 2**	**SE of diff.**	**N1**	**N2**	**q**	**DF**
12 hrs										
Y4I vs. pgaR::Tn5-Km^R	-1.6E+09	-3458942107 to 185608773	0.0705	5.07E+08	2.14E+09	4.2E+08	3	3	3.897	3.982
Y4I vs. phaR::Tn5-Km^R	1.67E+08	-1574661098 to 1907994431	0.9952	5.07E+08	3.4E+08	3.59E+08	3	3	0.4646	3.293
Y4I vs. phaI::pKNOCK	2E+08	-1635066898 to 2035066898	0.9812	5.07E+08	3.07E+08	3.38E+08	3	3	0.5915	2.818
Y4I vs. igiD::Tn5-Km^R	3.57E+08	-1695030280 to 2408363613	0.8026	5.07E+08	1.5E+08	3.19E+08	3	3	1.118	2.322
Y4I vs. SE45	5.06E+08	-1808069364 to 2820069364	0.5854	5.07E+08	666667	3.07E+08	3	3	1.649	2
Y4I vs. E37	5.06E+08	-1808084299 to 2820084299	0.5854	5.07E+08	666667	3.07E+08	3	3	1.649	2
Y4I vs. ISM	4.76E+08	-1830219916 to 2781553250	0.6231	5.07E+08	31000000	3.07E+08	3	3	1.548	2.008
Y4I vs. EE36	4.83E+08	-1817896975 to 2784563641	0.6136	5.07E+08	23333333	3.07E+08	3	3	1.573	2.012

Supplemental Table 3.3 Continued

Dunnett's multiple comparisons test	**Mean Diff.**	**95.00% CI of diff.**	**Adjusted P Value**	**Mean 1**	**Mean 2**	**SE of diff.**	**N1**	**N2**	**q**	**DF**
24 hrs										
Y4I vs. pgaR::Tn5-Km^R	3.33E+08	-2964783912 to 3631450579	0.9931	5E+09	4.67E+09	6.67E+08	3	3	0.5	3.2
Y4I vs. phaR::Tn5-Km^R	3.33E+08	-2964783912 to 3631450579	0.9931	5E+09	4.67E+09	6.67E+08	3	3	0.5	3.2
Y4I vs. phaI::Tn5-Km^R	1.5E+09	-8719300922 to 11719300922	0.9026	5E+09	3.5E+09	1.71E+09	3	3	0.8783	2.508
Y4I vs. igiD::Tn5-Km^R	2.47E+09	-5367326110 to 10300659444	0.5236	5E+09	2.53E+09	1.42E+09	3	3	1.736	2.762
Y4I vs. SE45	4.99E+09	638530539 to 9344136128	0.0384	5E+09	8666667	5.77E+08	3	3	8.645	2
Y4I vs. E37	5E+09	645733008 to 9352866992	0.0383	5E+09	700000	5.77E+08	3	3	8.659	2
Y4I vs. ISM	4.84E+09	598039490 to 9081960510	0.0385	5E+09	1.6E+08	5.82E+08	3	3	8.322	2.059
Y4I vs. EE36	4.81E+09	696808109 to 8916525224	0.0363	5E+09	1.93E+08	5.87E+08	3	3	8.185	2.138

Supplemental Table 3.3 Continued

Dunnett's multiple comparisons test	**Mean Diff.**	**95.00% CI of diff.**	**Adjusted P Value**	**Mean 1**	**Mean 2**	**SE of diff.**	**N1**	**N2**	**q**	**DF**
48 hrs										
Y4I vs. pgaR::Tn5-Km^R	4E+09	-1712506639 to 9712506639	0.1292	7E+09	3E+09	1.15E+09	3	3	3.464	3.2
Y4I vs. phaR::Tn5-Km^R	4E+09	-353567306 to 8353567306	0.0588	7E+09	3E+09	5.77E+08	3	3	6.928	2
Y4I vs. phaI::Tn5-Km^R	2.33E+09	-964783912 to 5631450579	0.1259	7E+09	4.67E+09	6.67E+08	3	3	3.5	3.2
Y4I vs. igiD::Tn5-Km^R	1.33E+09	-6768050708 to 9434717375	0.8893	7E+09	5.67E+09	1.45E+09	3	3	0.9177	2.725
Y4I vs. SE45	6.99E+09	2633363954 to 11339969379	0.0199	7E+09	13333333	5.77E+08	3	3	12.1	2
Y4I vs. E37	7E+09	2642527953 to 11349472047	0.0198	7E+09	4000000	5.77E+08	3	3	12.12	2
Y4I vs. ISM	6.27E+09	2014152884 to 10519180449	0.0231	7E+09	7.33E+08	5.81E+08	3	3	10.78	2.053
Y4I vs. EE36	3.63E+09	-12341969691 to 19608636358	0.6301	7E+09	3.37E+09	2.4E+09	3	3	1.513	2.244

Supplemental Table 3.4 PERMANOVA on all mixed communities for all time points on either a complex carbon source or a minimal carbon source.

Variable	Df	SumsOfSqs	MeanSqs	F.Model	R2	Pr(>F)
carbon	1	2.4154	2.4154	56.12	0.37274	0.000666
time_point	1	1.898	1.89799	44.099	0.29289	0.000666
syn_comm	1	0.0427	0.04273	0.993	0.00659	0.389074
carbon:time_point	1	0.4817	0.48169	11.192	0.07433	0.000666
carbon: syn_comm	1	0.0381	0.03808	0.885	0.00588	0.41439
time_point: syn_comm	1	0.0075	0.00754	0.175	0.00116	0.84477
carbon:time_point: syn_comm	1	0.0042	0.00421	0.098	0.00065	0.896736
Residuals	37	1.5925	0.04304	0.24575		
Total	44	6.4801	1			

Supplemental Table 3.5 PERMANOVA on all mixed communities for the Day 0 time point on either a complex or a minimal carbon source.

Variable	Df	SumsOfSqs	MeanSqs	F.Model	R2	Pr(>F)
carbon	1	0.39274	0.39274	33.475	0.804	0.002665
syn_comm	1	0.02636	0.02636	2.247	0.05396	0.154564
carbon:syn_comm	1	-0.00101	-0.00101	-0.086	-0.00207	0.974017
Residuals	6	0.07039	0.01173	0.14411		
Total	9	0.48848	1			

Supplemental Table 3.6 PERMANOVA on all mixed communities for the Day 1 time point on either a complex or a minimal carbon source.

Variable	Df	SumsOfSqs	MeanSqs	F.Model	R2	Pr(>F)
carbon	1	1.90778	1.90778	361.01	0.94121	0.001332
syn_comm	1	0.0325	0.0325	6.15	0.01604	0.04064
carbon: syn_comm	1	0.05495	0.05495	10.4	0.02711	0.021319
Residuals	6	0.03171	0.00528	0.01564		
Total	9	2.02694	1			

Supplemental Table 3.7 PERMANOVA on all mixed communities for the paired Day 2/Day 9 time point on either a complex or a minimal carbon source.

Variable	Df	SumsOfSqs	MeanSqs	F.Model	R2	Pr(>F)
carbon	1	0.42584	0.42584	12.4807	0.62754	0.001332
syn_comm	1	0.01813	0.01813	0.5314	0.02672	0.536309
carbon: syn_comm	1	0.0299	0.0299	0.8763	0.04406	0.41439
Residuals	6	0.20472	0.03412	0.30168		
Total	9	0.67859	1			

Supplemental Table 3.8 PERMANOVA on all mixed communities for the paired Day 3/Day 14 time point on either a complex or a minimal carbon source.

Variable	Df	SumsOfSqs	MeanSqs	F.Model	R2	Pr(>F)
carbon	1	0.057908	0.057908	3.7557	0.32038	0.03464
syn_comm	1	0.00662	0.00662	0.4293	0.03662	0.74684
carbon: syn_comm	1	0.023706	0.023706	1.5374	0.13115	0.26249
Residuals	6	0.092513	0.015419	0.51184		
Total	9	0.180746	1			

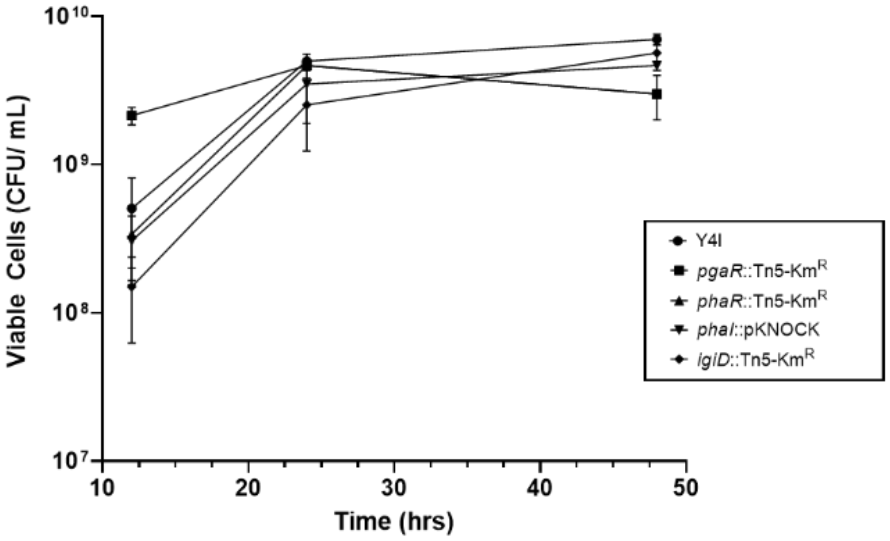

Supplemental Figure 3.1 Surface colonization of Y4I variants as they colonize a glass bead in complex medium over time. Viable cell abundance of wildtype Y4I (circles), *pgaR*::Tn5-Km^R (squares), *phaR*::Tn5-Km^R (upward triangles), *phaI*::pKNOCK (downward triangles), and *igiD*::Tn5-Km^R (diamonds) was assessed. Each data point represents the average of three biological replicates. Error bars represent the standard error from the mean.

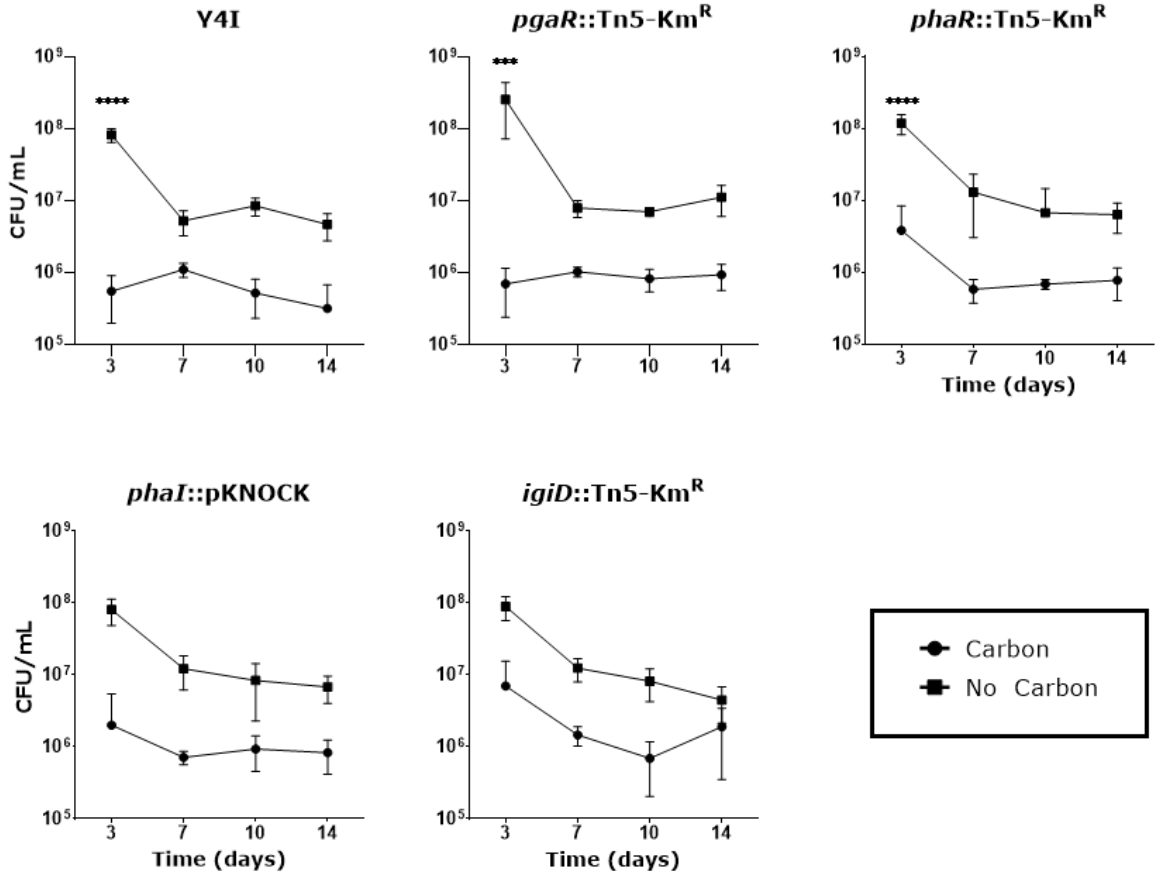

Supplemental Figure 3.2 Y4I variants in liquid cultures in the presence of carbon (2 mM coumarate - circles) and no carbon (squares). Y4I variants in liquid cultures in the presence of carbon (2 mM coumarate - circles) and no carbon (squares). Each data point represents the average of three replicates. Error bars represent standard deviation of the mean. Asterisks represent statistical significance [**** (p < 0.0001), *** (p < 0.005)] using a two-way ANOVA with Sidak's multiple comparisons test as a post hoc test. Inclusion of carbon was significantly different from no carbon control in all analyses (p < 0.01).

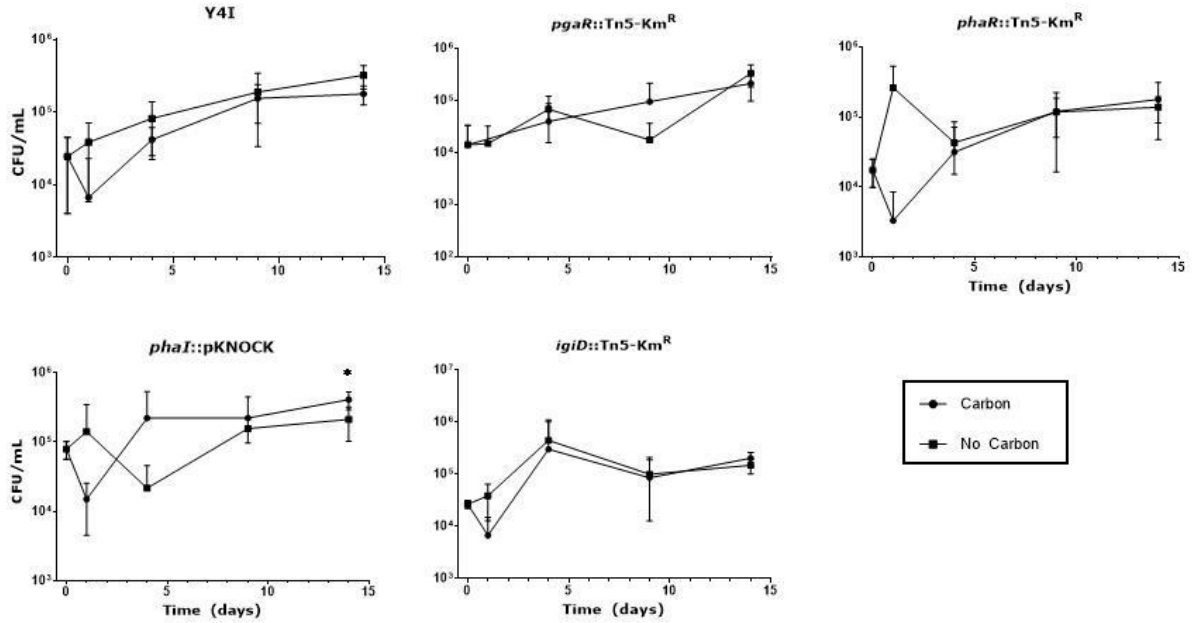

Supplemental Figure 3.3 Synthetic mixed biofilm cultures containing Y4I variants (labelled above respective graph) in the presence of carbon (2 mM coumarate - circles) and no carbon (squares). Each data point represents the average of three replicates. Error bars represent standard deviations. Asterisks represent statistical significance ($p < 0.05$) with a two-way ANOVA using Tukey's HSD test as post hoc tests.

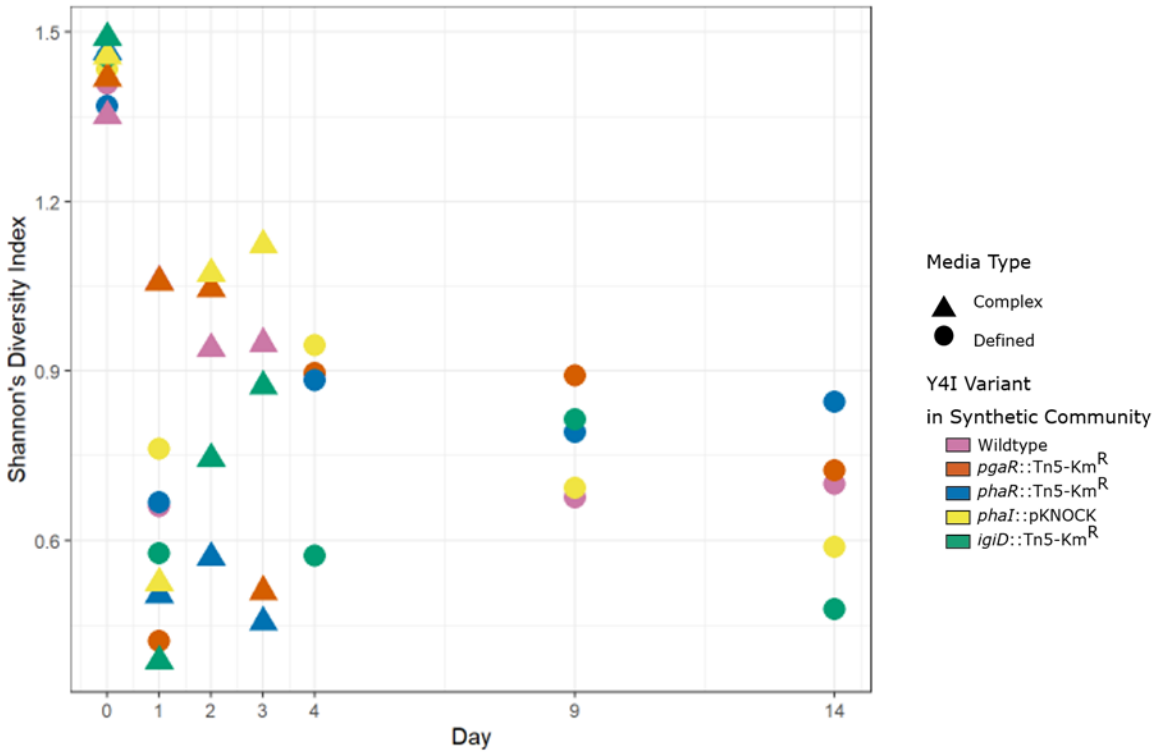

Supplemental Figure 3.4 Shannon's Diversity Index for all synthetic communities at each time point based on viable cell counts. Synthetic communities are denoted by color and carbon source (complex or defined/minimal) are designated by triangles or circles, respectively.

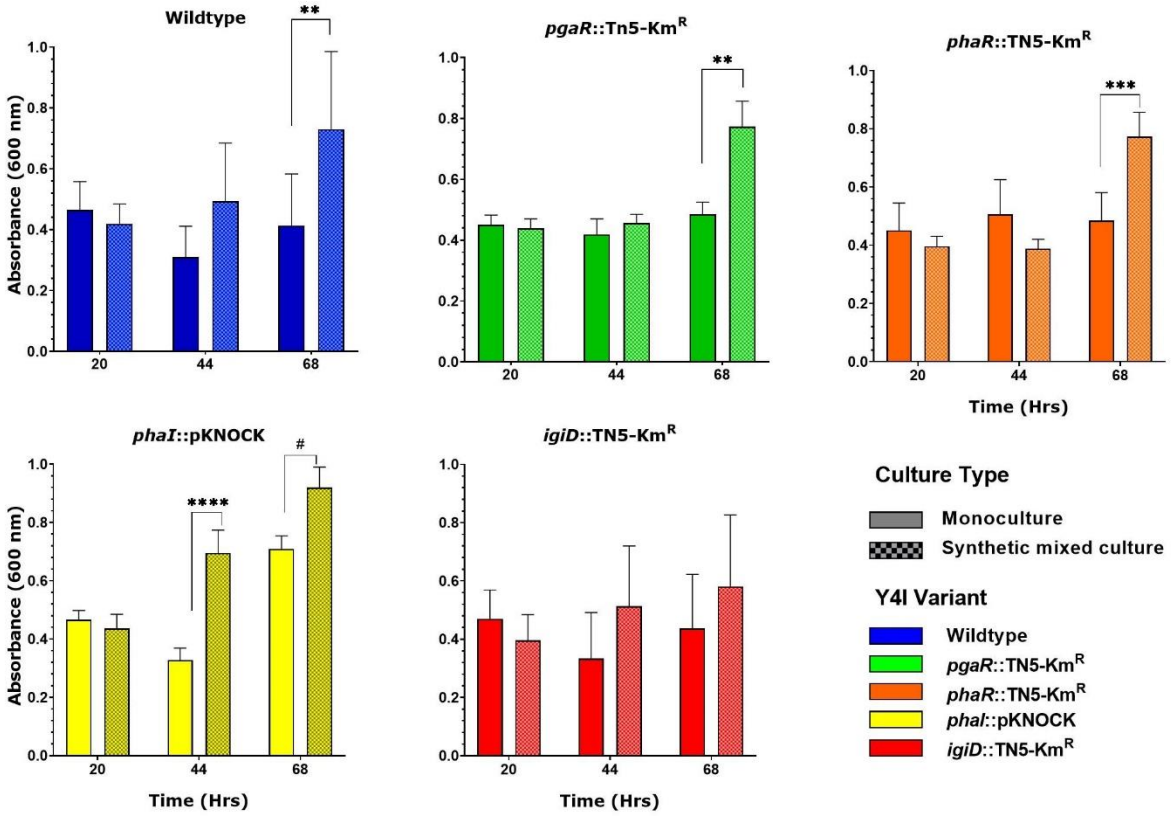

Supplemental Figure 3.5 Biofilm production on glass beads from Y4I variants in complex medium over time for monoculture (solid colors) and synthetic mixed cultures (patterned) as determined by crystal violet assay. Data is representative of the mean of three biological and three technical replicates. Error bars represent the standard deviation from the mean. Asterisks denote statistical significance at $p < 0.01$ (**), 0.001 (***), 0.0001 (****). Octothrope represents significance at $p < 0.1$.

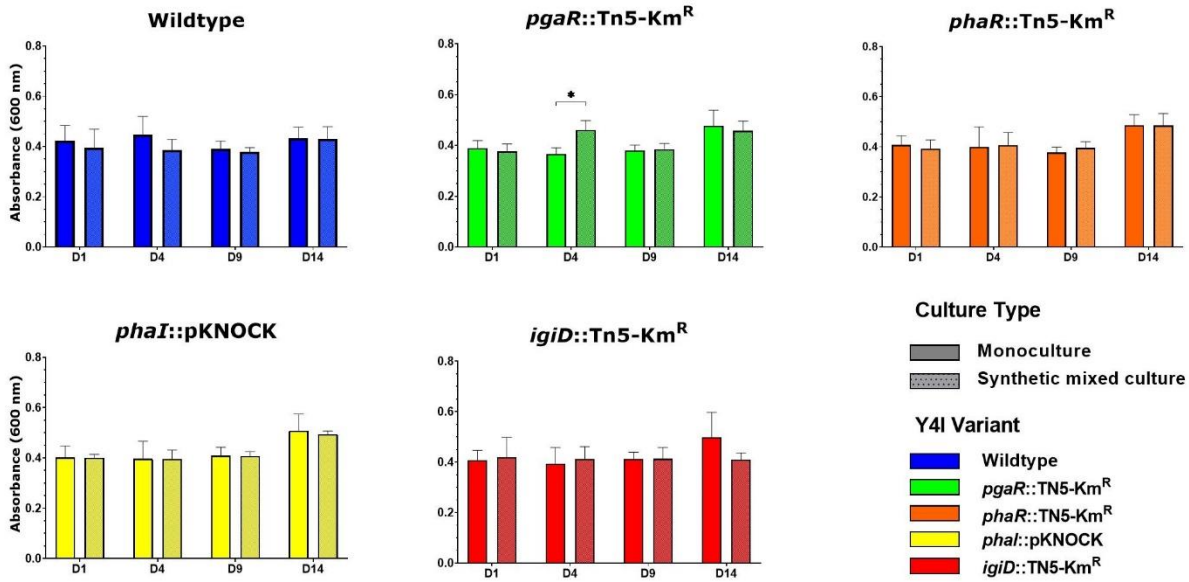

Supplemental Figure 3.6 Biofilm production on glass beads from Y4I variants in defined medium over time for monoculture (solid colors) and synthetic mixed cultures (patterned) as determined by crystal violet assay. Data is representative of the mean of three biological and three technical replicates. Error bars represent the standard deviation from the mean. Asterisks denote statistical significance at $p < 0.05$ (*).

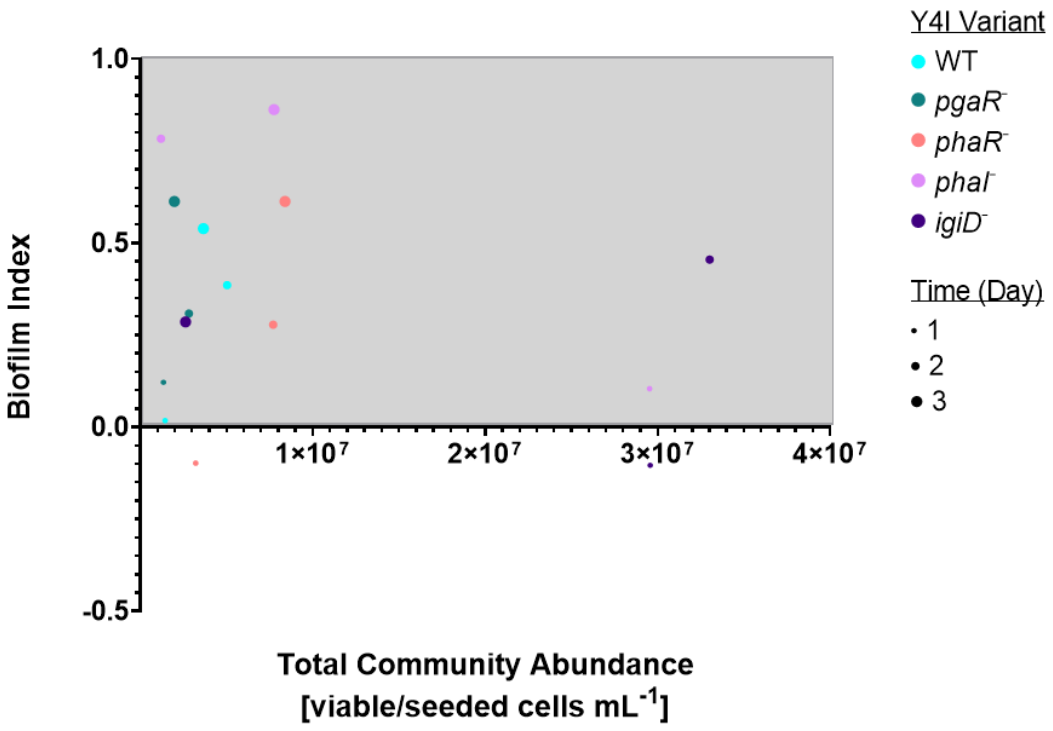

Supplemental Figure 3.7 Biofilm production index of synthetic communities harboring Y4I variants in complex medium. Y4I variants within communities are color coded according to the legend and time point at which data was extracted varies by size of dots. Each data point represents the average of 9 replicates. Communities outside of gray box indicate greatest evidence for community cooperation or competition depending on Y4I variant included over time.

Chapter 4 : QUORUM SENSING IN ROSEOBACTERS: CLADE SPECIFIC ROSEOBOX IDENTIFIES GENES LIKELY REGULATED BY QUORUM SENSING.

This chapter was written by April C. Armes, Taylor M. Royalty, and Alison Buchan and is intended to be submitted for publication.

A.C.A and T.M.R. designed the bioinformatic workflow, performed analysis, and wrote the manuscript. Specifically, A.C.A retrieved the sequences, utilized MSA and phylogenetic relatedness to narrow the sequences. T.R. generated motifs, modeled the motif to increase confidence, ran motifs against individual genomes. A.C.A. and T.R. analyzed the results and wrote the manuscript. A.B. edited the manuscript. All authors contributed equally to this project.

I. Abstract

Bacterial cell-to-cell communication, or quorum sensing (QS) mediates bacterial social behaviors, such as biofilm formation; antimicrobial production; metabolism; and SOS response, that are beneficial to the microbial community. Quorum sensing regulatory networks are complex and in the simplest of systems involve transcriptional regulators, signaling molecules and their synthases, as well as cis-acting elements such as DNA binding sites. These DNA binding regions are short, palindromic sequences often referred to as 'boxes'. This type of QS system is present in Proteobacteria and was first described in the Gamma-proteobacterium Vibrio fischeri. A prevalent class of signaling molecule among Proteobacteria are N-acylhomoserine lactones (AHLs). AHLs, produced by their cognate synthases (luxI homologs) bind to their cognate transcriptional regulators (LuxR homologs), creating a LuxR-AHL complex. This activated LuxR then binds to a cis-acting site in the DNA to facilitate transcription of downstream genes. Model QS bacteria have been well characterized in regards to their transcriptional elements and 'boxes'. Despite the abundance of QS features found in members of the Roseobacter clade of marine Alpha-proteobacteria, little work has been done to characterize a QS box and subsequently regulated genes. As a first attempt to generate a clade specific DNA regulatory motif, termed 'roseo box', we focused on the Phaeobacter-Leisingera sister clades recently identified by core-genome sequencing. We isolated the intergenic region between LuxRI homologs from 30 Phaeobacter-Leisingera genomes and found conserved elements indicative of LuxR binding sites. We then surveyed these Phaeobacter-Leisingera genomes for matches to roseo box motifs and found genes putatively regulated by QS. This initial analysis into QS regulated motifs within the Roseobacter clade provides gene candidates involved in biofilm formation, SOS response, antimicrobial resistance, and metabolism worthy of future investigation.

II. Introduction

Bacterial cell-to-cell communication regulates essential behaviors: from monitoring environmental conditions to regulating social behaviors (1). This type of cell-to-cell communication is often referred to as quorum sensing (QS) as it depends on the concentration of small, diffusible signaling molecules known as autoinducers (AI). Local concentrations of AIs elicit a quorum by binding to their cognate transcriptional regulators (denoted by -*R*) and facilitate population level responses. Gram negative bacteria typically use AIs such as acylhomoserine lactones (AHLs). AHL-based quorum sensing involves a two-component regulatory system: AHL synthases (LuxI homologs) produce the signaling molecules which then bind to transcriptional regulators, belonging to the LuxR family of transcriptional regulators. Once bound to its cognate AI, the LuxR-AI protein complex binds to a regulatory DNA sequence, often in proximity to the sigma 70 promoter region (2–4). This regulatory DNA element has been previously termed the "lux box" and was first identified in *Vibrio fischeri* (5). While AHL-based QS has been well studied in the *V. fischeri* model system (6), as well as human pathogen models such as *Pseudomonas aeruginosa* (7) relatively little work outside these genera has been done to characterize lux box sequences, especially within marine bacteria.

A prevalent class of marine heterotrophic Alpha-proteobacteria, known as the Roseobacter Clade, are arguably some of the most ecologically relevant marine microorganisms. Members of the clade can comprise up to 20% of microbial abundance in marine ecosystems. Their contributions to global biogeochemical cycles, such as carbon, sulfur, and phosphorous largely stem from their vast array of diverse metabolisms (8, 9). Many Roseobacter physiologies are regulated by QS (10–12). Furthermore, we recently demonstrated that QS impacts community composition and dynamics in multi-species biofilms (Chapter 2). Thus, understanding the regulatory elements influencing Roseobacter physiologies aids in our ability to utilize Roseobacters as model organisms for marine ecology. Recent genomic evidence suggests up to 87% of sequenced Roseobacter genomes contain at least one QS systems (12). Of those, half contain multiple QS systems (12, 13). Despite this prevalence for QS in clade members, relatively few strains have been studied with regards to QS. QS systems are often fairly conserved within members of the Roseobacter clade (14). This conservation in genes allows researchers to use bioinformatic tools to generate consensus motifs and predict relationships between genes and their regulators (15, 16). However, the bioinformatic tools available to identify DNA regulatory elements, such as the *lux* box, within the Roseobacter clade have proven insufficient, presumably because these tools utilize consensus motifs from more phylogenetically distinct organisms (e.g., the Gamma-Proteobacteria *V. fischeri* and *Pseudomonas aeruginosa* [4, 17]). While some conservation within LuxRI homologs spans across Proteobacteria classes, studies have demonstrated that even within similar species, *lux* box consensus sequences do not fully capture all genes regulated by QS in a signal organism (18–21). Thus, applying consensus motifs generated for Gamma-proteobacteria is inadequate to identify QS-regulated genes in members of the Roseobacter clade.

In this study, we employed a bioinformatic approach independent of previous approaches by constructing a *de novo* consensus sequence using members of the *Phaeobacter-Leisingera* lineages of the Roseobacter clade. One member of this

lineage, Rhodobacterales strain Y4I (formerly *Phaeobacter sp.* strain Y4I), is a competitive member of biofilm communities due to its two QS systems: *pgaRI* and *phaRI* (22, 23) Chapter 2). Thirty genomes in the *Phaeobacter-Leisingera* lineage possessed homologs to *pgaI* and only 10 genomes contained *phaI* homologs. This conservation in *pgaI* homologs among the *Phaeobacter-Leisingera* lineage catalyzed our investigation to identity a clade-specific DNA binding site (termed 'roseo box') for LuxR family transcriptional regulators for the *Phaeobacter-Leisingera* lineage of the Roseobacter clade. We then queried these 30 genomes for matches to the roseo box in effort to identify putative genes regulated by QS. Given the prevalence of QS in members of the Roseobacter clade, their diverse metabolic capabilities, abundance in marine ecosystems, and predilection for colonizing surfaces, we posit QS is a critical regulatory mechanism employed by Roseobacters aiding in the aforementioned processes. Because the complexity of QS and its role in regulating a variety of behaviors, it is impossible to experimentally characterize the vast network that is QS in the Roseobacter clade. Thus, the identification of a clade-specific roseo box provides a genetic tool for future researchers when selecting genes putatively regulated by QS for hypothesis driven research.

III. Methodology

Sequence retrieval, gene homology search, phylogenetic relatedness

Roseobacter genome sequences (374) were retrieved from the Integrated Microbial Genomes and Microbiomes Database at the Joint Genome Institute [IMG (https://img.jgi.doe.gov/cgi-bin/mer/main.cgi), **Supplementary Table 4.1**]. Genome sequences were queried for the presence of homologous genes to *pgaI* in Y4I using a cutoff of 50 % amino acid similarity. Of the 374 genomes queried, 214 genomes possessed 218 gene homologs with 50 % or greater protein similarity to PgaI (**Supplementary Table 4.2**). Of those, 34 gene sequences shared < 60 % protein identity to PgaI in Y4I, 30 of which belong to the *Phaeobacter-Leisingera*. In addition, 10 *Phaeobacter-Leisingera* genomes shared < 60 % protein identity to PhaI in Y4I, with *Leisingera* species possessing the highest identity scores with the lowest e-values (**Supplementary Table 4.2**). Two of the 34 genomes, *Roseobacter* sp. MED 193 (638341182) and *Ruegeria* sp. R11 (647533206) were eliminated from this study. The other two genomes, *Phaeobacter gallaeciensis* BS107 (641380432) and Rhodobacterales strain Y4I (647533203), were unavailable for download through IMG and genome annotation was suppressed due to poor quality through the National Center for Biotechnology Information (NCBI).

Initial motif model

We extracted the intergenic region between *luxRI* homologs from 30 *Phaeobacter-Leisingera* genomes. Intergenic regions were used to build a model consensus sequence using Gapped Local Alignment of Motifs (GLAM2) software [https://meme-suite.org/meme/tools/glam2, (24)]. GLAM2 parameters were left as default (GLAM2 -M -z 2 -a 2 -b 100 -w 20 -r 10 -n 2000 -D 0.1 -E 2.0 -I 0.02 -J 1.0). Motif matches containing a putative sigma 70 consensus sequence (TATAA) were identified using BPROM (25) and used for further analysis. Two motif structures were evident in the consensus sequences: The first motif was chosen primarily due to its palindromic sequence spanning base pairs ~2-32 (**Figure 4.1A**)**.** The second motif was built using isolated components of the intergenic region between *luxRI* sequences not included in the first motif (**Figure 4.1B**).

Significant positive hits to the consensus sequence were determined as follows: The intergenic regions for individual *Roseobacter* genomes were randomized 1000 times with fasta-shuffle-letters (MEME Suite). This program shuffles sequences so that a given intergenic region's length and GC content is maintained after randomization. For each iteration, the randomized intergenic regions were queried against the two motif models using GLAM2SCAN (-2 -t -n 1000; [26]). The top bitscore hits for both motifs, respectively, were retained from this query. These bitscores corresponded to the maximum false positive bitscores expected relative to randomized intergenic region sequences. The final significance threshold could then be defined as a quantile of false positive bitscores for individual Roseobacter genomes. This quantile was adjustable to change the motif model sensitivity such that regions of varying sequence homology could be labelled as putative positive hits to the motifs. The final significance threshold was established by comparing the median bitscore for putative motifs versus the bitscore quantile. The bitscore quantile leading to a rapid decrease in putative matched bitscores was defined as the significance threshold (**Figure 4.2**). This is based on the rationale that there should be a clear demarcation in which sequences are and are not homologous with the roseo box motifs. Initially, these thresholds were 0.50 and 0.74 for the primary and secondary motifs, respectively (**Figure 4.2A,B**). These motifs were then compared with previously described motifs in CollecTF, Prodoric (v8.9), and RegTransBase (v4) using TOMTOM (27). There were no significant matches, with the lowest match e-values being, respectively, 1.56 and 6.54 for the primary and secondary motif.

Iterative model used to construct roseo boxes

In an attempt to improve model specificity for both motifs, an iterative approach was taken that constructed new motif models using positive matches from the earlier motif model queries (**Supplemental Tables 4.3 and 4.4**). Similar approaches have been taken with tools such as JackHMMER (28) and PSI-BLAST (29). Briefly, the motifs were constructed as before and queried against the intergenic regions of the 30 *Phaeobacter-Leisingera* genomes using GLAM2SCAN (-2 -t -n 1000). As before, intergenic regions from the *Phaeobacter-Leisingera* genomes were randomized using fasta-shuffle-letters and analyzed for the maximum false positive bitscore. The 95th quantile from the maximum false positive bitscores was taken as the threshold for defining a significant match. Next, all significant matches from the initial GLAM2SCAN query were used to construct new motifs, termed roseo box motif 1 and 2 with GLAM2. These new models were then used to query for new putative matches based on new false positive bitscore thresholds. New models were iteratively constructed in this fashion until model scores did not improve by more than 5 % for two iterations in a row. This required five and seven iterations (including the initial model) for roseo box motifs 1 and 2, respectively. Last, the roseo box motifs were compared with previously described motifs using TOMTOM (27). Again, there were no significant matches, with the lowest match e-values being 0.74 and 1.58 for roseo box motifs 1, and 2, respectively.

Genome query

The final models were used to find putative motifs in the 30 *Phaeobacter-Leisingera* genomes. Final significance threshold for false positives was established using the approach described in the previous section, where median bitscores for putative matches were compared against the false positive bitscore quantiles. Using this approach, the final thresholds were 0.7 and 0.96 for roseo box motifs 1 and 2, respectively (**Figure 4.2C,D**). To test whether our motif model could be applied

more broadly to identify putative matches to the motif, we search the intergenic regions of a divergently related roseobacter and non-roseobacter species, *Ruegeria denitrificans* and *Pseudomonas aeruginosa* PA17 respectively. Additionally, we identified homologous genes corresponding to those identified as putative positive matches to roseobox 1 in Y4I. Using the upstream region of those genes, we manually searched for motif matches.

IV. Results and Discussion

We surveyed 374 publicly available Roseobacter genomes (**Supplementary Table 4.1**) for genes encoding LuxI homologs. Of those, 57 % shared amino acid identity to LuxI homologs in Rhodobacterales strain Y4I. We found 218 genes and 11 genes with 50 % or greater protein identity with LuxI homologs, PgaI and PhaI, respectively (**Supplemental Table 4.2**). Given the overwhelming number of Roseobacters containing LuxI homologs that share protein identity to PgaI and that this AHL synthase produces a relatively common AHL, C8-HSL in Y4I, we used these sequences to generate two roseo box motifs. Motifs were chosen due to their sequence length, the presence of a palindromic sequence, and proximity to putative sigma 70 promoter region all of which are typical of lux box regulatory elements (30, 31).

Our analysis of QS regulated genes using the regulatory elements of these gene homologs focused on the *Phaeobacter-Lesingera* lineage in the Roseobacter clade that clustered as sister clades based on core genome sequences (13). Previously, Rhodobacterales strain Y4I (formerly *Phaeobacter sp.* Y4I) belonged to the *Phaeobacter* clade as determined by 16S rRNA phylogeny in the early 2000's (10, 32). Since then, Y4I has been stripped of its genus designation and remains without classification beyond order. Computational analysis using whole genome sequences, indicates Y4I is more closely related to *Leisingera* species but still aligns closely with *Phaeobacter* in select genes (data not shown). Given that Y4I falls somewhere between these two sister clades, we surveyed 30 *Phaeobacter-Leisingera* genomes for matches to our iterative motif models, roseo box 1 and roseo box 2 (**Figure 4.1A,B**, respectively). These models and subsequent queries were constructed with the assumption that regulatory elements would be found within intergenic regions (**Figure 4.1C**). Gene orientation was conserved regardless of stranded-ness so that the downstream annotated gene is the putative target for regulation (**Tables 4.1, Supplemental Tables 4.3-4.6**). Due to both differences in transcription binding site locations (33) as well as the imprecise nature of automatic genome annotations (34), we consider positive hits to our motifs whose distance from the transcriptional start site of the downstream annotated gene is less than 500 bp (**Table 4.1, Supplemental Tables 4.4, 4.5**) as more likely to be transcriptional regulated by QS.

***QS putatively regulates less than 0.1% of* Phaeobacter-Leisingera *genomes directly*.** Intergenic regions matching roseo box motifs 1 and 2 were extracted and together with the sequences used to generate the primary and secondary motifs, roseo box motifs 1 and 2 were generated (**Figure 4.1A,B**, respectively). Of the 72 positive hits, that is matches to the motif above the significance bitscore threshold (0.7), 16 were identified as putatively regulated by roseo box motif 1 due to proximity of downstream annotated gene to motif match (**Table 4.1**). Likewise, a total of 36 positive hits to roseo box motif 2 were found

above the significance threshold of 0.96. Of those, 13 annotated genes were identified as likely to be regulated by roseo box motif 2 based on distance from the transcriptional start site of the annotated gene (**Supplemental Table 4.5**). We calculated the percentage of putative transcriptional regulation by QS of these genes based on total gene counts (data not shown). QS putatively regulates 0.020 – 0.067 % of total genes across 9 independent *Phaeobacter-Leisingera* strains for roseo box motif 1. Of those, *Leisingera* sp. ANG-S5 possessed the most matches (three) to roseo box motif 1 representing 0.067% of its genome. While the lowest percentage of QS regulated genes (0.020%) was found in *Leisingera* sp. ANG-Vp (**Table 4.1**). Likewise, using roseo box motif 2 QS putatively regulates 0.023 % to 0.053 % of genes represented by the 10 unique strains represented. Two genes (0.053%) in *Phaeobacter inhinbens* 2.10 are considered to be under the regulation of QS by binding to roseo box motif 2, while only one gene (0.023 %) is regulated by QS in *Leisingera* sp. ANG-DT. Previous studies estimate QS to regulate 1-30 % of genes. However, these estimates were derived from expression analysis incorporating genes both directly and indirectly regulated by QS (35–37). QS may directly bind to a smaller percentage of the genome for transcriptional activation than previously thought. Many regulatory networks, such as those involving QS, are modified post-transcriptionally (38–41). This type of regulatory redundancy allows for fine tuning of energetically expensive metabolic processes.

In canonical QS systems, AHL synthase genes are positively autoregulated by their LuxR-AI complex and mediate regulation of their own operon in a positive feedback loop (30, 35, 42). In support of this, we found acyl homoserine lactone synthases represented 70 % and 25 % of positive matches within distinct genomes across for roseo box motif 1 and 2, respectively. These findings indicate that roseo box motif 1 might be a stronger candidate when considering genes transcriptionally regulated by QS in the *Phaeobacter-Leisingera* lineage of the Roseobacter clade. For this reason, we largely focused on examining genes putatively regulated by QS through the DNA regulatory element identified as roseo box motif 1 (**Table 4.1**). However, roseo box motif 2 resulted in positive matches upstream to CheR which warrants inclusion in the discussion below (**Supplemental Table 4.5**).

Transporters and receptors are likely regulated directly by QS in* Phaeobacter-Leisingera *genomes. A common feature appearing as positive matches to roseo box motif 1 were proteins involved in ABC-type transport such as: spermidine/putrescine transport system substrate-binding protein and microcin C transport ATP binding protein. A quarter of positive matches to roseo box motif 1 were annotated as spermidine/putrescine transport system substrate-binding protein, termed PotD. All of these positive matches belonged to *Leisingera* species, but not all members of this genera came back with positive hits. The three strains (ANG-Vp, ANG-S, and ANG-M6) had positive matches to roseo box motif 1 ~400 bp upstream of *potD* on the negative strand with bitscores ranging from (10.4-18.2, **Table 4.1**). PotD and subsequent genes (PotA/B/C) belong to a polyamine transport system involved in stress response (43). It has been demonstrated that PotD stimulates biofilm production through increased polyamine (preferentially spermidine) metabolism resulting in increased expression of SOS response genes (44). Our results, while preliminary, indicate *potD* as a target gene candidate linking QS to both biofilm formation and SOS response among the *Phaeobacter-Leisingera* lineage within the Roseobacter clade. This strategy has been exploited by a divergent member of the clade, *Dinoroseobacter shibae* (45).

Another transporter system putatively regulated by roseo box motif 1 in *Leisignera* sp. ANG-M7 is annotated as a microcin C transport ATP binding protein, termed *yejF*. YejF is part of a bacteriocin ABC import system which preferentially binds microcin. Microcins are antimicrobial peptides produced by a variety of hosts including those in marine environments (46, 47). A recent study demonstrated microcin c activity is proximity dependent and is influenced by QS in a growth-dependent manner in *Escherichia coli* (48). The *YejABEF* operon has also been demonstrated to confer resistance to a variety of antimicrobial peptides including some Roseobacters (49, 50). It is possible that evolution of these two systems (e.g., antimicrobial peptides and their inhibitors) both emerged as a type of "chemical warfare" and are both regulated by similar mechanisms, such as QS. Competition, such as this, is common in environmental ecosystems (51, 52)

Evidence of metabolic enzymes regulated by QS in* Phaeobacter-Leisingera *genomes. A gene annotated as cytochrome C peroxidase (CCP) was found downstream of roseo box motif 1 in two *Leisingera* genomes: ANG-M6 and ANG-S5 with a bitscore of 11.1 for each (**Table 4.1**). The CCPs in both genomes putatively contain heme groups and are likely responsible for reducing radical oxygen species (ROS) based on their KEGG pathways [EC:1.11.1.5]. CCPs can be linked to QS in two ways: (i) ROS are typically used as quorum quenching (QQ) mechanism by hosts against pathogens. QQ has been posited to induce QS in *P. aerogenesis* (53). Perhaps the integration of CCPs into this network serves as a mechanism to combat QQ in members of the Roseobacter clade. (ii) Another possibility is that CCPs are involved in the synthesis of a specialized AHL and are thus regulated by QS. Ongoing research in *P. aeruginosa* indicates that CCPs are involved in the production of 2-heptyl-3-hydroxy-4-quinolone, a signaling molecule in the specialized *Pseudomonas* quinolone signal system (PQS) quorum sensing pathway through oxidation of fatty acid biosynthesis (54–58). Utilization of unique signaling molecules is not unprecedented in members of the Roseobacter clade: *Ruegeria pomeryi* DSS-3 of the Roseobacter Clade can incorporate exogenously supplied p-coumaroyl into its AHL chain catalyzed by *S*-adenosylmethionine (SAM) (59).

Many metabolic pathways utilize SAM (also called AdoMet) as a methyl donor through catalytic reaction with methyltransferases (60, 61). Matches to roseo box motifs 1 and 2 were respectively found upstream of the transcriptional start site of annotated methyl transferases RsmD and CheR. A positive hit to roseo box motif 1 for RsmD was found in *L.* sp. ANG-S5 with a bitscore of 14.5 (**Table 4.1**). In comparison, three positive matches to roseo box motif 2 for CheR were found in *P. gallaeciensis* DSM 17935, *P. inhibens* 2.10, and *P. inhibens* T5, DSM 16374 each with the same bitscore of 13.2 (**Supplement Table 4.5**). Methyltransferases such as these catalyze the reaction between a methyl donor, such as SAM, and their substrate. The substrate for RsmD is the guanosine 966 residue, specifically, in 16S rRNA (62). In the case of CheR, glutamate residues on chemotaxis transmembrane chemoreceptors (MCPs). serve as the substrate (63, 64). In both cases, *S*-adenosyl-L-homocysteine (SAH) is a resulting by-product (65, 66). While biological function of the catalytic reaction of RsmD for methylation of 16S rRNA at guanosine 966 is still unclear, it is a nearly universal mechanism among bacteria (62). The role of CheR, on the other hand, has been well characterized as a chemotaxis protein in diverse bacteria (67–70). The methylation of the certain glutamate residues on MCPs by CheR activates a cascade response ultimately leading to flagellar motility in response to stimuli (71). A number of studies provide evidence linking QS to chemotaxis

through the regulation of CheR (72–74). Interestingly, CheR is constitutively expressed in diverse proteobacteria (66). Our results indicate that CheR may be upregulated during QS in members of the Roseobacter clade indicating that . Indeed, the nucleotide residues which match roseo box motif 2 in the sequences corresponding to the upstream region of CheR proteins may unveil highly conserved features not previously included in our model.

All pathways lead to* S-*adenosylmethionine (SAM). As an intermediate in a variety of metabolic transformations including methylation, polyamine biosynthesis, vitamin synthesis, and AHL synthesis in bacteria, SAM is integral to cellular processes (61, 75). Several of the aspects previously discussed are linked to SAM. In an attempt to better contextualize the link between these putative QS regulated genes and SAM, we present a working model that incorporates the principal mechanisms and information discussed previously (**Figure 4.3**). For brevity, direct transcriptional regulation of genes, with the exception of the *luxRI* operon, are not shown. SAM combined with an acyl-ACP, which is derived from acetyl-CoA, is involved in the synthesis of AHLs (76, 77). A by-product of all SAM methyltransferases is SAH (indicated here by RsmD) (75). In the same way SAM contributes to the synthesis of AHLs, SAH contributes to the synthesis of AI2 (78). Both AIs can bind to their cognate LuxR which forms the LuxR-AI complex (79). Activated LuxR-AI putatively mediates the transcription of *yejF* – conferring antimicrobial resistance (49); *potD* – mediating biofilm formation, SOS response, and polyamine transport (43, 44, 80, 81); and CCP – presumably involved in the oxidation of the fatty acids which can be passed into the generation of acetyl-CoA (82) leading to the generation of acyl-ACP completing the cycle.

Motif model is specific for the *Phaeobacter-Leisingera* lineage of the Roseobacter Clade*.* We tested our motif model for matches to roseo box 1 and 2 using the threshold cutoffs of 0.7 and 0.96 respectively to determine if our roseo box motifs could be broadly applied to members of the Roseobacter clade. To this end, we scanned intergenic regions of the genome of a divergently related member of the Roseobacter clade, *Ruegeria denitrificans* CECT 5091*,* and a non-Roseobacter member, *Pseudomonas aeruginosa* PA 17, for matches to the roseo box motifs. For both organisms, roseo box 1 motif was identified upstream of unique genes, that is genes not previously identified as putatively regulated by rose box motifs. Only one positive match (bitscore = 14.4) was identified in *R. denitrificans* CECT 5091 upstream of a Flp/Tad pilus biosynthetic cluster (Ga0125401_10393). The Flp biosynthetic cluster is absent from microarray data indicating that it is not transcriptionally controlled by QS in another proteobacteria (83, 84). Two positive matches to roseo box motif 1 were identified in *P. aeruginosa* PA 17: a heme oxygenase (*hemO*, Ga0112696_100114) and a xanthine permease (Ga0112696_1012919) with bitscores of 13.8 and 10.0 respectively. Both genes found in *P. aeruginosa* are downregulated in the presence of QS molecules (85–87). That we found positive matches to these genes in a non-Roseobacter suggests an evolutionary role for QS cross-talk and competition between Proteobacteria. No positive matches to roseo box 2 were identified in either organism. Additionally, we searched for gene homologs to genes identified as downstream of positive matches to roseo box 1 motif in Y4I. Specifically, we manually surveyed upstream regions (up to ~500 bp) of gene homologs to *potD*, *yejF*, *rsmD*, and CCP for matches to roseo box 1 motif. We identified a positive match to roseo box 1 motif in the intergenic region between *luxRI* homologs, *pgaRI* (bitscore – 19.9). Given the high threshold

cutoffs included in our model, it is possible our model was too rigid and did not allow for sufficient variation between the consensus sequence and the sequence matches in the genome. Despite this, we have demonstrated that our motif model identifies genes likely regulated by QS in members of the *Phaeobacter-Leisingera* lineages specifically. In addition, our bioinformatic pipeline could be applied more broadly with the inclusion of more divergent sequences or relaxing the stringency.

V. Future Directions

We have demonstrated that the annotated genes putatively regulated by QS in the *Phaeobacter-Leisingera* lineage of the Roseobacter clade have strong ties to bacterial social behaviors such as SOS response, biofilm formation/motility, antimicrobial resistance, and metabolism. These processes are integral to cooperation and competition between multispecies bacterial interaction. The role of QS in these social behaviors have been the focus of multiple reviews (3, 88–95). Traditional genetic analysis, in addition to transcriptomics, is typically used to assess QS-regulated genes in a single organism. However, these approaches are limited to lab-based studies and cannot be applied to meta-data. Additionally, these types of analysis may encompass genes indirectly regulated by QS as they rely on expression data (i.e., the increases and decreases in gene expression in the presence and absence of a mutated system). While both approaches are valuable in providing a set of possible genes to explore when examining the role of QS. Unlike traditional approaches, our analysis targets the intergenic region between genes. It is here where direct transcriptional regulation takes place (33). Given, motif modeling for roseo box consensus sequences used the sigma 70 consensus (TATAA) as a guide to target regions where this clade specific "lux box" would be found. Therefore, it is possible we isolated genetic regulatory elements corresponding to the sigma 70 motif instead. Nonetheless, our results reflect a selection of candidate genes, and associated phenotypes and conditions which warrant additional investigation. Herein, we present a DNA regulatory element indicative of with the palindromic 'lux box' with proximity to promoter start sites that have high conservation in the *Phaeobacter-Leisingera* lineage of the Roseobacter clade.

References

1. Williams P, Winzer K, Chan WC, Cámara M. 2007. Look who's talking: communication and quorum sensing in the bacterial world. Philos Trans R Soc Lond B Biol Sci 362:1119–34.
2. Bassler BL. 1999. How bacteria talk to each other: Regulation of gene expression by quorum sensing. Curr Opin Microbiol. Current Biology Ltd.
3. Miller MB, Bassler BL. 2001. Quorum Sensing in Bacteria. Annu Rev Microbiol 55:165–99.
4. Egland KA, Greenberg EP. 1999. Quorum sensing in *Vibrio fischeri*: elements of the *luxI* promoter. Mol Microbiol 31:1197–1204.
5. Devine JH, Shadel GS, Baldwint T 0, Heckel R, Johnston TC, Lin J-W. 1989. Identification of the operator of the *lux* regulon from the *Vibrio fischeri* strain ATCC7744 (bioluminescence/regulation/autoinduction/repression/activator) Proc. NatI Acad Sci USA 86:5688-5692.
6. Liu J, Fu K, Wu C, Qin K, Li F, Zhou L. 2018. "In-Group" Communication in Marine *Vibrio*: A Review of N-Acyl Homoserine Lactones-Driven Quorum Sensing. Front Cell Infect Microbiol 8:139.
7. Brindhadevi K, LewisOscar F, Mylonakis E, Shanmugam S, Verma TN, Pugazhendhi A. 2020. Biofilm and Quorum sensing mediated pathogenicity in *Pseudomonas aeruginosa*. Process Biochem 96:49–57.
8. Buchan A, González JM, Moran MA. 2005. Overview of the marine *Roseobacter* lineage. Appl Environ Microbiol 71:5665–5677.
9. Wagner-Döbler I, Biebl H. 2006. Environmental biology of the marine Roseobacter lineage. Annu Rev Microbiol 60:255–280.
10. Slightom RN, Buchan A. 2009. Surface colonization by marine roseobacters: integrating genotype and phenotype. Appl Environ Microbiol 75:6027–37.
11. Cude WN, Buchan A. 2013. Acyl-homoserine lactone-based quorum sensing in the Roseobacter clade: Complex cell-to-cell communication controls multiple physiologies. Front Microbiol 4:336.
12. Zan J, Liu Y, Fuqua C, Hill R. 2014. Acyl-Homoserine Lactone Quorum Sensing in the Roseobacter Clade. Int J Mol Sci 15:654–669.
13. Liang KYH, Orata FD, Boucher YF, Case RJ. 2021. Roseobacters in a Sea of Poly- and Paraphyly: Whole Genome-Based Taxonomy of the Family Rhodobacteraceae and the Proposal for the Split of the "Roseobacter Clade" Into a Novel Family, Roseobacteraceae fam. nov. Front Microbiol 0:1635.
14. Buchan A, Mitchell A, Nathan Cude NW, Campagna S. 2016. Acyl-Homoserine Lactone-Based Quorum Sensing in Members of the Marine Bacterial Roseobacter Clade: Complex Cell-to-Cell Communication Controls Multiple Physiologies. Stress Environ Regul Gene Expr Adapt Bact 1:225–233.
15. Wasserman WW, Sandelin A. 2004. Applied bioinformatics for the identification of regulatory elements. Nat Rev Genet 5:276–287.
16. Subramoni S, Florez Salcedo DV, Suarez-Moreno ZR. 2015. A bioinformatic survey of distribution, conservation, and probable functions of LuxR solo regulators in bacteria. Front Cell Infect Microbiol 5:1–17.
17. Pesci EC, Pearson JP, Seed PC, Iglewski BH. 1997. Regulation of *las* and *rhl* quorum sensing in *Pseudomonas aeruginosa.* J Bacteriol 179:3127–3132.
18. Fuqua C, Winans SC. 1996. Conserved cis-acting promoter elements are required for density-dependent transcription of *Agrobacterium tumefaciens* conjugal transfer genes. J Bacteriol 178:435.
19. de Kievit TR, Kakai Y, Register JK, Pesci EC, Iglewski BH. 2002. Role of the

Pseudomonas aeruginosa las and *rhl* quorum-sensing systems in *rhlI* regulation. FEMS Microbiol Lett 212:101–106.
20. Antunes LCM, Ferreira RBRR, Lostroh CP, Greenberg EP. 2008. A mutational analysis defines *Vibrio fischeri* LuxR binding sites. J Bacteriol 190:4392–4397.
21. Kimbrough JH, Stabb E V. 2017. Comparative analysis reveals regulatory motifs at the *ainS*/*ainR* pheromone-signaling locus of *Vibrio fischeri*. Sci Rep 7:1–14.
22. Cude WN, Mooney J, Tavanaei AA, Hadden MK, Frank AM, Gulvik CA, May AL, Buchan A. 2012. Production of the antimicrobial secondary metabolite indigoidine contributes to competitive surface colonization by the marine roseobacter *Phaeobacter sp.* strain Y4I. Appl Environ Microbiol 78:4771–4780.
23. Quigley LNM, Edwards A, Steen AD, Buchan A, Fagervold SK. 2019. Characterization of the Interactive Effects of Labile and Recalcitrant Organic Matter on Microbial Growth and Metabolism. Front Microbiol 10:1–15.
24. Frith MC, Saunders NFW, Kobe B, Bailey TL. 2008. Discovering Sequence Motifs with Arbitrary Insertions and Deletions. PLoS Comput Biol 4:e1000071.
25. Solovyev V, Salamov A. 2011. Automatic Annotation of Microbial Genomes and Metagenomic Sequences. In Metagenomics and its Applications in Agriculture, Biomedicine and Environmental Studies (Ed. R.W. Li), Nova Science Publishers, p.61-78., p. 61–78. *In* .
26. Frith MC, Saunders NFW, Kobe B, Bailey TL. 2008. Discovering Sequence Motifs with Arbitrary Insertions and Deletions. PLOS Comput Biol 4:e1000071.
27. Gupta S, Stamatoyannopoulos JA, Bailey TL, Noble WS. 2007. Quantifying similarity between motifs. Genome Biol 8.
28. Johnson LS, Eddy SR, Portugaly E. 2010. Hidden Markov model speed heuristic and iterative HMM search procedure. BMC Bioinforma 2010 111 11:1–8.
29. Altschul SF, Madden TL, Schäffer AA, Zhang J, Zhang Z, Miller W, Lipman DJ. 1997. Gapped BLAST and PSI-BLAST: A new generation of protein database search programs. Nucleic Acids Res 25:3389–3402.
30. Fuqua C, Parsek MR, Greenberg EP. 2001. Regulation of Gene Expression by Cell-to-Cell Communication: Acyl-Homoserine Lactone Quorum Sensing. Annu Rev Genet 35:439–468.
31. Finney AH, Blick RJ, Murakami K, Ishihama A, Stevens AM. 2002. Role of the C-terminal domain of the alpha subunit of RNA polymerase in LuxR-dependent transcriptional activation of the *lux* operon during quorum sensing. J Bacteriol 184:4520–4528.
32. Buchan A, Neidle EL, Moran MA. 2004. Diverse Organization of Genes of the *B*-Ketoadipate Pathway in Members of the Marine Roseobacter Lineage. Appl Environ Microbiol 70:1658–68.
33. McGrath PT, Lee H, Zhang L, Iniesta AA, Hottes AK, Tan MH, Hillson NJ, Hu P, Shapiro L, McAdams HH. 2007. High-throughput identification of transcription start sites, conserved promoter motifs and predicted regulons. Nat Biotechnol 25:584–592.
34. Salzberg SL. 2019. Next-generation genome annotation: we still struggle to get it right. Genome Biol 2019 201 20:1–3.
35. Schuster M, Lostroh CP, Ogi T, Greenberg EP. 2003. Identification, timing, and signal specificity of *Pseudomonas aeruginosa* quorum-controlled genes: a transcriptome analysis. J Bacteriol 185:2066–79.
36. Chen H, Teplitski M, Robinson JB, Rolfe BG, Bauer WD. 2003. Proteomic analysis of wild-type *Sinorhizobium meliloti* responses to *N*-acyl homoserine lactone quorum-sensing signals and the transition to stationary phase? J

Bacteriol 185:5029–5036.
37. Gao X, Wang X, Mao Q, Xu R, Zhou X, Ma Y, Liu Q, Zhang Y, Wang Q. 2018. VqsA, a Novel LysR-Type Transcriptional Regulator, Coordinates Quorum Sensing (QS) and Is Controlled by QS To Regulate Virulence in the Pathogen *Vibrio alginolyticus*. Appl Environ Microbiol 84:444–462.
38. Waters CM, Lu W, Rabinowitz JD, Bassler BL. 2008. Quorum sensing controls biofilm formation in *Vibrio cholerae* through modulation of cyclic Di-GMP levels and repression of *vpsT*. J Bacteriol 190:2527–2536.
39. Liang F, Zhang B, Yang Q, Zhang Y, Zheng D, Zhang L, Yan Q, Wu X. 2020. Cyclic-di-GMP Regulates the Quorum-Sensing System and Biocontrol Activity of *Pseudomonas fluorescens* 2P24 through the RsmA and RsmE Proteins. Appl Environ Microbiol 86.
40. Srivastava D, Waters CM. 2012. A tangled web: Regulatory connections between quorum sensing and cyclic Di-GMP. J Bacteriol 194:4485–4493.
41. Loh J, Pierson EA, Pierson LS, Stacey G, Chatterjee A. 2002. Quorum sensing in plant-associated bacteria. Curr Opin Plant Biol 5:285–290.
42. Schaefer AL, Hanzelka BL, Eberhard A, Greenberg EP. 1996. Quorum sensing in *Vibrio fischeri*: Probing autoinducer-LuxR interactions with autoinducer analogs. J Bacteriol 178:2897–2901.
43. Han KY, Seo HS, Song JA, Ahn KY, Park JS, Lee J. 2007. Transport proteins PotD and Crr of *Escherichia coli*, novel fusion partners for heterologous protein expression. Biochim Biophys Acta - Proteins Proteomics 1774:1536–1543.
44. Zhang X, Zhang Y, Liu J, Liu H. 2013. PotD protein stimulates biofilm formation by *Escherichia coli*. Biotechnol Lett 2013 357 35:1099–1106.
45. Koppenhöfer S, Wang H, Scharfe M, Kaever V, Wagner-Döbler I, Tomasch J. 2019. Integrated Transcriptional Regulatory Network of Quorum Sensing, Replication Control, and SOS Response in *Dinoroseobacter shibae*. Front Microbiol 10:803.
46. Hancock REW, Chapple DS. 1999. Peptide antibiotics. Antimicrob Agents Chemother 43:1317–1323.
47. Rather IA, Galope R, Bajpai VK, Lim J, Paek WK, Park Y-H. 2017. Diversity of Marine Bacteria and Their Bacteriocins: Applications in Aquaculture. Rev Fish Sci Aquac 25:257–269.
48. Lu S-Y, Zhao Z, Avillan JJ, Liu J, Call DR. 2017. Autoinducer-2 Quorum Sensing Contributes to Regulation of Microcin PDI in *Escherichia coli*. Front Microbiol 8:1–12.
49. Tanaka KJ, Song S, Mason K, Pinkett HW. 2018. Selective substrate uptake: The role of ATP-binding cassette (ABC) importers in pathogenesis. Biochim Biophys Acta - Biomembr 1860:868–877.
50. Wang R, Gallant É, Seyedsayamdost MR. 2016. Investigation of the genetics and biochemistry of roseobacticide production in the Roseobacter clade bacterium *Phaeobacter inhibens*. MBio 7.
51. Prasad S, Morris PC, Hansen R, Meaden PG, Austin B. 2005. A novel bacteriocin-like substance (BLIS) from a pathogenic strain of *Vibrio harveyi*. Microbiology 151:3051–3058.
52. Desriac F, Defer D, Bourgougnon N, Brillet B, Le Chevalier P, Fleury Y. 2010. Bacteriocin as Weapons in the Marine Animal-Associated Bacteria Warfare: Inventory and Potential Applications as an Aquaculture Probiotic. Mar Drugs 8:1153–1177.
53. Tang H, Zhang Y, Ma Y, Tang M, Shen D, Wang M. 2018. Regulation of Nicotine Tolerance by Quorum Sensing and High Efficiency of Quorum

Quenching Under Nicotine Stress in *Pseudomonas aeruginosa* PAO1. Front Cell Infect Microbiol 0:88.
54. Déziel E, Gopalan S, Tampakaki AP, Lépine F, Padfield KE, Saucier M, Xiao G, Rahme LG. 2004. The contribution of MvfR to *Pseudomonas aeruginosa* pathogenesis and quorum sensing circuitry regulation: multiple quorum sensing-regulated genes are modulated without affecting *lasRI*, *rhlRI* or the production of *N*-acyl- *l*-homoserine lactones. Mol Microbiol 55:998–1014.
55. Pesci EC, Milbank JBJ, Pearson JP, McKnight S, Kende AS, Greenberg EP, Iglewski BH. 1999. Quinolone signaling in the cell-to-cell communication system of *Pseudomonas aeruginosa*. Proc Natl Acad Sci 96:11229–11234.
56. Martínez E, Estupiñán M, Pastor FIJ, Busquets M, Díaz P, Manresa A. 2013. Functional characterization of ExFadLO, an outer membrane protein required for exporting oxygenated long-chain fatty acids in *Pseudomonas aeruginosa*. Biochimie 95:290–298.
57. Estupiñán M, Álvarez-García D, Barril X, Diaz P, Manresa A. 2015. *In Silico*/*In Vivo* Insights into the Functional and Evolutionary Pathway of *Pseudomonas aeruginosa* Oleate-Diol Synthase. Discovery of a New Bacterial Di-Heme Cytochrome C Peroxidase Subfamily. PLoS One 10:e0131462.
58. Martínez E, Cosnahan RK, Wu M, Gadila SK, Quick EB, Mobley JA, Campos-Gómez J. 2019. Oxylipins mediate cell-to-cell communication in *Pseudomonas aeruginosa*. Commun Biol 2019 21 2:1–10.
59. Schaefer AL, Greenberg EP, Oliver CM, Oda Y, Huang JJ, Bittan-Banin G, Peres CM, Schmidt S, Juhaszova K, Sufrin JR, Harwood CS. 2008. A new class of homoserine lactone quorum-sensing signals. Nat 2008 4547204 454:595–599.
60. Cheng X, Roberts RJ. 2001. AdoMet-dependent methylation, DNA methyltransferases and base flipping. Nucleic Acids Res 29:3784.
61. Sufrin JR, Finckbeiner S, Oliver CM. 2009. Marine-Derived Metabolites of *S*-Adenosylmethionine as Templates for New Anti-Infectives. Mar Drugs 2009, Vol 7, Pages 401-434 7:401–434.
62. Lesnyak D V, Osipiuk J, Skarina T, Sergiev P V, Bogdanov AA, Edwards A, Savchenko A, Joachimiak A, Dontsova OA. 2007. Methyltransferase That Modifies Guanine 966 of the 16 S rRNA Functional Identification And Tertiary Structure. J Biol Chem 282:5880–5887.
63. Goy MF, Springer MS, Adler J. 1977. Sensory transduction in *Escherichia coli*: Role of a protein methylation reaction in sensory adaptation. Proc Natl Acad Sci 74:4964–4968.
64. Yi X, Weis RM. 2002. The receptor docking segment and S-adenosyl-L-homocysteine bind independently to the methyltransferase of bacterial chemotaxis. Biochim Biophys Acta - Protein Struct Mol Enzymol 1596:28–35.
65. Simms SA, Subbaramaiah K. 1991. The kinetic mechanism of *S*-adenosyl-L-methionine: glutamylmethyltransferase from salmonella typhimurium. J Biol Chem 266:12741–12746.
66. Wadhams GH, Armitage JP. 2004. Making sense of it all: bacterial chemotaxis. Nat Rev Mol Cell Biol 5:1024–1037.
67. Martin AC, Wadhams GH, Shah DSH, Porter SL, Mantotta JC, Craig TJ, Verdult PH, Jones H, Armitage JP. 2001. CheR- and CheB-Dependent Chemosensory Adaptation System of *Rhodobacter sphaeroides*. J Bacteriol 183:7135.
68. Liu W, Sun Y, Shen R, Dang X, Liu X, Sui F, Li Y, Zhang Z, Alexandre G, Elmerich C, Xie Z. 2018. A Chemotaxis-Like Pathway of *Azorhizobium caulinodans* Controls Flagella-Driven Motility, Which Regulates Biofilm Formation, Exopolysaccharide Biosynthesis, and Competitive Nodulation.

Molecular Plant-Microbe Interactions 31:737–749.
69. Partridge JD, Nhu NTQ, Dufour YS, Harshey RM. 2019. *Escherichia coli* remodels the chemotaxis pathway for swarming. MBio 10.
70. Xu X, Li H, Qi X, Chen Y, Qin Y, Zheng J, Jiang X. 2021. *cheA*, *cheB*, *cheR*, *cheV*, and *cheY* Are Involved in Regulating the Adhesion of *Vibrio harveyi*. Front Cell Infect Microbiol 0:850.
71. Bren A, Eisenbach M. 2000. How signals are heard during bacterial chemotaxis: Protein-protein interactions in sensory signal propagation. J Bacteriol 182:6865–6873.
72. Hegde M, Englert DL, Schrock S, Cohn WB, Vogt C, Wood TK, Manson MD, Jayaraman A. 2011. Chemotaxis to the quorum-sensing signal AI-2 requires the Tsr chemoreceptor and the periplasmic LsrB AI-2-binding protein. J Bacteriol 193:768–773.
73. Laganenka L, Colin R, Sourjik V. 2016. Chemotaxis towards autoinducer 2 mediates autoaggregation in *Escherichia coli*. Nat Commun 2016 71 7:1–11.
74. Zhang L, Li S, Liu X, Wang Z, Jiang M, Wang R, Xie L, Liu Q, Xie X, Shang D, Li M, Wei Z, Wang Y, Fan C, Luo Z-Q, Shen X. 2020. Sensing of autoinducer-2 by functionally distinct receptors in prokaryotes. Nat Commun 2020 111 11:1–13.
75. Parveen N, Cornell KA. 2011. Methylthioadenosine/S-adenosylhomocysteine nucleosidase, a critical enzyme for bacterial metabolism. Mol Microbiol 79:7–20.
76. Heath RJ, Rock CO. 1995. Regulation of Malonyl-CoA Metabolism by Acyl-Acyl Carrier Protein and β-Ketoacyl-Acyl Carrier Protein Synthases in *Escherichia coli*. J Biol Chem 270:15531–15538.
77. Reading NC, Sperandio V. 2006. Quorum sensing: the many languages of bacteria. FEMS Microbiol Lett 254:1–11.
78. Zhao G, Wan W, Mansouri S, Alfaro JF, Bassler BL, Cornell KA, Zhou ZS. 2003. Chemical synthesis of *S*-ribosyl-l-homocysteine and activity assay as a LuxS substrate. Bioorg Med Chem Lett 13:3897–3900.
79. Pérez PD, Weiss JT, Hagen SJ. 2011. Noise and crosstalk in two quorum-sensing inputs of *Vibrio fischeri*. BMC Syst Biol 5.
80. Karatan E, Duncan TR, Watnick PI. 2005. NspS, a predicted polyamine sensor, mediates activation of *Vibrio cholerae* biofilm formation by norspermidine. J Bacteriol 187:7434–7443.
81. Mou X, Sun S, Rayapati P, Moran M. 2010. Genes for transport and metabolism of spermidine in *Ruegeria pomeroyi* DSS-3 and other marine bacteria. Aquat Microb Ecol 58:311–321.
82. Val DL, Cronan JE. 1998. In Vivo Evidence that *S*-Adenosylmethionine and Fatty Acid Synthesis Intermediates Are the Substrates for the LuxI Family of Autoinducer Synthases. J Bacteriol 180:2644–2651.
83. Liu H, Coulthurst SJ, Pritchard L, Hedley PE, Ravensdale M, Humphris S, Burr T, Takle G, Brurberg MB, Birch PRJ, Salmond GPC, Toth IK. 2008. Quorum sensing coordinates brute force and stealth modes of infection in the plant pathogen *Pectobacterium atrosepticum*. PLoS Pathog 4.
84. Kõiv V, Andresen L, Broberg M, Frolova J, Somervuo P, Auvinen P, Pirhonen M, Tenson T, Mäe A. 2013. Lack of RsmA-Mediated Control Results in Constant Hypervirulence, Cell Elongation, and Hyperflagellation in *Pectobacterium wasabiae*. PLoS One 8.
85. Abdalla MY, Hoke T, Seravalli J, Switzer BL, Bavitz M, Fliege JD, Murphy PJ, Britigan BE. 2017. *Pseudomonas* quinolone signal induces oxidative stress and inhibits heme oxygenase-1 expression in lung epithelial cells. Infect Immun

85.
86. Rasmussen TB, Bjarnsholt T, Skindersoe ME, Hentzer M, Kristoffersen P, Köte M, Nielsen J, Eberl L, Givskov M. 2005. Screening for quorum-sensing inhibitors (QSI) by use of a novel genetic system, the QSI selector. J Bacteriol 187:1799–1814.
87. Zhou JW, Muhammad J, Sun B, Yang R, Wadood A, Wang JS, Jia AQ. 2019. Metabolomic analysis of quorum sensing inhibitor hordenine on *Pseudomonas aeruginosa*. Appl Microbiol Biotechnol 103:6271–6285.
88. Waters CM, Bassler BL. 2005. QUORUM SENSING: Cell-to-Cell Communication in Bacteria. Annu Rev Cell Dev Biol 21:319–346.
89. Silva DP da, Schofield MC, Parsek MR, Tseng BS. 2017. An Update on the Sociomicrobiology of Quorum Sensing in Gram-Negative Biofilm Development. Pathog 2017, Vol 6, Page 51 6:51.
90. Li Y-H, Tian X-L. 2016. Quorum Sensing and Bacterial Social Interactions in Biofilms: Bacterial Cooperation and Competition, p. 1195–1205. *In* Stress and Environmental Regulation of Gene Expression and Adaptation in Bacteria. John Wiley & Sons, Inc., Hoboken, NJ, USA.
91. Chen R, Déziel E, Groleau MC, Schaefer AL, Greenberg EP. 2019. Social cheating in a *Pseudomonas aeruginosa* quorum-sensing variant. Proc Natl Acad Sci U S A.
92. Bruger EL, Snyder DJ, Cooper VS, Waters CM. 2020. Quorum sensing provides a molecular mechanism for evolution to tune and maintain investment in cooperation. ISME J 2020 154 15:1236–1247.
93. LaSarre B, Federle MJ. 2013. Exploiting Quorum Sensing To Confuse Bacterial Pathogens. Microbiol Mol Biol Rev 77:73–111.
94. Hmelo LR. 2016. Quorum Sensing in Marine Microbial Environments. Ann Rev Mar Sci 9:257–281.
95. Sharma A, Singh P, Sarmah BK, Nandi SP. 2020. Quorum sensing: its role in microbial social networking. Res Microbiol 171:159–164.

Appendix: Tables

Table 4.1 Positive matches to roseo box motif 1 likely to be regulated by QS

Genome.ID	Genome.Name	contig	downstream_annotation	motif distance	bitscore
2713896966	*Leisingera aquaemixtae* CECT 8399	Ga0125397_110	acyl homoserine lactone synthase [EC:2.3.1.184]	5	27.6
2667527653	*Leisingera* sp. ANG-M6	Ga0112165_113	cytochrome c peroxidase [EC:1.11.1.5]	372	11.1
		Ga0112165_101	spermidine/putrescine transport system substrate-binding protein	419	10.4
2690316282	*Leisingera* sp. ANG-M7	Ga0112167_105	acyl homoserine lactone synthase [EC:2.3.1.184]	5	31.2
		Ga0112167_107	microcin C transport system permease protein	100	12
2657244983	*Leisingera* sp. ANG-S	Ga0112170_101	acyl homoserine lactone synthase [EC:2.3.1.184]	5	29
		Ga0112170_124	spermidine/putrescine transport system substrate-binding protein	419	10.4
2690316342	*Leisingera* sp. ANG-S5	Ga0112166_127	acyl homoserine lactone synthase [EC:2.3.1.184]	5	29
		Ga0112166_110	16S rRNA (guanine966-N2)-methyltransferase [EC:2.1.1.171]	133	14.5
		Ga0112166_110	cytochrome c peroxidase [EC:1.11.1.5]	372	11.1
2695420551	*Leisingera* sp. ANG-Vp	Ga0112990_1088	spermidine/putrescine transport system substrate-binding protein	421	18.2
2706794654	*Phaeobacter italicus* CECT 7321	Ga0124145_113	acyl homoserine lactone synthase [EC:2.3.1.184]	4	36.7
		Ga0124146_131	acyl homoserine lactone synthase [EC:2.3.1.184]	4	36.7
2713896965	*Phaeobacter* sp. CECT 5382	Ga0125396_106	acyl homoserine lactone synthase [EC:2.3.1.184]	6	30.7
		Ga0125396_107	aerotaxis receptor	529	12.7
2502171179	*Phaeobacter* sp. LSS9	PHLS_contig00027	sorbitol/mannitol transport system permease protein	388	12

Appendix: Figures

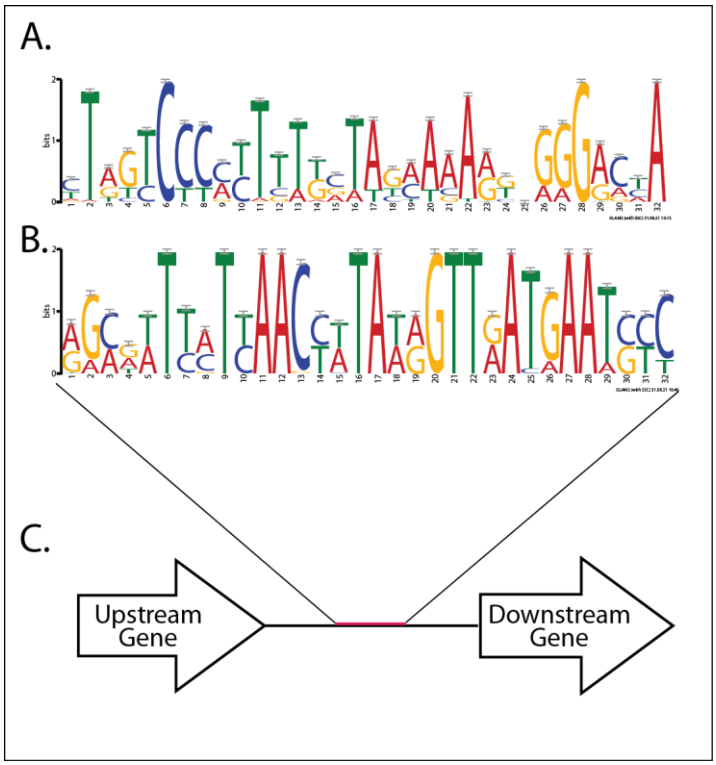

Figure 4.1 Roseo box motifs sequence logos and gene orientation for roseo box motifs 1 (A.) and 2 (B.). Multilevel consensus sequence based on Gapped Local Alignment of Motifs using MEME suite (meme-suite.org). Palindromic sequence typical of lux box motifs can be seen between 6 bp and 28 bp in in A. Motifs were constructed from intergenic region between upstream and downstream genes represented by C. Genomic query for motif matches preserved orientation or upstream and downstream regions regardless of strandedness.

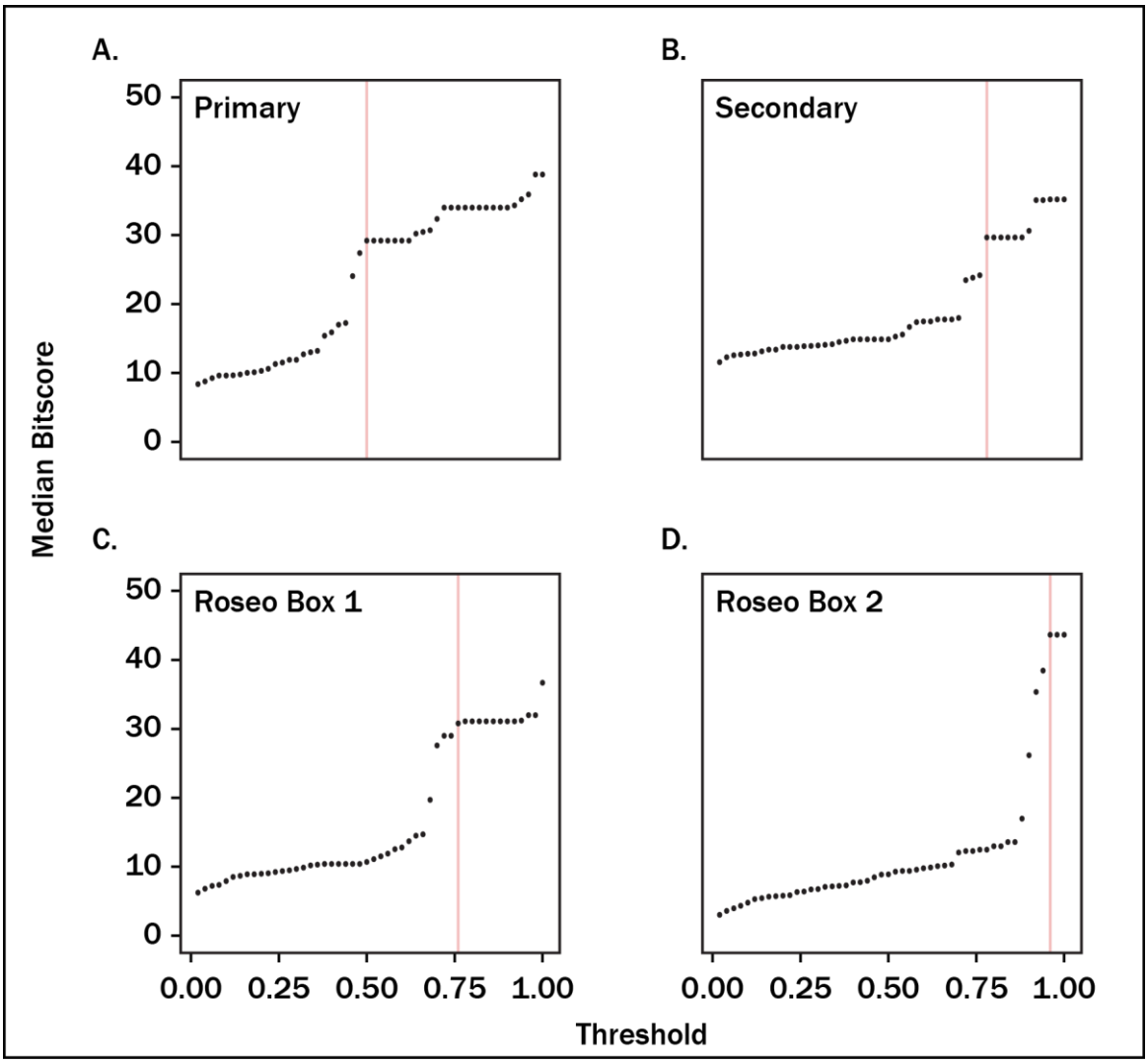

Figure 4.2 Bitscore quantile to determine optimal bitscore threshold for model specificity and sensitivity. Bitscore quantile to determine optimal bitscore threshold for model specificity and sensitivity for primary (A) and secondary (B), in addition to roseo box motif 1 (C) and roseo box motif 2 (D). Median bitscore represents the average bitscore across 30 genomes for motif matches, while bitscore threshold signifies the average maximum false positive constructed for every genome based on fasta-shuffle-fasta. A sharp shift in the bitscore threshold (red line) was used to define the cutoff for putative positive hits to motifs

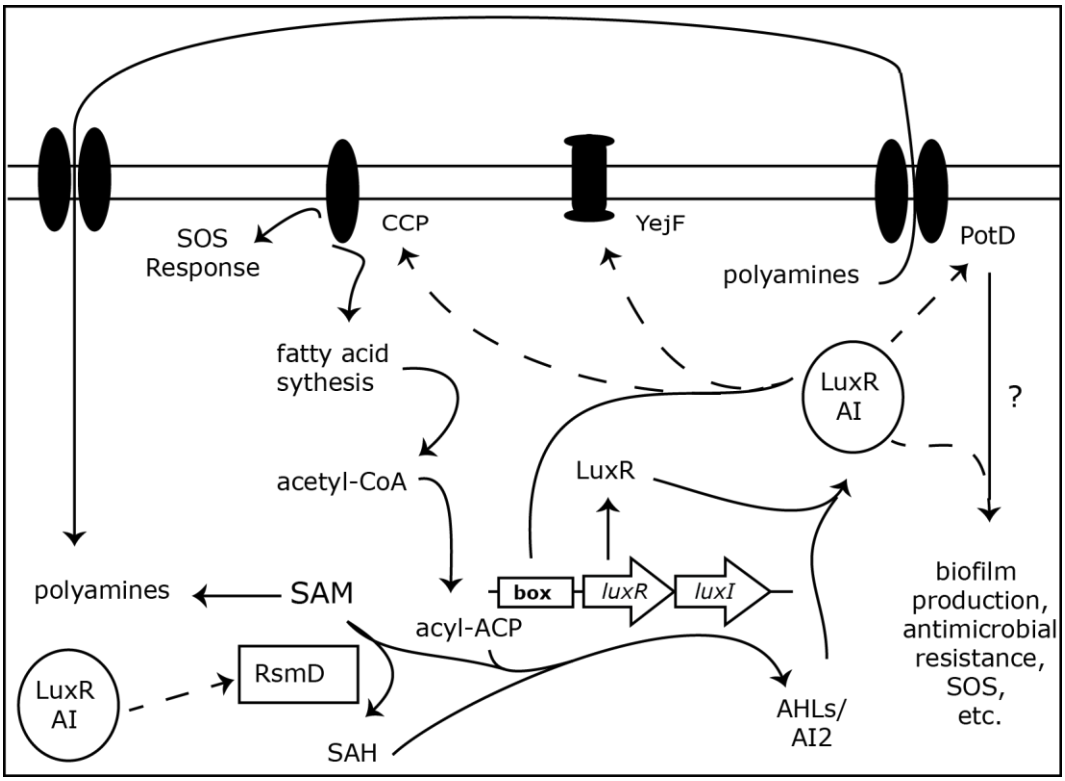

Figure 4.3 Working model of putative QS regulated genes discovered by computational analysis using roseobox motif 1. Black filled ellipses represent transmembrane proteins: PotD (synthesized by *potD*); YejF (synthesized by *yefF*); CCP (cytochrome c peroxidase). Unfilled shapes represent cytoplasmic proteins such as RsmD (synthesized by *rsmD*, protein product represented by retangle) and the LuxR-AI complex (synthesis illustrated and denoted by block arrows). SOS response = bacterial response to DNA and oxidative damage; SAM = S-adenosylmethionine; SAH = S-adenosylhomocysteine; acyl-ACP = acyl-acyl carrier protein; AHLs = acyl homoserine lactones; AI = autoinducer; box = DNA regulatory motif. Solid lines indicate previously reported pathways/mechanisms, dotted lines indicate suggested pathways/mechanisms discussed here.

Appendix: Supplemental Materials

Supplemental Table 4.1 Roseobacter genomes retrieved from IMG

Genome Name	IMG.Genome.ID
Roseobacter sp. AG-891-A04	2894917955
Pseudooceanicola nanhaiensis DSM 18065	2558309102
Wenxinia saemankumensis DSM 100565	2695421046
Epibacterium scottomollicae DSM 25328	2728369517
Dinoroseobacter shibae DFL-12, DSM 16493	2501004205
Roseobacter sp. CCS2	640612221
Roseobacter sp. R2A57	2521172554
Phaeobacter inhibens P66	2814123350
Roseobacter sp. SCGC AB-661-L17	2671180212
Roseobacter sp. AG-359-A03	2894956587
Rhodobacterales sp. HTCC2150	640612203
Sulfitobacter noctilucae NB-68	2579778790
Poseidonocella pacifica DSM 29316	2687453774
Ketogulonicigenium vulgare Y25	649633059
Roseobacter denitrificans FDAARGOS_309	2841198529
Phaeobacter gallaeciensis P129	2814123089
Roseobacter sp. AG-914-O23	2894954409
Ketogulonicigenium vulgare Hbe602	2675903356
Sulfitobacter donghicola DSW-25, KCTC 12864	2574180243
Ketogulonicigenium vulgare SPU B805	2718218202
Celeribacter indicus P73	2528768207
Roseobacter sp. AG-461-K23	2897641642
Ruegeria sp. ANG-R	2660238111
Leisingera sp. ANG-M1	2690316183
Ruegeria marisrubri ZGT118	2724679120
Mameliella alba CGMCC 1.7290	2663762746
Pelagicola litoralis DSM 18290	2574179735
Actibacterium mucosum KCTC 23349	2667527933
Sulfitobacter mediterraneus	2671181181
Planktomarina temperata RCA23, DSM 22400	2548877138
Rhodobacteraceae bacterium bin08	2608642200
Litoreibacter halocynthiae DSM 29467	2681812955
Sedimentitalea nanhaiensis DSM 24252	2521172577
Celeribacter indicus DSM 27257	2693429899
Ruegeria denitrificans CECT 5091	2713896969
Loktanella vestfoldensis DSM 16212	2521172635
Phaeobacter inhibens P10/01/009	2814123246

Supplemental Table 4.1 Continued

Genome Name	IMG.Genome.ID
Leisingera caerulea DSM 24564	2512047087
Phaeobacter gallaeciensis DSM 17395	2510065029
Roseobacter sp. SCGC AG-487_B13 (contamination screened)	2731639170
Roseobacter sp. SCGC AG-487_B10 (contamination screened)	2731639249
Sulfitobacter geojensis MM-124	2582580979
Leisingera sp. ANG-S3	2667528003
Octadecabacter antarcticus 307	2510461047
Yoonia sediminilitoris DSM 29955	2734482292
Litoreibacter janthinus DSM 26921	2617270836
Ponticoccus litoralis DSM 18986	2574179734
Oceanicola sp. MCTG156(1a)	2579779169
Roseobacter sp. N2S	2838011328
Leisingera aquaemixtae CECT 8399	2713896966
Rhodobacteraceae sp. HIMB11	2514885042
Roseovarius sp. MCTG156(2b)	2576861823
Pseudooceanicola antarcticus CGMCC 1.12662	2721755848
Pseudoruegeria sabulilitoris GJMS-35	2728369071
Lutimaribacter pacificus CGMCC 1.10970	2663762718
Epibacterium mobile F1926	2788500500
Roseovarius sp. TM1035	640963035
Phaeobacter inhibens P74	2814123299
Celeribacter persicus DSM 100434	2734482187
Ruegeria intermedia DSM 29341	2695420938
Ruegeria marina CGMCC 1.9108	2617270884
Sulfitobacter guttiformis DSM 11458	2737471612
Limimaricola soesokkakensis DSM 29956	2728369479
Leisingera sp. ANG1	2556921661
Yoonia tamlensis DSM 26879	2619619642
Sulfitobacter noctilucicola NB-77	2574180182
Phaeobacter gallaeciensis P63	2814123091
Roseobacter sp. SAT8	2788500504
Donghicola eburneus DSM 29127	2684622851
Poseidonocella sedimentorum DSM 29315	2634166304
Phaeobacter inhibens P51	2814123291
Yoonia maritima DSM 101533	2731639257
Oceanicola sp. HL-35	2540341247
Jannaschia aquimarina GSW-M26	2603880180
Jhaorihella thermophila DSM 23413	2675903694

Supplemental Table 4.1 Continued

Genome Name	IMG.Genome.ID
Roseovarius tolerans EL-164	2740892180
Tropicibacter naphthalenivorans CECT 7648	2713896963
Ruegeria conchae TW15	2513237272
Celeribacter ethanolicus NH195	2728369167
Donghicola sp. S598	2551306419
Roseovarius lutimaris DSM 28463	2622736530
Planktotalea frisia SH6-1	2703719202
Thalassococcus halodurans DSM 26915	2617270859
Loktanella sp. 5RATIMAR09	2648501310
Phaeobacter gallaeciensis BS107	641380432
Roseobacter sp. SCGC AB-661-I11	2671180213
Sulfitobacter mediterraneus DSM 12244	2734482289
Mameliella alba UMTAT08	2636415558
Octadecabacter temperatus SB1	2654588005
Ruegeria pomeroyi DSS-3	637000267
Sulfitobacter litoralis DSM 17584	2622736527
Rhodobacteraceae bacterium REDSEA-S03_B4	2651870274
Marivivens sp. JLT3646	2721755812
Thalassobacter stenotrophicus CECT 5294	2713896961
Limimaricola hongkongensis DSM 17492	2517434011
Pseudooceanicola nitratireducens CGMCC 1.7292	2663762743
Phaeobacter gallaeciensis P73	2814123117
Rhodobacteraceae bacterium KLH11	647533201
Sulfitobacter sp. NAS-14.1	638341212
Roseovarius mucosus DSM 17069	2518285587
Rhodobacteraceae bacterium bin07 (version 2)	2608642199
Roseobacter denitrificans OCh 114	639633056
Rhodobacteraceae bacterium bin09	2585428049
Ruegeria lacuscaerulensis DSM 11314	2698536695
Salipiger thiooxidans DSM 10146	2615840719
Octadecabacter arcticus 238, DSM 13978	2512564006
Phaeobacter italicus CECT 7645	2706794655
Yoonia maricola DSM 29128	2695420968
Roseobacter sp. GAI101	647533205
Aliiroseovarius sp. PrR006	2890912079
Tropicimonas isoalkanivorans DSM 19548	2615840715
Roseovarius indicus B108 cultivar:MA	2731957848
Marivita geojedonensis DSM 29432	2728369485
Yangia sp. PrR003	2890487060

Supplemental Table 4.1 Continued

Genome Name	IMG.Genome.ID
Sulfitobacter pseudonitzschiae DSM 26824	2695420945
Roseobacter sp. AG-359-L15	2894907910
Roseobacter sp. AG-891-D09	2898190329
Jannaschia seosinensis CECT 7799	2711768077
Citreicella sp. SE45	647533124
Roseobacter sp. AG-911-A11	2894959566
Ruegeria lacuscaerulensis ITI-1157	647533208
Loktanella sp. 3ANDIMAR09	2648501806
Sulfitobacter pontiacus DSM 10014	2622736431
Rhodobacteraceae bacterium REDSEA-S34_B6	2651870280
Shimia abyssi DSM 100673	2728369514
Roseobacter sp. NP7	2788500503
Roseobacter sp. AG-903-P13	2894895117
Yangia sp. PrR004	2890457238
Salipiger profundus DSM 27508	2693429894
Leisingera daeponensis DSM 23529	2521172619
Leisingera sp. ANG-DT	2657245004
Sulfitobacter mediterraneus KCTC 32188	2574179802
Rhodobacteraceae bacterium bin18 (version 2)	2608642210
Octadecabacter temperatus DSM 26878	2698536702
Phaeobacter porticola P97	2718218026
Epibacterium multivorans CECT 7557	2713896962
Litoreibacter ascidiaceicola DSM 100566	2695420937
Roseobacter sp. SP159	2788500509
Litoreibacter albidus DSM 26922	2617270827
Phaeobacter gallaeciensis P75	2814123081
Thalassobacter sp. 16PALIMAR09	2627854218
Halocynthiibacter namhaensis RA2-3	2636415494
Marinovum algicola DSM 10251	2615840718
Phaeobacter gallaeciensis DSM 26640	2558309061
Ruegeria sp. P4	2710724219
Epibacterium mobile 45A6	2504756012
Marinovum algicola DG 898	2513237001
Epibacterium multivorans DSM 26470	2615840706
Leisingera sp. ANG-Vp	2695420551
Roseobacter sp. MED193	638341182
Ruegeria conchae DSM 29317	2734482173
Phaeobacter italicus CECT 7321	2706794654
Pseudophaeobacter arcticus DSM 23566	2521172622

Supplemental Table 4.1 Continued

Genome Name	IMG.Genome.ID
Tateyamaria sp. ANG-S1	2698536347
Celeribacter baekdonensis DSM 27375	2616644820
Pseudooceanicola nitratireducens DSM 29619	2687453758
Monaibacterium marinum C7	2710264757
Oceaniovalibus guishaninsula JLT2003	2519899589
Phaeobacter sp. 11ANDIMAR09	2645728037
Pseudooceanicola batsensis HTCC2597	638341139
Jannaschia helgolandensis DSM 14858	2622736446
Rhodobacteraceae bacterium REDSEA-S02_B3	2651870273
Salipiger aestuarii DSM 22011	2615840712
Sulfitobacter delicatus DSM 16477	2634166359
Antarctobacter heliothermus DSM 11445	2619619037
Shimia gijangensis DSM 100564	2700988697
Rhodobacterales sp. HTCC2083	647533202
Cognatiyoonia koreensis DSM 17925	2619619643
Rhodobacteraceae bacterium bin 12	2608642204
Thalassobacter stenotrophicus	2627854264
Phaeobacter gallaeciensis JL2886	2814123072
Leisingera sp. ANG-M7	2690316282
Jannaschia faecimaris DSM 100420	2693429889
Roseobacter sp. SAG-O19 SCGC AAA160-J18 (contamination screened)	2627853514
Loktanella sp. S4079	2711768163
Yoonia rosea DSM 29591	2681812930
Roseovarius azorensis DSM 100674	2693429884
Pacificibacter marinus DSM 25228	2622736522
Roseobacter sp. AG-*920-O19*	2898191822
Sulfitobacter brevis DSM 11443	2619619004
Roseobacter sp. SK209-2-6	640612220
Aliiroseovarius crassostreae CV919-312	2645727822
Roseobacter sp. AzwK-3b	640963029
Celeribacter halophilus DSM 26270	2593339274
Jannaschia sp. CCS1	637000137
Roseovarius indicus DSM 26383	2619618997
Phaeobacter inhibens DOK1-1	2811995358
Shimia marina DSM 26895	2619618961
Phaeobacter inhibens P70	2814123315
Epibacterium mobile DSM 23403	2693429875
Citreimonas salinaria DSM 26880	2693429906
Oceanicola sp. S124	2526164698

Supplemental Table 4.1 Continued

Genome Name	IMG.Genome.ID
Yoonia vestfoldensis SKA53	638341119
Roseobacter sp. TSBP12	2894961754
Sulfitobacter indolifex HEL-45	641380424
Salipiger pacificus CGMCC 1.3455	2617270881
Roseovarius nanhaiticus CGMCC 1.10961	2667528179
Shimia marina CECT 7688	2713896960
Jannaschia donghaensis CECT 7802	2671180308
Lutimaribacter pacificus DSM 29620	2695420927
Roseovarius tolerans DSM 11457	2619619026
Leisingera sp. ANG-M6	2667527653
Litoreibacter ponti DSM 100977	2734482799
Pelagimonas varians DSM 23678	2734482185
Sulfitobacter donghicola JCM 14565	2588253841
Roseobacter sp. CPC4	2788500506
Leisingera sp. ANG-S	2657244983
Ruegeria atlantica CECT 4292	2713896959
Phaeobacter inhibens P92	2814123287
Roseobacter sp. CHAB-I-5 SCGC AAA076-I17 (contamination screened)	2627853511
Ruegeria sp. PrR005	2895591741
Shimia thalassica CECT 7735	2690315772
Leisingera sp. ANG-S5	2690316342
Ruegeria halocynthiae DSM 27839	2693429872
Phaeobacter gallaeciensis P128	2814123083
Roseobacter sp. NP10	2788500502
Phaeobacter gallaeciensis P11	2814123108
Rhodobacteraceae bacterium EBPR_Bin_228	2619618911
Jannaschia rubra CECT 5088	2711768026
Phaeobacter inhibens P59	2814123324
Phaeobacter inhibens 2.10	2510065028
Aliiroseovarius sediminilitoris DSM 29439	2687453744
Sulfitobacter sp. EE-36	638341211
Pseudaestuariivita atlantica 22II-S11-z3	2645727674
Roseobacter sp. SP57	2788500508
Planktotalea frisia DSM 23709	2593339277
Tropicibacter phthalicicus DSM 26923	2734482174
Roseobacter sp. AG-899-G23	2894943273
Thalassobius gelatinovorus CECT 4357	2684622622
Nereida ignava CECT 5292	2706794653
Maritimibacter sp. HL-12	2545555844

Supplemental Table 4.1 Continued

Genome Name	IMG.Genome.ID
Roseobacter denitrificans DSM 7001	2693429868
Roseovarius marisflavi DSM 29327	2700988702
Roseobacter sp. LE17	2504756015
Phaeobacter inhibens T5, DSM 16374	2574179718
Jannaschia rubra DSM 16279	2622736430
Phaeobacter sp. S60	2675903626
Roseovarius pacificus DSM 29589	2700988706
Phaeobacter inhibens P30/M4-3.1A	2814123329
Phaeobacter inhibens BS107	2841416095
Loktanella fryxellensis DSM 16213	2622736532
Celeribacter halophilus ZXM137	2728369168
Phaeobacter italicus DSM 26436	2622736589
Rhodobacterales sp. Y4I	647533203
Pseudoruegeria haliotis DSM 29328	2728369471
Yangia sp. PrR007	2890359682
Marivita hallyeonensis DSM 29431	2695421018
Sulfitobacter dubius DSM 16472	2616644813
Roseobacter sp. CHAB-I-5 SCGC AAA076-M18 (contamination screened)	2627853512
Maritimibacter sp. REDSEA-S40_B3	2651870217
Ketogulonicigenium robustum SPU_B003	2751185723
Rhodobacteraceae bacterium GWE1_64_9	2721755242
Phaeobacter inhibens S4Sm	2724679070
Maritimibacter alkaliphilus HTCC2654	648276686
Brevirhabdus pacifica DSM 27767	2728369741
Maribius pelagius DSM 26893	2616644821
Roseovarius sp. 217	638341184
Phaeobacter sp. CECT 5382	2713896965
Phaeobacter inhibens P48/M21-2.3	2814123348
Maribius salinus DSM 26892	2619618996
Ruegeria sp. TrichCH4B	647533209
Roseobacter sp. SAG-O19 SCGC AAA015-L03 (contamination screened)	2627853513
Lutimaribacter saemankumensis DSM 28010	2675903213
Thalassobacter stenotrophicus DSM 16310	2585427601
Sulfitobacter pontiacus 3SOLIMAR09	2663763423
Roseovarius nubinhibens ISM	638341183
Ponticoccus marisrubri SJ5A-1	2724679114
Epibacterium mobile S1942	2711768164
Oceanicola sp.	2582581249

Supplemental Table 4.1 Continued

Genome Name	IMG.Genome.ID
Loktanella sp. SE62	2517487002
Salipiger marinus DSM 26424	2615840707
Jannaschia pohangensis DSM 19073	2622736536
Shimia sp. SK013	2645727935
Oceanicola litoreus DSM 29440	2698536701
Pseudoruegeria lutimaris DSM 25294	2622736598
Roseobacter litoralis Och 149	2510065042
Phaeobacter gallaeciensis JL2872	2834652479
Roseovarius litoreus DSM 28249	2700988728
Ruegeria halocynthiae MOLA R1/13b	2597490221
Celeribacter neptunius DSM 26471	2617270870
Salinihabitans flavidus DSM 27842	2634166353
Roseobacter sp. AI77	2894903407
Mameliella alba DSM 26384	2593339298
Roseobacter sp. CHAB-I-5 SCGC AAA076-A02 (contamination screened)	2627853510
Lutimaribacter litoralis DSM 29506	2724679730
Aliiroseovarius halocynthiae DSM 27840	2617270828
Nereida ignava DSM 16309	2599185238
Celeribacter halophilus CGMCC 1.8891	2617270905
Roseovarius nanhaiticus DSM 29590	2681812935
Sulfitobacter sp. 20_GPM-1509m	2556921091
Roseobacter sp. MED633	2788500507
Pseudoruegeria marinistellae SF-16	2728368996
Maritimibacter alkaliphilus DSM 100037	2693429867
Ruegeria profundi ZGT108	2724679119
Phaeobacter sp. LSS9	2502171179
Phaeobacter inhibens P83	2814123277
Ruegeria sp. TM1040	637000268
Thalassobius mediterraneus DSM 16398	2681813506
Litoreibacter meonggei DSM 29466	2681812954
Loktanella sp. 1ANDIMAR09	2648501493
Salipiger bermudensis HTCC2601	648276709
Celeribacter marinus DSM 100036	2693429905
Jannaschia aquimarina DSM 28248	2681813552
Phaeobacter inhibens P88	2814123341
Sulfitobacter pseudonitzschiae H3	2585427828
Shimia haliotis DSM 28453	2619619046
Ruegeria atlantica CECT 4293	2713896958
Oceanicola granulosus HTCC2516	638341140

Supplemental Table 4.1 Continued

Genome Name	IMG.Genome.ID
Phaeobacter inhibens P72	2814123347
Donghicola tyrosinivorans DSM 100212	2731639258
Cognatishimia maritima DSM 28223	2617270829
Loktanella atrilutea DSM 29326	2695420928
Sulfitobacter sp. CB2047	2617271224
Loktanella salsilacus DSM 16199	2622736595
Leisingera aquimarina DSM 24565	2521172617
Cognatishimia activa CECT 5113	2713896968
Loktanella sp. DSM 29012	2675903145
Shimia aestuarii DSM 15283	2616644822
Roseibaca calidilacus HL-91	2603880215
Aestuariivita boseongensis BS-B2	2648501248
Yoonia litorea DSM 29433	2687453745
Pseudooceanicola atlanticus 22II-S11g	2645727778
Cognatiyoonia sediminum DSM 28715	2695421013
Ruegeria sp. R11	647533206
Phaeobacter inhibens P80	2814123328
Citreicella sp. 357	2513237353
Pseudooceanicola flagellatus CGMCC 1.12644	2718217653
Ruegeria sp. ANG-S4	2663763207
Litorimicrobium taeanense DSM 22007	2615840713
Sulfitobacter guttiformis KCTC 32187	2579778904
Shimia isoporae DSM 26433	2728369275
Thalassobium sp. R2A62	647533238
Ketogulonicigenium vulgare SKV	2811995318
Phaeobacter sp. O365	2687453711
Pseudodonghicola xiamenensis DSM 18339	2524023213
Roseobacter sp. EAC695	2788500505
Ketogulonicigenium vulgare WSH-001	2511231188
Ruegeria faecimaris DSM 28009	2724679780
Celeribacter marinus IMCC12053	2654587720
Phaeobacter inhibens P54	2814123349
Shimia sagamensis DSM 29734	2724679805
Phaeobacter inhibens P57	2814123273
Sulfitobacter marinus DSM 23422	2619619641
Roseovarius halotolerans DSM 29507	2728369466
Salipiger pacificus DSM 26894	2619618962
Limimaricola cinnabarinus LL-001	2602041674
Thalassobius mediterraneus CECT 5383	2713896964

Supplemental Table 4.1 Continued

Genome Name	IMG.Genome.ID
Thalassobius gelatinovorus DSM 5887	2622736435
Sediminimonas qiaohouensis DSM 21189	2523533612
Maribius sp. MOLA 401	2597490207
Yangia sp. PrR002	2890379745
Epibacterium ulvae U95	2622736501
Ruegeria sp. 6PALISEP08	2634166458
Phaeobacter inhibens P78	2814123300
Tropicibacter naphthalenivorans DSM 19561	2622736506
Hasllibacter halocynthiae DSM 29318	2681812958
Lentibacter algarum DSM 24677	2693429861
Nautella sp. ECSMB14104	2627854045
Sedimentitalea nanhaiensis CGMCC 1.10959	2667527411
Roseobacter sp. SCGC AB-661-M21	2671180211
Phaeobacter piscinae S26	2671181183
Celeribacter baekdonensis B30	2519899583
Cognatishimia activa CECT 5114	2698536607
Maritimibacter sp. REDSEA-S28_B5	2651870216
Salipiger mucosus DSM 16094	2523231081
Sagittula stellata E-37	640612219
Phaeobacter inhibens P24/M2-4.4	2814123342
Leisingera methylohalidivorans MB2, DSM 14336	2512564009
Wenxinia marina DSM 24838	2515154190
Sulfitobacter sp. SA11	2519103045
Phaeobacter gallaeciensis C3M10	2834656465
Aliiroseovarius crassostreae DSM 16950	2619619030
Sulfitobacter sp. AM1-D1	2721755576
Hwanghaeicola aestuarii DSM 22009	2593339276

Supplemental Table 4.2. Roseobacter PgaI/PhaI homologs with a 50% protein identify threshold cutoff

		PgaI Homologs				PhaI Homologs			
Genome.ID	Genome.Name	Gene.Id	E.value	Identities	Coverage	Gene.Id	E.value.	Identities	Coverage
647533203	Rhodobacterales sp. Y4I	647618890	3.00E-163	100	213	647616507	2.00E-167	100	221
2521172619	*Leisingera daeponensis* DSM 23529	2521645937	1.00E-161	99	213	2521647319	5.00E-165	99	221
2512047087	*Leisingera caerulea DSM* 24564	2512536472	5.00E-156	95	213	2512537815	7.00E-149	90	221
2713896966	*Leisingera aquaemixtae* CECT 8399	2715048052	5.00E-156	94	213	2715049187	2.00E-159	95	221
2690316183	*Leisingera* sp. ANG-M1	2692597578	3.00E-137	83	213				
2695420551	*Leisingera* sp. ANG-Vp	2696489217	2.00E-135	81	213				
2512564009	*Leisingera methylohalidivorans* MB2, DSM 14336	2512613835	2.00E-115	74	213	2512615344	1.00E-116	74	221
2556921661	*Leisingera* sp. ANG1	2558250491	3.00E-118	74	213				
2657245004	*Leisingera* sp. ANG-DT	2657707777	3.00E-118	74	213				
2667527653	*Leisingera* sp. ANG-M6	2668947550	3.00E-118	74	213				
2657244983	*Leisingera* sp. ANG-S	2657626006	3.00E-118	74	213				
2667528003	*Leisingera* sp. ANG-S3	2670393176	3.00E-118	74	213				
2690316342	*Leisingera* sp. ANG-S5	2693277602	3.00E-118	74	213				
2521172617	*Leisingera aquimarina* DSM 24565	2521633632	6.00E-117	72	213				
2690316282	*Leisingera* sp. ANG-M7	2693016765	1.00E-117	72	213	2693018497	1.00E-126	75	221
2814123329	*Phaeobacter inhibens* P30/M4-3.1A	2815622585	6.00E-49	69	101				
2718218026	*Phaeobacter porticola* P97	2719802526	5.00E-111	68	213				

Supplemental Table 4.2 Continued

		PgaI Homologs				PhaI Homologs			
Genome.ID	Genome.Name	Gene.Id	E.value	Identities	Coverage	Gene.Id	E.value.	Identities	Coverage
2558309061	*Phaeobacter gallaeciensis* DSM 26640	2558538489	2.00E-110	67	213				
2834652479	*Phaeobacter gallaeciensis* JL2872	2834653884	3.00E-107	67	213				
2814123072	*Phaeobacter gallaeciensis* JL2886	2814712172	3.00E-107	67	213				
2814123108	*Phaeobacter gallaeciensis* P11	2814827496	2.00E-110	67	213				
2814123083	*Phaeobacter gallaeciensis* P128	2814752684	1.00E-110	67	213				
2814123089	*Phaeobacter gallaeciensis* P129	2814778134	1.00E-110	67	213				
2814123091	*Phaeobacter gallaeciensis* P63	2814788702	2.00E-110	67	213				
2814123117	*Phaeobacter gallaeciensis* P73	2814857398	2.00E-110	67	213				
2814123081	*Phaeobacter gallaeciensis* P75	2814746517	2.00E-110	67	213				
2510065028	*Phaeobacter inhibens* 2.10	2510175116	3.00E-109	67	213	2510176667	8.00E-96	62	235
2671181183	*Phaeobacter piscinae* S26	2675854848	2.00E-111	67	213	2675854659	2.00E-94	61	235
2502171179	*Phaeobacter* sp. LSS9	2502320848	4.00E-111	67	246				
2675903626	*Phaeobacter* sp. S60	2678680233	2.00E-111	67	213	2678680401	2.00E-94	61	235
2521172622	*Pseudophaeobacter arcticus* DSM 23566	2521660572	4.00E-109	67	213				
641380432	*Phaeobacter gallaeciensis* BS107	641477384	1.00E-108	66	213				
2510065029	*Phaeobacter gallaeciensis* DSM 17395	2510178954	1.00E-108	66	213				
2841416095	*Phaeobacter inhibens* BS107	2841416487	1.00E-108	66	213				

Supplemental Table 4.2 Continued

Genome.ID	Genome.Name	PgaI Homologs				PhaI Homologs			
		Gene.Id	E.value	Identities	Coverage	Gene.Id	E.value.	Identities	Coverage
2811995358	*Phaeobacter inhibens* DOK1-1	2814046713	1.00E-108	66	213				
2814123246	*Phaeobacter inhibens* P10/01/009	2815315383	1.00E-108	66	213				
2814123342	*Phaeobacter inhibens* P24/M2-4.4	2815674143	2.00E-108	66	213				
2814123348	*Phaeobacter inhibens* P48/M21-2.3	2815697831	1.00E-108	66	213				
2814123291	*Phaeobacter inhibens* P51	2815472527	1.00E-108	66	213				
2814123349	*Phaeobacter inhibens* P54	2815701441	1.00E-108	66	213				
2814123273	*Phaeobacter inhibens* P57	2815400644	1.00E-108	66	213				
2814123324	*Phaeobacter inhibens* P59	2815601796	3.00E-108	66	213				
2814123350	*Phaeobacter inhibens* P66	2815708485	2.00E-108	66	213				
2814123315	*Phaeobacter inhibens* P70	2815570623	2.00E-108	66	213				
2814123347	*Phaeobacter inhibens* P72	2815693590	2.00E-108	66	213				
2814123299	*Phaeobacter inhibens* P74	2815508653	2.00E-108	66	213				
2814123300	*Phaeobacter inhibens* P78	2815515329	1.00E-108	66	213				
2814123328	*Phaeobacter inhibens* P80	2815620805	2.00E-108	66	213				
2814123277	*Phaeobacter inhibens* P83	2815418577	2.00E-108	66	213				
2814123341	*Phaeobacter inhibens* P88	2815669641	2.00E-108	66	213				
2814123287	*Phaeobacter inhibens* P92	2815457027	2.00E-108	66	213				

Supplemental Table 4.2 Continued

		PgaI Homologs				PhaI Homologs			
Genome.ID	Genome.Name	Gene.Id	E.value	Identities	Coverage	Gene.Id	E.value.	Identities	Coverage
2724679070	*Phaeobacter inhibens* S4Sm	2725334607	8.00E-109	66	213	2725332037	9.00E-95	62	235
2574179718	*Phaeobacter inhibens* T5, DSM 16374	2574250588	1.00E-108	66	213	2574252193	2.00E-94	62	235
2645728037	*Phaeobacter* sp. 11ANDIMAR09	2648045913	4.00E-105	65	213				
638341182	*Roseobacter* sp. MED193	638933006	2.00E-106	65	213				
2521172554	*Roseobacter* sp. R2A57	2521413937	9.00E-57	65	123				
647533238	*Thalassobium* sp. R2A62	647777443	4.00E-27	65	78				
2627854045	*Nautell*a sp. ECSMB14104	2629996650	8.00E-103	64	213				
2706794655	*Phaeobacter italicus* CECT 7645	2707822120	5.00E-103	64	213				
2622736589	*Phaeobacter italicus* DSM 26436	2623437402	5.00E-103	64	213				
2713896965	*Phaeobacter* sp. CECT 5382	2715044697	2.00E-105	64	213				
647533206	*Ruegeria* sp. R11	647637122	4.00E-103	64	213				
2648501248	*Aestuariivita boseongensis* BS-B2	2649150261	2.00E-93	63	212				
2706794654	*Phaeobacter italicus* CECT 7321	2707816858	8.00E-100	63	211				
2814123329	*Phaeobacter inhibens* P30/M4-3.1A	2815622588	6.00E-53	62	128				
2834656465	*Phaeobacter gallaeciensis* C3M10	2834660013	8.00E-91	61	212				
2894903407	*Roseobacte*r sp. AI77	2894903978	1.00E-88	61	212				
2695420945	*Sulfitobacter pseudonitzschiae* DSM 26824	2698164249	2.00E-90	61	212				

Supplemental Table 4.2 Continued

		PgaI Homologs				PhaI Homologs			
Genome.ID	Genome.Name	Gene.Id	E.value	Identities	Coverage	Gene.Id	E.value.	Identities	Coverage
2585427828	*Sulfitobacter pseudonitzschiae* H3	2586895770	2.00E-90	61	212				
2700988706	*Roseovarius pacificus* DSM 29589	2701217768	1.00E-88	60	210				
2582580979	*Sulfitobacter geojensis* MM-124	2584129863	4.00E-85	60	211				
2556921091	*Sulfitobacter* sp. 20_GPM-1509m	2557389984	6.00E-89	60	212				
2663762746	*Mameliella alba* CGMCC 1.7290	2664204694	1.00E-83	59	213				
2593339298	*Mameliella alba* DSM 26384	2595668600	1.00E-83	59	213				
2724679114	*Ponticoccus marisrubri* SJ5A-1	2725509504	4.00E-85	59	212				
2693429868	*Roseobacter denitrificans* DSM 7001	2694923001	4.00E-89	59	212				
2841198529	*Roseobacter denitrificans* FDAARGOS_309	2841202115	4.00E-89	59	212				
639633056	*Roseobacter denitrificans* OCh 114	639635080	4.00E-89	59	212				
2510065042	*Roseobacter litoralis* Och 149	2510236598	1.00E-88	59	212				
2894917955	*Roseobacter* sp. AG-891-A04	2894918687	7.00E-24	59	78				
637000267	*Ruegeria pomeroyi* DSS-3	637287864	4.00E-88	59	212				
2667527411	*Sedimentitalea nanhaiensis* CGMCC 1.10959	2668049690	4.00E-91	59	212				
2521172577	*Sedimentitalea nanhaiensis* DSM 24252	2521520239	4.00E-91	59	212				
2690315772	*Shimia thalassica* CECT 7735	2691038137	1.00E-87	59	212				

Supplemental Table 4.2 Continued

		PgaI Homologs				PhaI Homologs			
Genome.ID	Genome.Name	Gene.Id	E.value	Identities	Coverage	Gene.Id	E.value.	Identities	Coverage
2619619004	*Sulfitobacter brevis* DSM 11443	2620355733	2.00E-77	59	192				
2698536347	*Tateyamaria* sp. ANG-S1	2698718636	1.00E-81	59	211				
2713896963	*Tropicibacter naphthalenivorans* CECT 7648	2715037021	1.00E-86	59	212				
2622736506	*Tropicibacter naphthalenivorans* DSM 19561	2623184230	1.00E-86	59	212				
2619619037	*Antarctobacter heliothermus* DSM 11445	2620498147	2.00E-84	58	212				
2693429906	*Citreimonas salinaria* DSM 26880	2695084676	7.00E-87	58	227				
2675903694	*Jhaorihella thermophila* DSM 23413	2678963136	5.00E-85	58	223				
2636415558	*Mameliella alba* UMTAT08	2637050256	4.00E-83	58	213				
2728369485	*Marivita geojedonensis* DSM 29432	2730545812	4.00E-85	58	212				
2695421018	*Marivita hallyeonensis* DSM 29431	2698434642	1.00E-82	58	212				
2574179735	*Pelagicola litoralis* DSM 18290	2574316886	5.00E-83	58	213				
2627853510	*Roseobacter* sp. CHAB-I-5 SCGC AAA076-A02 (contamination screened)	2627883052	4.00E-11	58	61				
647533205	*Roseobacte*r sp. GAI101	647646372	3.00E-83	58	211				

Supplemental Table 4.2 Continued

Genome.ID	Genome.Name	PgaI Homologs				PhaI Homologs			
		Gene.Id	E.value	Identities	Coverage	Gene.Id	E.value.	Identities	Coverage
2698536695	*Ruegeria lacuscaerulensis* DSM 11314	2700130482	1.00E-80	58	212				
647533208	Ruegeria lacuscaerulensis ITI-1157	647838199	1.00E-80	58	212				
640612219	Sagittula stellata E-37	640643757	6.00E-82	58	212				
2634166353	Salinihabitans flavidus DSM 27842	2635339879	2.00E-80	58	212				
2700988697	*Shimia gijangensis* DSM 100564	2701178612	1.00E-84	58	214				
2615840713	*Litorimicrobium taeanense* DSM 22007	2616592786	1.00E-84	57	212				
2593339277	*Planktotalea frisia* DSM 23709	2595589918	4.00E-84	57	211				
2703719202	*Planktotalea frisia* SH6-1	2705892174	4.00E-84	57	211				
2894954409	*Roseobacte*r sp. AG-914-O23	2894954541	2.00E-27	57	92				
2724679780	*Ruegeria faecimaris* DSM 28009	2728043131	3.00E-81	57	212				
2693429872	*Ruegeria halocynthiae* DSM 27839	2694939882	2.00E-82	57	212				
2695420938	*Ruegeria intermedia* DSM 29341	2698138481	1.00E-80	57	212				
2698536695	*Ruegeria lacuscaerulensis* DSM 11314	2700131912	6.00E-81	57	221				
647533208	*Ruegeria lacuscaerulensis* ITI-1157	647839284	6.00E-81	57	221				
2724679120	*Ruegeria marisrubri* ZGT118	2725536902	1.00E-81	57	212				
2634166458	*Ruegeria* sp. 6PALISEP08	2635754306	5.00E-81	57	212				

Supplemental Table 4.2 Continued

		PgaI Homologs				PhaI Homologs			
Genome.ID	Genome.Name	Gene.Id	E.value	Identities	Coverage	Gene.Id	E.value.	Identities	Coverage
2660238111	*Ruegeria* sp. ANG-R	2661076398	3.00E-83	57	212				
2895591741	*Ruegeria* sp. PrR005	2895593658	1.00E-84	57	212				
2615840707	*Salipiger marinus* DSM 26424	2616568982	1.00E-79	57	214				
2616644822	*Shimia aestuarii* DSM 15283	2616718007	4.00E-83	57	212				
2619619641	*Sulfitobacter marinus* DSM 23422	2622718838	4.00E-81	57	211				
2579778790	*Sulfitobacter noctilucae* NB-68	2580992102	2.00E-82	57	211				
2574180182	*Sulfitobacter noctilucicola* NB-77	2575896298	2.00E-83	57	211				
2724679730	*Lutimaribacter litoralis* DSM 29506	2727917226	3.00E-84	56	212				
2721755812	*Marivivens* sp. JLT3646	2724054074	3.00E-81	56	210				
2728369471	*Pseudoruegeria haliotis* DSM 29328	2730483723	8.00E-73	56	214				
647533201	*Rhodobacteraceae bacterium* KLH11	647668484	5.00E-82	56	212				
2713896958	*Ruegeria atlantica* CECT 4293	2715016549	5.00E-81	56	212				
2734482173	*Ruegeria conchae* DSM 29317	2735473802	2.00E-82	56	212				
2513237272	*Ruegeria conchae* TW15	2514313393	2.00E-82	56	212				
2713896969	*Ruegeria denitrificans* CECT 5091	2715060965	2.00E-81	56	212				
2597490221	*Ruegeria halocynthiae* MOLA R1/13b	2598760842	3.00E-80	56	212				
2617270884	*Ruegeria marina* CGMCC 1.9108	2617889734	4.00E-85	56	212				
2724679119	*Ruegeria profundi* ZGT108	2725532134	1.00E-80	56	212				

Supplemental Table 4.2 Continued

Genome.ID	Genome.Name	PgaI Homologs				PhaI Homologs			
		Gene.Id	E.value	Identities	Coverage	Gene.Id	E.value.	Identities	Coverage
2693429894	*Salipiger profundus* DSM 27508	2695029478	4.00E-80	56	212				
2728369514	*Shimia abyssi* DSM 100673	2730668113	2.00E-82	56	215				
2645727822	*Aliiroseovarius crassostreae* CV919-312	2647118074	1.00E-75	55	216				
2619619030	*Aliiroseovarius crassostreae* DSM 16950	2620456446	1.00E-75	55	216				
647533124	*Citreicella* sp. SE45	647841250	7.00E-79	55	211				
2615840718	*Marinovum algicola* DSM 10251	2616612792	6.00E-79	55	210				
2622736598	*Pseudoruegeria lutimaris* DSM 25294	2623472697	8.00E-74	55	212				
2693429884	*Roseovarius azorensis* DSM 100674	2694983240	3.00E-76	55	208				
2663763207	*Ruegeria* sp. ANG-S4	2666090598	2.00E-80	55	212				
2617270859	*Thalassococcus halodurans* DSM 26915	2617773595	5.00E-82	55	211				
2728369167	*Celeribacter ethanolicus* NH195	2729475817	2.00E-73	54	212				
2734482187	*Celeribacter persicus* DSM 100434	2735529169	2.00E-74	54	212				
2513237353	*Ci*treicella sp. 357	2514595725	6.00E-76	54	211				
2513237001	*Marinovum algicola* DG 898	2513244918	8.00E-80	54	210				
2545555844	*Maritimibacter* sp. HL-12	2545718731	5.00E-64	54	215				
2574179734	*Ponticoccus litoralis* DSM 18986	2574314549	2.00E-81	54	212				

Supplemental Table 4.2 Continued

		PgaI Homologs				PhaI Homologs			
Genome.ID	Genome.Name	Gene.Id	E.value	Identities	Coverage	Gene.Id	E.value.	Identities	Coverage
2634166304	*Poseidonocella sedimentorum* DSM 29315	2635110626	5.00E-77	54	211				
2645727674	*Pseudaestuariivita atlantica* 22II-S11-z3	2646473668	7.00E-77	54	210				
2718217653	*Pseudooceanicola flagellatus* CGMCC 1.12644	2718371102	1.00E-80	54	212				
2728369071	*Pseudoruegeria sabulilitoris* GJMS-35	2729008511	2.00E-76	54	212				
2622736530	*Roseovarius lutimaris* DSM 28463	2623275602	6.00E-82	54	208				
2700988702	*Roseovarius marisflavi* DSM 29327	2701200911	9.00E-80	54	208				
2895591741	*Ruegeria* sp. PrR005	2895594844	5.00E-71	54	193				
2615840712	*Salipiger aestuarii* DSM 22011	2616586881	6.00E-76	54	211				
2523231081	*Salipiger mucosus* DSM 16094	2523509616	6.00E-79	54	211				
2615840719	*Salipiger thiooxidans* DSM 10146	2616618122	1.00E-77	54	211				
2734482292	*Yoonia sediminilitoris* DSM 29955	2735950330	2.00E-78	54	211				
2617270828	*Aliiroseovarius halocynthiae* DSM 27840	2617672683	2.00E-70	53	216				
2519899583	*Celeribacter baekdonensis* B30	2520219623	1.00E-72	53	212				
2616644820	*Celeribacter baekdonensis* DSM 27375	2616710789	2.00E-72	53	212				

Supplemental Table 4.2 Continued

Genome.ID	Genome.Name	PgaI Homologs				PhaI Homologs			
		Gene.Id	E.value	Identities	Coverage	Gene.Id	E.value.	Identities	Coverage
2617270905	*Celeribacter halophilus* CGMCC 1.8891	2617972339	2.00E-72	53	212				
2593339274	*Celeribacter halophilus* DSM 26270	2595579730	2.00E-72	53	212				
2728369168	*Celeribacter halophilus* ZXM137	2729479253	2.00E-72	53	212				
2617270870	*Celeribacter neptunius* DSM 26471	2617826380	1.00E-74	53	212				
2693429867	*Maritimibacter alkaliphilus* DSM 100037	2694917004	4.00E-70	53	213				
648276686	*Maritimibacter alkaliphilus* HTCC2654	648278257	4.00E-70	53	213				
2651870216	*Maritimibacter* sp. REDSEA-S28_B5	2654134524	2.00E-69	53	215				
2651870217	*Maritimibacter* sp. REDSEA-S40_B3	2654140265	2.00E-69	53	215				
2582581249	*Oceanicola* sp.	2585045553	3.00E-70	53	211				
2734482185	*Pelagimonas varians* DSM 23678	2735522648	1.00E-80	53	221				
2608642200	*Rhodobacteraceae bacterium* bin08	2609099027	3.00E-70	53	211				
2585428049	*Rhodobacteraceae bacterium* bin09	2587698236	3.00E-67	53	217				
2894961754	*Roseobacter* sp. TSBP12	2894965322	1.00E-72	53	212				
2574180243	*Sulfitobacter donghicola* DSW-25, KCTC 12864	2576119543	2.00E-73	53	211				
2588253841	*Sulfitobacter donghicola* JCM 14565	2588962487	2.00E-73	53	211				
2519103045	*Sulfitobacter* sp. SA11	2519255589	1.00E-70	53	245				

Supplemental Table 4.2 Continued

Genome.ID	Genome.Name	PgaI Homologs				PhaI Homologs			
		Gene.Id	E.value	Identities	Coverage	Gene.Id	E.value.	Identities	Coverage
2615840715	*Tropicimonas isoalkanivorans* DSM 19548	2616600143	2.00E-71	53	214				
2890912079	*Al*iiroseovarius sp. PrR006	2890913925	3.00E-70	52	216				
2693429899	*Celeribacter indicus* DSM 27257	2695054990	2.00E-70	52	212				
2528768207	*Celeribacter indicus* P73	2529193760	2.00E-70	52	212				
2619619643	*Cognatiyoonia koreensis* DSM 17925	2622725072	2.00E-69	52	209				
2593339276	*Hwanghaeicola aestuarii* DSM 22009	2595586164	1.00E-71	52	212				
2734482799	*Litoreibacter ponti* DSM 100977	2737437574	2.00E-71	52	220				
2695420928	*Loktanella atrilutea* DSM 29326	2698096077	1.00E-69	52	212				
2622736595	*Loktanella salsilacus* DSM 16199	2623467449	2.00E-72	52	212				
2706794653	*Nereida ignava* CECT 5292	2707814681	5.00E-74	52	237				
2599185238	*Nereida ignava* DSM 16309	2599732352	5.00E-74	52	237				
2698536701	*Oceanicola litoreus* DSM 29440	2700155418	1.00E-76	52	212				
2510461047	*Octadecabacter antarcticus* 307	2510759375	8.00E-73	52	212				
2687453774	*Poseidonocella pacifica* DSM 29316	2690121817	8.00E-71	52	213				
2894959566	*Roseobacter* sp. AG-911-A11	2894960889	9.00E-52	52	164				
2898191822	*Roseobacter* sp. AG-920-O19	2898193607	7.00E-52	52	164				
2731957848	*Roseovarius indicus* B108 cultivar:MA	2733476913	4.00E-76	52	211				

Supplemental Table 4.2 Continued

Genome.ID	Genome.Name	PgaI Homologs				PhaI Homologs			
		Gene.Id	E.value	Identities	Coverage	Gene.Id	E.value.	Identities	Coverage
2619618997	*Roseovarius indicus* DSM 26383	2620330715	4.00E-76	52	211				
2523533612	*Sediminimonas qiaohouensis* DSM 21189	2523944979	6.00E-78	52	211				
2737471612	*Sulfitobacter guttiformis* DSM 11458	2737514737	2.00E-73	52	211				
2579778904	*Sulfitobacter guttiformis* KCTC 32187	2581483017	2.00E-73	52	211				
2734482174	*Tropicibacter phthalicicus* DSM 26923	2735475891	4.00E-77	52	221				
2695421013	*Cognatiyoonia sediminum* DSM 28715	2698405886	1.00E-69	51	209				
2636415494	*Halocynthiibacter namhaensis* RA2-3	2636809389	5.00E-70	51	210				
2693429861	*Lentibacter algarum* DSM 24677	2694891015	3.00E-72	51	211				
2617270836	*Litoreibacter janthinus* DSM 26921	2617712094	3.00E-67	51	210				
2622736522	*Pacificibacter marinus* DSM 25228	2623242520	6.00E-71	51	217				
2728368996	*Pseudoruegeria marinistellae* SF-16	2728740874	3.00E-69	51	214				
647533202	Rhodobacterales sp. HTCC2083	647612720	1.00E-75	51	207				
2894956587	*Roseobacter* sp. AG-359-A03	2894957316	5.00E-51	51	164				
640963029	*Roseobacter* sp. AzwK-3b	641155385	3.00E-67	51	212				
2576861823	*Roseovarius* sp. MCTG156(2b)	2579755962	1.00E-67	51	208				

Supplemental Table 4.2 Continued

		PgaI Homologs				PhaI Homologs			
Genome.ID	Genome.Name	Gene.Id	E.value	Identities	Coverage	Gene.Id	E.value.	Identities	Coverage
2619619642	*Yoonia tamlensis* DSM 26879	2622722072	2.00E-71	51	211				
2687453744	*Aliiroseovarius sediminilitoris* DSM 29439	2689997833	8.00E-68	50	216				
2693429905	*Celeribacter marinus* DSM 100036	2695081274	1.00E-69	50	213				
2654587720	*Celeribacter marinus* IMCC12053	2655545080	1.00E-69	50	213				
2501004205	*Dinoroseobacter shibae* DFL-12, DSM 16493	2501024736	7.00E-71	50	206				
2681812954	*Litoreibacter meonggei* DSM 29466	2682261909	1.00E-67	50	210				
2517487002	*Loktanella* sp. SE62	2517495029	2.00E-70	50	211				
2700988728	*Roseovarius litoreus* DSM 28249	2701327190	7.00E-66	50	212				
2731639257	*Yoonia maritima* DSM 101533	2731932731	2.00E-69	50	211				
2512047087	*Leisingera caerulea* DSM 24564					2512537815	7.00E-149	90	221

Supplemental Table 4.3. Positive matches to primary motif using initial model

Genome.ID	Genome.Name	contig	strand	downstream_annotation	motif distance	bitscore
2713896966	*Leisingera aquaemixtae* CECT 8399	Ga0125397_110	-	conserved hypothetical protein	3195	35.9
		Ga0125397_110	+	acyl homoserine lactone synthase	2	30.2
2521172617	*Leisingera aquimarina* DSM 24565	NA	NA	NA	NA	
2512047087	*Leisingera caerulea* DSM 24564	PhacaeDRAFT_Scaffold1.6	+	(R)-ethylmalonyl-CoA mutase	5326	33.6
		PhacaeDRAFT_Scaffold1.6	-	DNA-binding transcriptional regulator, CsgD family	57	17
		PhacaeDRAFT_Scaffold3.7	-	methyl-accepting chemotaxis protein	1492	13.9
		PhacaeDRAFT_Scaffold2.3	+	NADPH2:quinone reductase	4384	10.4
2521172619	*Leisingera daeponensis* DSM 23529	NA	NA	NA	NA	
2512564009	*Leisingera methylohalidivorans* MB2, DSM 14336	Leime_Contig76.3	-	conserved hypothetical protein	3155	30.7
		Leime_Contig76.3	+	N-acyl-L-homoserine lactone synthetase	3	30
		Leime_Contig75.2	-	iron(III) transport system permease protein	1234	10.8
2556921661	*Leisingera* sp. ANG1	ANG1_gi328751003.54	+	(R)-ethylmalonyl-CoA mutase	4122	38.8
		ANG1_gi328751003.54	-	DNA-binding transcriptional regulator, CsgD family	56	29.2
		ANG1_gi328751055.2	+	bifunctional NMN adenylyltransferase/nudix hydrolase	670	11.5
		ANG1_gi328751025.32	+	uridylate kinase	6360	11.3
2657245004	*Leisingera* sp. ANG-DT	Ga0112991_111	+	(R)-ethylmalonyl-CoA mutase	4122	38.8
		Ga0112991_111	-	DNA-binding transcriptional regulator, CsgD family	56	29.2
		Ga0112991_101	+	uridylate kinase	6360	13
2690316183	*Leisingera* sp. ANG-M1	Ga0112989_106	+	(R)-ethylmalonyl-CoA mutase	4125	35.8
		Ga0112989_106	-	regulatory protein, luxR family	60	17
		Ga0112989_108	+	uridylate kinase	6682	17
		Ga0112989_127	-	DNA-binding transcriptional regulator, ArsR family	354	11.8
		Ga0112989_130	-	DNA-binding protein H-NS	4471	10.9
		Ga0112989_130	+	hypothetical protein	2902	10.6

Supplemental Table 4.3 Continued

Genome.ID	Genome.Name	contig	strand	downstream_annotation	motif distance	bitscore
2667527653	*Leisingera* sp. ANG-M6	Ga0112165_121	+	(R)-ethylmalonyl-CoA mutase	4122	38.8
		Ga0112165_121	-	DNA-binding transcriptional regulator, CsgD family	56	29.2
		Ga0112165_117	+	uridylate kinase	6359	13
2690316282	*Leisingera* sp. ANG-M7	Ga0112167_105	-	conserved hypothetical protein	3146	40.1
		Ga0112167_105	+	acyl homoserine lactone synthase	2	30.7
		Ga0112167_104	+	transcriptional regulator, LacI family	6142	13.6
		Ga0112167_113	-	hypothetical protein	111	11.9
2657244983	*Leisingera* sp. ANG-S	Ga0112170_101	-	conserved hypothetical protein	3060	38.8
		Ga0112170_101	+	acyl homoserine lactone synthase	2	29.2
		Ga0112170_120	-	Predicted ATP-dependent endonuclease of the OLD family, contains P-loop ATPase and TOPRIM domains	1453	11.5
		Ga0112170_109	+	uridylate kinase	6360	11.3
2667528003	*Leisingera* sp. ANG-S3	Ga0112164_105	+	(R)-ethylmalonyl-CoA mutase	4122	38.8
		Ga0112164_105	-	DNA-binding transcriptional regulator, CsgD family	56	29.2
		Ga0112164_120	+	bifunctional NMN adenylyltransferase/nudix hydrolase	670	11.5
		Ga0112164_102	+	uridylate kinase	6360	11.3
2690316342	*Leisingera* sp. ANG-S5	Ga0112166_127	-	conserved hypothetical protein	3060	38.8
		Ga0112166_127	+	acyl homoserine lactone synthase	2	29.2
		Ga0112166_110	+	16S rRNA (guanine966-N2)-methyltransferase	130	15.9
		Ga0112166_103	+	uridylate kinase	6366	11.3
2695420551	*Leisingera* sp. ANG-Vp	Ga0112990_1047	+	(R)-ethylmalonyl-CoA mutase	4125	34.6
		Ga0112990_1047	-	regulatory protein, luxR family	57	22.5
		Ga0112990_1028	+	transcriptional regulator, GntR family	3586	11.7

Supplemental Table 4.3 Continued

Genome.ID	Genome.Name	contig	strand	downstream_annotation	motif distance	bitscore
641380432	*Phaeobacter gallaeciensis* BS107	NA	NA	NA	NA	
2510065029	*Phaeobacter gallaeciensis* DSM 17395	PGA1_c	+	N-acyl-L-homoserine lactone synthetase	2	41.5
		PGA1_c	-	conserved hypothetical protein	3140	40.4
2558309061	*Phaeobacter gallaeciensis* DSM 26640	CP006966	-	regulatory protein, luxR family	57	41.5
		CP006966	+	polyphosphate kinase 2, PA0141 family	1421	15.4
2510065028	*Phaeobacter inhibens* 2.10	PGA2_c	+	N-acyl-L-homoserine lactone synthetase	2	41.5
		PGA2_c	-	transcriptional regulator, AsnC family	449	11.6
2724679070	*Phaeobacter inhibens* S4Sm	Ga0126028_177	-	regulatory protein, luxR family	57	41.5
		Ga0126028_177	+	Putative transposase of IS4/5 family (DUF4096)	2610	40.4
		Ga0126028_178	-	Carbon monoxide dehydrogenase subunit G	1469	10.8
2574179718	*Phaeobacter inhibens* T5, DSM 16374	Phain_cP05.1	+	N-acyl-L-homoserine lactone synthetase	2	41.5
		Phain_cP05.1	-	conserved hypothetical protein	3140	40.4
2706794654	*Phaeobacter italicus* CECT 7321	Ga0124145_113	+	acyl homoserine lactone synthase	1	40.7
		Ga0124145_113	-	conserved hypothetical protein	3000	34
		Ga0124145_137	-	DNA-binding transcriptional response regulator, NtrC family, contains REC, AAA-type ATPase, and a Fis-type DNA-binding domains	5573	10.1
2706794655	*Phaeobacter italicus* CECT 7645	Ga0124146_131	+	acyl homoserine lactone synthase	1	40.7
		Ga0124146_131	-	conserved hypothetical protein	3006	34
		Ga0124146_135	+	RNA polymerase, sigma-24 subunit, RpoE	3667	10.1

Supplemental Table 4.3 Continued

Genome.ID	Genome.Name	contig	strand	downstream_annotation	motif distance	bitscore
2622736589	*Phaeobacter italicus* DSM 26436	Ga0070236_102	-	DNA-binding transcriptional regulator, CsgD family	57	40.7
		Ga0070236_102	+	(R)-ethylmalonyl-CoA mutase	4181	34
		Ga0070236_108	-	DNA-binding transcriptional response regulator, NtrC family, contains REC, AAA-type ATPase, and a Fis-type DNA-binding domains	5573	10.1
2671181183	*Phaeobacter piscinae* S26	Ga0124422_105	-	hypothetical protein	57	45.2
		Ga0124422_105	+	(R)-ethylmalonyl-CoA mutase	4284	43.8
		Ga0124422_116	-	transcriptional regulator, AsnC family	449	15.4
		Ga0124422_110	+	hypothetical protein	1063	13.4
2718218026	*Phaeobacter porticola* P97	Ga0175981_13	-	regulatory protein, luxR family	57	42.7
2645728037	*Phaeobacter* sp. 11ANDIMAR09	Ga0098778_1004	+	N-acyl-L-homoserine lactone synthetase	4	25.6
		Ga0098778_1004	-	conserved hypothetical protein	3273	17.5
		Ga0098778_1011	-	Ammonia channel protein AmtB	228	13.3
		Ga0098778_1028	-	EamA domain-containing membrane protein RarD	52	11.9
		Ga0098778_1019	+	SnoaL-like domain-containing protein	148	11.3
2713896965	*Phaeobacter* sp. CECT 5382	Ga0125396_106	+	acyl homoserine lactone synthase	4	29.3
		Ga0125396_120	-	glutathione S-transferase	2905	19.8
		Ga0125396_106	-	conserved hypothetical protein	3292	16.7
		Ga0125396_104	+	hypothetical protein	51	13
		Ga0125396_103	+	PTS IIA-like nitrogen-regulatory protein PtsN	368	12.7

Supplemental Table 4.3 Continued

Genome.ID	Genome.Name	contig	strand	downstream_annotation	motif distance	bitscore
2502171179	*Phaeobacter* sp. LSS9	PHLS_contig00030	+	N-acyl-L-homoserine lactone synthetase	2	44.2
		PHLS_contig00030	-	conserved hypothetical protein	3142	43
		PHLS_contig00020	+	polyphosphate kinase 2, PA0141 family	1422	15.4
2675903626	*Phaeobacter* sp. S60	Ga0124421_112	-	regulatory protein, luxR family	57	45.2
		Ga0124421_112	+	hypothetical protein	4053	43.8
		Ga0124421_114	-	DNA-binding transcriptional regulator, Lrp family	449	15.4
		Ga0124421_101	+	Sporulation related domain-containing protein	1063	13.4
		Ga0124421_116	-	hypothetical protein	235	11.7
2521172622	*Pseudophaeobacter arcticus* DSM 23566	NA	NA	NA	NA	

Supplemental Table 4.4. Positive matches to secondary motif using initial model

Genome.ID	Organism Name	contig	strand	downstream_annotation	motif distance	bitscore
2713896966	*Leisingera aquaemixtae* CECT 8399	Ga0125397_107	-	type VI secretion system protein VasG	71	15.4
2521172617	*Leisingera aquimarina* DSM 24565	NA	NA	NA	NA	NA
2512047087	*Leisingera caerulea* DSM 24564	PhacaeDRAFT_Contig182.8	-	two-component system, cell cycle response regulator CtrA	1692	14.9
			+	hypothetical protein	34	14.9
2521172619	*Leisingera daeponensis* DSM 23529	NA	NA	NA	NA	NA
2512564009	*Leisingera methylohalidivorans* MB2, DSM 14336	Leime_Contig76.3	+	2,4-dienoyl-CoA reductase	644	16.3
2556921661	*Leisingera* sp. ANG1	ANG1_gi328751003.54	+	(R)-ethylmalonyl-CoA mutase	4089	29.3
		ANG1_gi328751003.54	-	DNA-binding transcriptional regulator, CsgD family	15	17.6
2657245004	*Leisingera* sp. ANG-DT	Ga0112991_111	+	(R)-ethylmalonyl-CoA mutase	4089	31.2
2690316183	*Leisingera* sp. ANG-M1	NA	NA	NA	NA	NA
2667527653	*Leisingera* sp. ANG-M6	Ga0112165_121	+	(R)-ethylmalonyl-CoA mutase	4089	31.5
		Ga0112165_118	+	copper-resistance protein, CopA family	8962	15.6
2690316282	*Leisingera* sp. ANG-M7	Ga0112167_105	+	acyl homoserine lactone synthase	47	23.8
		Ga0112167_101	-	salicylate hydroxylase	317	16.2
2657244983	*Leisingera* sp. ANG-S	Ga0112170_101	-	conserved hypothetical protein	3097	29.3
		Ga0112170_101	+	acyl homoserine lactone synthase	48	17.6
2667528003	*Leisingera* sp. ANG-S3	Ga0112164_105	+	(R)-ethylmalonyl-CoA mutase	4089	29.3
		Ga0112164_105	-	DNA-binding transcriptional regulator, CsgD family	15	17.6
2690316342	*Leisingera* sp. ANG-S5	Ga0112166_127	-	conserved hypothetical protein	3097	29.3
		Ga0112166_103	+	MoxR-like ATPase	9993	23.8
		Ga0112166_127	+	acyl homoserine lactone synthase	48	17.6
2695420551	*Leisingera* sp. ANG-Vp	NA	NA	NA	NA	NA

Supplemental Table 4.4 Continued

Genome.ID	Organism Name	contig	strand	downstream_annotation	motif distance	bitscore
2627854045	*Nautella* sp. ECSMB14104	Ga0077307_102	+	N-acyl-L-homoserine lactone synthetase	45	33.7
2510065029	*Phaeobacter gallaeciensis* DSM 17395	PGA1_c	+	N-acyl-L-homoserine lactone synthetase	45	38.9
		PGA1_c	-	homogentisate 1,2-dioxygenase	79	17.4
2558309061	*Phaeobacter gallaeciensis* DSM 26640	CP006966	-	regulatory protein, luxR family	16	38.9
		CP006966	+	(R)-ethylmalonyl-CoA mutase	4374	34.8
		CP006967	-	hypothetical protein	359	23.1
2510065028	*Phaeobacter inhibens* 2.10	PGA2_c	+	N-acyl-L-homoserine lactone synthetase	45	38.9
		PGA2_c	-	Protein of unknown function (DUF3307)	2119	16.4
2724679070	*Phaeobacter inhibens* S4Sm	Ga0126028_177	-	regulatory protein, luxR family	16	38.9
		Ga0126028_177	+	Putative transposase of IS4/5 family (DUF4096)	2564	34.8
		Ga0126028_138	-	homogentisate 1,2-dioxygenase	76	17.4
		Ga0126028_156	-	acetyl esterase	1851	17
		Ga0126028_132	-	Protein of unknown function (DUF3307)	2119	16.4
2574179718	*Phaeobacter inhibens* T5, DSM 16374	Phain_cP05.1	+	N-acyl-L-homoserine lactone synthetase	45	38.9
2706794654	*Phaeobacter italicus* CECT 7321	Ga0124145_113	+	acyl homoserine lactone synthase	45	34.7
2706794655	*Phaeobacter italicus* CECT 7645	Ga0124146_131	+	acyl homoserine lactone synthase	45	34.7
		Ga0124146_134	-	Transposase InsO and inactivated derivatives	6470	17.1
2622736589	*Phaeobacter italicus* DSM 26436	Ga0070236_102	-	DNA-binding transcriptional regulator, CsgD family	16	34.7
		Ga0070236_107	-	Transposase InsO and inactivated derivatives	6470	17.1
2671181183	*Phaeobacter piscinae* S26	Ga0124422_105	-	hypothetical protein	16	38.9
		Ga0124422_105	+	(R)-ethylmalonyl-CoA mutase	4238	34.8
		Ga0124422_126	-	homogentisate 1,2-dioxygenase	80	17.4

Supplemental Table 4.4 Continued

Genome.ID	Organism Name	contig	strand	downstream_annotation	motif distance	bitscore
2718218026	*Phaeobacter porticola* P97	Ga0175981_13	-	regulatory protein, luxR family	16	40.2
		Ga0175981_13	+	ATP-dependent Clp protease adaptor protein ClpS	1039	17.1
2645728037	*Phaeobacter* sp. 11ANDIMAR09	Ga0098778_1011	-	Transposase	483	17.1
		Ga0098778_1002	-	ATP-binding cassette, subfamily C, LapB	1106	16.1
2713896965	*Phaeobacter* sp. CECT 5382	Ga0125396_115	-		760	17
		Ga0125396_106	+	acyl homoserine lactone synthase	78	16.4
2502171179	*Phaeobacter* sp. LSS9	PHLS_contig00030	+	N-acyl-L-homoserine lactone synthetase	45	38.9
		PHLS_contig00030	-	conserved hypothetical protein	3189	34.8
2675903626	*Phaeobacter* sp. S60	Ga0124421_112	-	regulatory protein, luxR family	16	38.9
		Ga0124421_112	+	hypothetical protein	4007	34.8
		Ga0124421_121	+	Glyoxylase, beta-lactamase superfamily II	1260	17.4

Supplemental Table 4.5. Positive matches to roseo box motif 2

Genome.ID	Genome.Name	contig	strand	downstream_annotation	motif distance	bitscore
2713896966	*Leisingera aquaemixtae* CECT 8399	Ga0125397_130	+	uridylate kinase [EC:2.7.4.22]	14350	12.1
2512047087	*Leisingera caerulea* DSM 24564	PhacaeDRAFT_Contig178.5	-	serine/threonine protein phosphatase Stp1 [EC:3.1.3.16]	7003	12.6
2556921661	*Leisingera* sp. ANG1	ANG1_gi328751020.37	+	small subunit ribosomal protein S16	91	12.6
2657245004	*Leisingera* sp. ANG-DT	Ga0112991_105	+	small subunit ribosomal protein S16	91	12.6
2690316183	*Leisingera* sp. ANG-M1	Ga0112989_101	-	phage terminase small subunit	25512	14.6
		Ga0112989_101	+	RHH-type transcriptional regulator, proline utilization regulon repressor / proline dehydrogenase / delta 1-pyrroline-5-carboxylate dehydrogenase [EC:1.5.5.2 1.2.1.88]	55051	13.1
2667527653	*Leisingera* sp. ANG-M6	Ga0112165_110	-	signal recognition particle subunit SRP54	2281	12.6
2657244983	*Leisingera* sp. ANG-S	Ga0112170_128	+	small subunit ribosomal protein S16	91	12.6
2667528003	*Leisingera* sp. ANG-S3	Ga0112164_129	+	small subunit ribosomal protein S16	91	12.6
2690316342	*Leisingera* sp. ANG-S5	Ga0112166_105	+	small subunit ribosomal protein S16	91	12.6
		Ga0112166_103	-	phospholipid/cholesterol/gamma-HCH transport system ATP-binding protein	130	11
2510065029	*Phaeobacter gallaeciensis* DSM 17395	PGA1_262p	-	chemotaxis protein methyltransferase CheR [EC:2.1.1.80]	125	13.2
		PGA1_c	+	exodeoxyribonuclease V [EC:3.1.11.5]	799	43.3
2558309061	*Phaeobacter gallaeciensis* DSM 26640	CP006966	-	crotonyl-CoA carboxylase/reductase [EC:1.3.1.85]	1056	43.3
		CP006966	+	(2R)-ethylmalonyl-CoA mutase	4378	45.3

Supplemental Table 4.5 Continued

Genome.ID	Genome.Name	contig	strand	downstream_annotation	motif distance	bitscore
2510065028	*Phaeobacter inhibens* 2.10	PGA2_239p	-	chemotaxis protein methyltransferase CheR [EC:2.1.1.80]	125	13.2
		PGA2_c	+	glutathione S-transferase [EC:2.5.1.18]	581	12.1
		PGA2_c	-		4077	45.3
2724679070	*Phaeobacter inhibens* S4Sm	Ga0126028_180	-	LPS-assembly lipoprotein	534	12.1
		Ga0126028_177	-	crotonyl-CoA carboxylase/reductase [EC:1.3.1.85]	1051	43.3
		Ga0126028_177	+	(2R)-ethylmalonyl-CoA mutase	6337	45.3
2574179718	*Phaeobacter inhibens* T5, DSM 16374	Phain_pP05_a.2	-	chemotaxis protein methyltransferase CheR [EC:2.1.1.80]	125	13.2
		Phain_cP05.1	+	exodeoxyribonuclease V [EC:3.1.11.5]	799	43.3
2706794654	*Phaeobacter italicus* CECT 7321	Ga0124145_113	+	acyl homoserine lactone synthase [EC:2.3.1.184]	49	38.1
		Ga0124146_131	+	acyl homoserine lactone synthase [EC:2.3.1.184]	49	38.1
2622736589	*Phaeobacter italicus* DSM 26436	Ga0070236_102	-	crotonyl-CoA carboxylase/reductase [EC:1.3.1.85]	1084	38.1
2671181183	*Phaeobacter piscinae* S26	Ga0124422_105	-	crotonyl-CoA carboxylase/reductase [EC:1.3.1.85]	1055	43.3
		Ga0124422_105	+	(2R)-ethylmalonyl-CoA mutase	4242	45.3
2718218026	*Phaeobacter porticola* P97	Ga0175981_13	-	crotonyl-CoA carboxylase/reductase [EC:1.3.1.85]	1066	43.6
		Ga0175981_13	+	(2R)-ethylmalonyl-CoA mutase	4164	43.1
2713896965	*Phaeobacter* sp. CECT 5382	Ga0125396_106	+	acyl homoserine lactone synthase [EC:2.3.1.184]	83	14.4

Supplemental Table 4.5 Continued

Genome.ID	Genome.Name	contig	strand	downstream_annotation	motif distance	bitscore
2502171179	Phaeobacter sp. LSS9	PHLS_contig00030	+	exodeoxyribonuclease V [EC:3.1.11.5]	799	43.3
		PHLS_contig00030	-	not annotated	4081	45.3
		PHLS_contig00007	+	GntR family transcriptional regulator / MocR family aminotransferase	10818	13.2
2675903626	*Phaeobacter* sp. S60	Ga0124421_112	-	crotonyl-CoA carboxylase/reductase [EC:1.3.1.85]	1056	43.3
		Ga0124421_112	+	(2R)-ethylmalonyl-CoA mutase	4243	45.3

Supplemental Table 4.6. Positive matches to roseo box motif 1 not likely to be regulated by QS

Genome.ID	Genome.Name	contig	strand	downstream_annotation	motif distance	bitscore
2713896966	*Leisingera aquaemixtae* CECT 8399	Ga0125397_111	+	sarcosine oxidase, subunit gamma [EC:1.5.3.1]	1456	10.5
		Ga0125397_111	-	trimethylamine monooxygenase [EC:1.14.13.148]	3812	11.9
		Ga0125397_110	-	uncharacterized protein	3986	31.1
2521172617	*Leisingera aquimarina* DSM 24565	NA	NA	NA	NA	NA
		PhacaeDRAFT_Scaffold1.6	+	spermidine/putrescine transport system permease protein	832	11.4
		PhacaeDRAFT_Scaffold1.6	-	crotonyl-CoA carboxylase/reductase [EC:1.3.1.85]	1151	23.6
2521172619	*Leisingera daeponensis* DSM 23529	NA	NA	NA	NA	NA
2512564009	*Leisingera methylohalidivorans* MB2, DSM 14336	Leime_Contig76.3	-	5,6-dimethylbenzimidazole synthase [EC:1.13.11.79]	649	10.9
2556921661	Leisinger*a* sp. ANG1	ANG1_gi328751003.54	-	crotonyl-CoA carboxylase/reductase [EC:1.3.1.85]	1132	29
		ANG1_gi328750991.66	-	putative phosphoribosyl transferase	4218	11.5
2657245004	*Leisingera* sp. ANG-DT	Ga0112991_111	-	crotonyl-CoA carboxylase/reductase [EC:1.3.1.85]	1132	29
2690316183	*Leisingera* sp. ANG-M1	Ga0112989_106	-	crotonyl-CoA carboxylase/reductase [EC:1.3.1.85]	1138	22.8
		Ga0112989_106	+	(2R)-ethylmalonyl-CoA mutase	4129	32
2667527653	*Leisingera* sp. ANG-M6	Ga0112165_121	-	crotonyl-CoA carboxylase/reductase [EC:1.3.1.85]	1132	29
		Ga0112165_111	+	error-prone DNA polymerase [EC:2.7.7.7]	1912	12.9
2667527653	*Leisingera* sp. ANG-M6	Ga0112165_121	+	(2R)-ethylmalonyl-CoA mutase	4126	31.1
2690316282	*Leisingera* sp. ANG-M7	Ga0112167_105	-	uncharacterized protein	3937	31.4
		Ga0112167_107	+	uncharacterized protein	4437	11.9
2657244983	*Leisingera* sp. ANG-S	Ga0112170_104	-	phenylalanyl-tRNA synthetase beta chain [EC:6.1.1.20]	6647	11.5

Supplemental Table 4.6 Continued

Genome.ID	Genome.Name	contig	strand	downstream_annotation	motif distance	bitscore
2667528003	*Leisingera* sp. ANG-S3	Ga0112164_105	-	crotonyl-CoA carboxylase/reductase [EC:1.3.1.85]	1132	29
		Ga0112164_118	-	phenylalanyl-tRNA synthetase beta chain [EC:6.1.1.20]	6647	11.5
		Ga0112164_104	+	nitrogen regulatory protein P-II 1	32759	11.7
2690316342	*Leisingera* sp. ANG-S5	Ga0112166_127	-	uncharacterized protein	3850	31.1
		Ga0112990_1047	-	crotonyl-CoA carboxylase/reductase [EC:1.3.1.85]	1138	27.4
		Ga0112990_1047	+	(2R)-ethylmalonyl-CoA mutase	4129	31.1
2510065029	*Phaeobacter gallaeciensis* DSM 17395	PGA1_c	+	exodeoxyribonuclease V [EC:3.1.11.5]	755	37.7
2558309061	*Phaeobacter gallaeciensis* DSM 26640	CP006966	-	crotonyl-CoA carboxylase/reductase [EC:1.3.1.85]	1100	37.7
2510065028	*Phaeobacter inhibens* 2.10	PGA2_c	+	exodeoxyribonuclease V [EC:3.1.11.5]	755	37.7
2724679070	*Phaeobacter inhibens* S4Sm	Ga0126028_177	-	crotonyl-CoA carboxylase/reductase [EC:1.3.1.85]	1095	37.7
		Ga0126028_177	+	(2R)-ethylmalonyl-CoA mutase	6382	38.6
		Ga0126028_169	-	fatty-acyl-CoA synthase [EC:6.2.1.-]	7682	14.9
2574179718	*Phaeobacter inhibens* T5, DSM 16374	Phain_cP05.1	+	exodeoxyribonuclease V [EC:3.1.11.5]	755	37.7
2706794654	*Phaeobacter italicus* CECT 7321	Ga0124145_139	+	spermidine/putrescine transport system permease protein	832	10.4
		Ga0124145_135	+	methyl-accepting chemotaxis protein	852	10.2
		Ga0124145_145	+	succinate-semialdehyde dehydrogenase / glutarate-semialdehyde dehydrogenase [EC:1.2.1.16 1.2.1.79 1.2.1.20]	1656	12.9
		Ga0124145_113	-	uncharacterized protein	3840	37.7
2706794655	*Phaeobacter italicus* CECT 7645	Ga0124146_122	+	spermidine/putrescine transport system permease protein	832	10.4
		Ga0124146_131	-	uncharacterized protein	3846	37.7

Supplemental Table 4.6 Continued

Genome.ID	Genome.Name	contig	strand	downstream_annotation	motif distance	bitscore
2622736589	*Phaeobacter italicus* DSM 26436	Ga0070236_102	-	crotonyl-CoA carboxylase/reductase [EC:1.3.1.85]	1128	36.7
		Ga0070236_102	+	(2R)-ethylmalonyl-CoA mutase	4184	37.7
2671181183	*Phaeobacter piscinae* S26	Ga0124422_105	-	crotonyl-CoA carboxylase/reductase [EC:1.3.1.85]	1099	39.8
		Ga0124422_105	+	(2R)-ethylmalonyl-CoA mutase	4287	41.3
		Ga0124422_107	-	iron complex transport system ATP-binding protein [EC:3.6.3.34]	10793	10.9
2718218026	*Phaeobacter porticola* P97	Ga0175981_13	-	crotonyl-CoA carboxylase/reductase [EC:1.3.1.85]	1110	39.8
2645728037	*Phaeobacter* sp. 11ANDIMAR09	Ga0098778_1004	+	exodeoxyribonuclease V [EC:3.1.11.5]	732	23
		Ga0098778_1028	+	transposase, IS30 family	2235	12.4
		Ga0098778_1004	-		4066	21.2
2713896965	*Phaeobacter* sp. CECT 5382	Ga0125396_107	+	aerotaxis receptor	529	12.7
		Ga0125396_120	-	cytochrome c biogenesis protein CcmG, thiol:disulfide interchange protein DsbE	3988	12.1
		Ga0125396_106	-	uncharacterized protein	4106	32.3
2502171179	*Phaeobacter* sp. LSS9	PHLS_contig00030	+	exodeoxyribonuclease V [EC:3.1.11.5]	755	39.8
		PHLS_contig00030	-		4037	40.4
		PHLS_contig00027	+	ribonuclease D [EC:3.1.13.5]	8388	12.7
2675903626	*Phaeobacter* sp. S60	Ga0124421_112	-	crotonyl-CoA carboxylase/reductase [EC:1.3.1.85]	1100	39.8
		Ga0124421_112	+	(2R)-ethylmalonyl-CoA mutase	4288	41.3
		Ga0124421_124	-	iron complex transport system ATP-binding protein [EC:3.6.3.34]	10793	10.9

Chapter 5 : CONCLUSIONS AND FUTURE DIRECTIONS

Bacterial social behaviors mediated by quorum sensing plays an important role in structuring microbial biofilms and may contribute to functions within those biofilms. These functions include but are not limited to antimicrobial production, biofilm formation, and metabolism (1–3). To date, only a handful of Roseobacter representatives are being studied regarding QS (4–8). Thus, the field lacks a sufficient model organism to characterize QS-mediated social behaviors between microorganisms. Rhodobacterales strain Y4I shows promise as an emerging model organism for demonstrating how QS mediates bacterial social behaviors both in monoculture and in multispecies marine biofilms.

Further characterization of the QS network in Y4I is needed to fully elucidate all the social behaviors mediated by Y4I. The work presented in this dissertation primarily focused on secondary metabolite production and biofilm formation as social behaviors in Y4I. Other bacterial social behaviors in Y4I may include co-metabolism, SOS response, and virulence. One example of virulence in Y4I could be a type VI secretion system (T6SS), homologs of which are present in the annotated genome of Y4I (see appendix). T6SSs have been investigated in pathogen models due to their role in microbe-microbe interactions (9). In *Pseudomonas fluorescens* T6SS may serve as a contact-dependent communication system among sister cells (10). The role of virulence in T6SS have been demonstrated in a pathogenic strain of *Vibrio cholerae*. In this system, *V. cholerae* uses a T6SS, in a contact-dependent manner, as a molecular harpoon targeting a commensal organism in the intestine of a zebrafish. The T6SS delivers a toxic product into the victim. This distress to the microbiome of the fish gut leads to death of the host (11). In other *Vibrio* species, T6SS have been linked to QS (12–14). A commonality between these pathogen models containing T6SS and Y4I is their colonization success. Most T6SS have been associated with colonization and play a role in antagonism between competing bacteria in polymicrobial environments (9). Similarly, colonization and antagonism are coupled in Y4I through the production of indigoidine. While studies have demonstrated that indigoidine in Y4I confers inhibitory properties (8, 15) the exact mechanism is not known. Determining if the inhibitory action of indigoidine is contact dependent could be a first step in linking indigoidine to T6SS activity in Y4I.

With the exception of *phaI*::pKNOCK, the Y4I mutants used in the works presented in this dissertation (Chapters 2 and 3), originated from a 6048 member mutant library generated in Cude *et al*. 2012. We have demonstrated in some mutants, complementation with exogenous AHLs leads to partial restoration of the blue pigmentation characteristic of indigoidine production in Y4I (8). In this way, Y4I has been used as its own bioreporter. This technique has been particularly useful as working with bioreporters is not without challenges and also eliminated the need for further genetic manipulation (i. e., expression plasmids). Thus, this type of chemical complementation with AHLs could serve as a screening technique to identify other QS regulated physiologies in the mutant library. In addition, some antimicrobials can serve as intracellular signals in Roseobacter clade members. Tropodithietic acid (TDA) is one such antimicrobial (6). It is possible that indigoidine may have similar functions in Y4I. Attempts have been made to characterize indigoidine in Y4I but were unsuccessful (see appendix). One challenge here is the redox reactive nature of indigoidine (16, 17). To date, only strong organic solvents have been able to fully solubilize indigoidine, many of which are toxic to microorganisms (18).

Another area of research necessary for the establishment of Y4I as a model organism is genetic characterization of global regulators, such as CtrA and cyclic-di-GMP (c-di-GMP). CtrA, is relatively conserved in alphaproteobacteria. This cell-cycle regulator is largely responsible for regulating the swim-stick switch that mediates motile and sessile lifestyles respectively (19–23). Furthermore, the CtrA phosphorelay system has been demonstrated to be integrated in QS in several Roseobacter species (24–29). Much preliminary work on

CtrA in Y4I has been established but remains incomplete (see appendix). Due to the global function of CtrA, it is possible that this master regulator is essential to bacterial growth dynamics in Y4I. An example of the essential nature of CtrA has been previously reported in another Roseobacter strain, *Dinoroseobacter shibae* KLH11 (26). In addition, c-di-GMP has been linked to both CtrA and members of the Roseobacter clade. Chapter 2 demonstrated that c-di-GMP was decreased in both QS and indigoidine mutants, indicating its integration into this network (**Figure 2.4B, C**). Interestingly, a metabolite necessary for biosynthesis for both c-di-GMP and indigoidine is glutamine (30, 31). Previously, it was hypothesized that differences in motility and surface attachment observed in the indigoidine mutant (*igiD*::TN5-Km^R) compared to wildtype Y4I were due to the availability of intracellular levels of glutamine in the mutant which resulted in increased biofilm formation (15). Typically, higher concentrations of c-di-GMP are observed in mature biofilms (32). However, in *igiD*::TN5-Km^R c-di-GMP levels are significantly reduced compared to wildtype Y4I contrary to the general paradigm (**Figure 2.4B,C**). Despite the presumed availability of intracellular glutamine in the *igiD*::TN5-Km^R mutant, c-di-GMP concentrates did not increase (Chapter 2). Further characterization of the role of intracellular glutamine on c-di-GMP and indigoidine concentrations between the QS and indigoidine null mutants, as well as, wildtype Y4I would further elucidate the regulatory mechanisms underlying this complex QS network. Several traditional genetic methodologies, innovative genetic techniques, and 'omics' approaches can be utilized to characterize these global regulators in Y4I. These approaches include expression plasmids, western blots, northern blots, crisper, RNA-seq, Chip-seq.

In tandem with the above analyses, co-culture and community-based studies could be performed with Y4I. One of the most interesting features in Y4I's QS network is that a common signaling molecule, C8-HSL, is at the top of the regulatory network for indigoidine synthesis (8, 15, 33). This signaling molecule is commonly produced by many marine bacteria, including *Aliivibrio fischeri*, an organism which indigoidine inhibits. In *A. fischeri*, C8-HSL is synthesized by AinS and binds to AinR in a canonical QS fashion (34, 35). It is currently unknown whether the production of C8-HSL from *A. fisheri* strains is able to interact with the Y4I AinR homolog, PgaR, facilitating its own inhibition (15). In addition, the cross-talk between C8-HSL produced by Y4I and AinR in *A. fischeri* is still unresolved. Utilization of the *A. fisheri* DC22 bioreporter assay developed by Kimbrough *et al*. (2013) could serve as a useful technique in exploring the interspecies interactions between these two marine organisms.

Potential cross-talk within members of the Roseobacter clade is another avenue of exploration. Additional investigations of putative cross-talk between Roseobacters could focus on synthetic community members. AHLs with masses corresponding to 186 and 284 during growth on a surface may be present among related synthetic community members (Chapter 3). Identification of the molecular structure in these putative overlapping AHLs would support this hypothesis. If cross-talk is possible between synthetic community members, exogenous addition of cell supernant or purified AHLs could restore pigmentation in select QS mutants (*phaR*::TN-Km^R and *phaI*::pKNOCK) using a similar AHL-addback assay illustrated in Chapter 2 (**Supplemental Figure 2.2**).

The role QS plays on influencing biofilm community function is another area that is not well understood within members of the Roseobacter clade. It was previously hypothesized that Roseobacter members set the stage for biofilm structure, function, and dynamics (36). The results within chapter 3 support this hypothesis regarding community structure and dynamics as, respectively, functions of composition, and cooperative and competitive interactions. That QS influences the dynamics between community members within a biofilm suggests that the function, or role, of the biofilm consortia as a whole are also affected. The role of biofilms in marine ecosystems have been a topic of several recent

reviews (37–41). The function of a biofilm consisting of a high abundance Roseobacter species is presumed to be the degradation of polyaromatic compounds (42–46). Isotope tracking of polyaromatic compounds of synthetic biofilm communities harboring Y4I QS mutants, in addition to confocal microscopy, would expound upon the role QS plays in mediating biofilm structure, function, and dynamics.

In chapter 4, a set of candidate genes contributing to bacterial social behaviors such as SOS response, biofilm formation and motility, antimicrobial resistance, and metabolism was found using the clade specific roseo box. These genes, putatively regulated by QS among the *Phaeobacter-Leisingera* lineage of the Roseobacter clade, merit exploration. Further extrapolation on the relationship between these genes and QS in Roseobacter models, such as Y4I, would improve confidence in our preliminary consensus sequence for the roseo box motif. In addition, considering the role of post-translational modification within QS regulatory networks may reveal additional genes under QS mediation. Both c-di-GMP and *S*-adenosylmethionine (SAM) have been demonstrated to modify genes and proteins linked to QS in diverse proteobacteria (47–50). One approach to improving our motif model would be to include differentially expressed genes from expression analysis (e.g. RT-qPCR, RNA-seq, transcriptomics) from a representative model such as Y4I. Similar approaches have been performed in model QS organisms, *Pseudomonas aeruginosa* and *A. fischeri* (51, 52). At the time of submission for this dissertation, current work is undergoing to analyze gene expression using RT-qPCR in Y4I mutant strains in which exogenous addition of AHLs have been added. This analysis may unveil whether the genes putatively regulate by roseo box motifs 1 and 2 are, indeed, regulated by QS.

With the exponential increase of genomic and transcriptomic data extrapolated from natural environments, there is a need for quick and efficient bioinformatic analysis methods. In order to apply the bioinformatic model used generated the roseo box motif for use in metagenome data sets additional optimization is warranted. Once refined, the motif model can be applied to metagenome and metatranscriptome datasets in natural environments to probe whether genes of interest from Chapter 4 are present (metagenomes) and upregulated (metatranscriptomes). Paired metagenome and metatranscriptome data sets from a temperate salt marsh estuary (i.e., Grove's Creek, Georgia, USA) have already been obtained (44). As Roseobacter abundance is greatest in coastal environments, such as salt marsh estuaries (53), these ecosystems provide a relevant system in which to study microbial interactions mediated by QS, such as those listed above. Refinement of the model used to generate the roseo box motif could lead to our ability to survey these paired metagenome and metatranscriptome data sets for presence for roseo box motifs. If successful, this methodology would aid in elucidating the role of bacterial social behaviors in natural ecosystems.

References

1. Brindhadevi K, LewisOscar F, Mylonakis E, Shanmugam S, Verma TN, Pugazhendhi A. 2020. Biofilm and Quorum sensing mediated pathogenicity in *Pseudomonas aeruginosa*. Process Biochem 96:49–57.
2. Irie Y, Parsek MR. 2008. Quorum Sensing and Microbial Biofilms, p. 67–84. *In* . Springer, Berlin, Heidelberg.
3. Goo E, An JH, Kang Y, Hwang I. 2015. Control of bacterial metabolism by quorum sensing. Trends Microbiol 23:567–576.
4. Zan J, Choi O, Meharena H, Uhlson CL, Churchill MEA, Hill RT, Fuqua C. 2015. A solo luxi-type gene directs acylhomoserine lactone synthesis and contributes to motility control in the marine sponge symbiont *Ruegeria* sp. KLH11. Microbiol (United Kingdom) 161:50–56.
5. Ziesche L, Rinkel J, Dickschat JS, Schulz S. 2018. Acyl-group specificity of AHL synthases involved in quorum-sensing in Roseobacter group bacteria. Beilstein J Org Chem 14:1309–1316.
6. Beyersmann PG, Tomasch JJ, Son K, Stocker R, Göker M, Wagner-Döbler I, Simon M, Brinkhoff T. 2017. Dual function of tropodithietic acid as antibiotic and signaling molecule in global gene regulation of the probiotic bacterium *Phaeobacter inhibens*. Sci Rep 7:730.
7. Johnson WM, Kido Soule MC, Kujawinski EB. 2016. Evidence for quorum sensing and differential metabolite production by a marine bacterium in response to DMSP. ISME J 10:2304–2316.
8. Armes AC, Buchan A. 2021. Cyclic di-GMP Is Integrated Into a Hierarchal Quorum Sensing Network Regulating Antimicrobial Production and Biofilm Formation in Roseobacter Clade Member *Rhodobacterales* Strain Y4I. Front Mar Sci 8:1–12.
9. Chen C, Yang X, Shen X. 2019. Confirmed and Potential Roles of Bacterial T6SSs in the Intestinal Ecosystem. Front Microbiol 0:1484.
10. Gallique M, Decoin V, Barbey C, Rosay T, Feuilloley MGJ, Orange N, Merieau A. 2017. Contribution of the *Pseudomonas fluorescens* MFE01 Type VI Secretion System to Biofilm Formation. PLoS One 12:e0170770.
11. Logan SL, Thomas J, Yan J, Baker RP, Shields DS, Xavier JB, Hammer BK, Parthasarathy R. 2018. The *Vibrio cholerae* type VI secretion system can modulate host intestinal mechanics to displace gut bacterial symbionts. Proc Natl Acad Sci 115:E3779–E3787.
12. Weber B, Hasic M, Chen C, Wai SN, Milton DL. 2009. Type VI secretion modulates quorum sensing and stress response in *Vibrio anguillarum*. Environ Microbiol 11:3018–3028.
13. Sheng L, Gu D, Wang Q, Liu Q, Zhang Y. 2011. Quorum sensing and alternative sigma factor RpoN regulate type VI secretion system I (T6SSVA1) in fish pathogen *Vibrio alginolyticus*. Arch Microbiol 2011 1945 194:379–390.
14. Gao X, Wang X, Mao Q, Xu R, Zhou X, Ma Y, Liu Q, Zhang Y, Wang Q. 2018. VqsA, a Novel LysR-Type Transcriptional Regulator, Coordinates Quorum Sensing (QS) and Is Controlled by QS To Regulate Virulence in the Pathogen *Vibrio alginolyticus*. Appl Environ Microbiol 84:444–462.
15. Cude WN, Mooney J, Tavanaei AA, Hadden MK, Frank AM, Gulvik CA, May AL, Buchan A. 2012. Production of the antimicrobial secondary metabolite indigoidine contributes to competitive surface colonization by the marine roseobacter *Phaeobacter sp.* strain Y4I. Appl Environ Microbiol 78:4771–4780.
16. Kuhn R, Starr MP, Kuhn DA, Bauer H, Knackmuss H-J. 1965. Indigoidine and other bacterial pigments related to 3,3-bipyridyl. Arch fr Mikrobiol 51:71–84.
17. Heumann W, Young D, Gottlich C. 1968. Leucoindigoidine formation by an

Arthrobacter species and its oxidation to indigoidine by other micro-organisms. Biochim Biophys Acta - Gen Subj 156:429–431.
18. Wehrs M, Gladden JM, Liu Y, Platz L, Prahl J-P, Moon J, Papa G, Sundstrom E, Geiselman GM, Tanjore D, Keasling JD, Pray TR, Simmons BA, Mukhopadhyay A. 2019. Sustainable bioproduction of the blue pigment indigoidine: Expanding the range of heterologous products in *R. toruloides* to include non-ribosomal peptides. Green Chem 21:3394–3406.
19. Ryan KR, Judd EM, Shapiro L. 2002. The CtrA response regulator essential for Caulobacter crescentus cell-cycle progression requires a bipartite degradation signal for temporally controlled proteolysis. J Mol Biol 324:443–55.
20. Laub MT, Chen SL, Shapiro L, McAdams HH. 2002. Genes directly controlled by CtrA, a master regulator of the *Caulobacter* cell cycle. Proc Natl Acad Sci 99:4632–4637.
21. Bellefontaine AF, Pierreux CE, Mertens P, Vandenhaute J, Letesson JJ, De Bolle X. 2002. Plasticity of a transcriptional regulation network among alpha-proteobacteria is supported by the identification of CtrA targets in *Brucella abortus*. Mol Microbiol 43:945–960.
22. Greene SE, Brilli M, Biondi EG, Komeili A. 2012. Analysis of the CtrA pathway in *Magnetospirillum* reveals an ancestral role in motility in alphaproteobacteria. J Bacteriol 194:2973–86.
23. Poncin K, Gillet S, De Bolle X. 2018. Learning from the master: targets and functions of the CtrA response regulator in *Brucella abortus* and other alpha-proteobacteria. FEMS Microbiol Rev. NLM (Medline).
24. Pini F, De Nisco NJ, Ferri L, Penterman J, Fioravanti A, Brilli M, Mengoni A, Bazzicalupo M, Viollier PH, Walker GC, Biondi EG. 2015. Cell Cycle Control by the Master Regulator CtrA in *Sinorhizobium meliloti*. PLoS Genet 11.
25. Leung MM, Brimacombe CA, Beatty JT. 2013. Transcriptional regulation of the *Rhodobacter capsulatus* response regulator CtrA. Microbiology 159:96–106.
26. Wang H, Ziesche L, Frank O, Michael V, Martin M, Petersen J, Schulz S, Wagner-Döbler I, Tomasch J. 2014. The CtrA phosphorelay integrates differentiation and communication in the marine alphaproteobacterium *Dinoroseobacter shibae*. BMC Genomics 15:130.
27. Zan J, Heindl JE, Liu Y, Fuqua C, Hill RT. 2013. The CckA-ChpT-CtrA Phosphorelay System Is Regulated by Quorum Sensing and Controls Flagellar Motility in the Marine Sponge Symbiont *Ruegeria* sp. KLH11. PLoS One 8:e66346.
28. Mercer RG, Callister SJ, Lipton MS, Pasa-Tolic L, Strnad H, Paces V, Beatty JT, Lang AS. 2010. Loss of the response regulator CtrA causes pleiotropic effects on gene expression but does not affect growth phase regulation in *Rhodobacter capsulatus*. J Bacteriol 192:2701–2710.
29. Brimacombe CA, Ding H, Beatty JT. 2014. *Rhodobacter capsulatus* DprA is essential for RecA-mediated gene transfer agent (RcGTA) recipient capability regulated by quorum-sensing and the CtrA response regulator. Mol Microbiol 92:1260–1278.
30. Reverchon S, Rouanet C, Expert D, Nasser W. 2002. Characterization of indigoidine biosynthetic genes in *Erwinia chrysanthemi* and role of this blue pigment in pathogenicity. J Bacteriol 184:654–665.
31. Tesmer JJG, Klem TJ, Deras ML, Davisson VJ, Smith JL. 1996. The crystal structure of GMP synthetase reveals a novel catalytic triad and is a structural paradigm for two enzyme families. Nat Struct Biol 3:74–86.
32. Römling U, Galperin MY, Gomelsky M. 2013. Cyclic di-GMP: the First 25 Years of a Universal Bacterial Second Messenger. Microbiol Mol Biol Rev 77:1–52.
33. Cude WN, Prevatte CW, Hadden MK, May AL, Smith RT, Swain CL, Campagna SR, Buchan A. 2015. *Phaeobacter sp.* strain Y4I utilizes two separate cell-to-cell communication systems to regulate production of the antimicrobial indigoidine. Appl Environ Microbiol 81:1417–1425.

34. Egland KA, Greenberg EP. 1999. Quorum sensing in *Vibrio fischeri*: elements of the luxI promoter. Mol Microbiol 31:1197–1204.
35. Kimbrough JH, Stabb E V. 2013. Substrate Specificity and Function of the Pheromone Receptor AinR in Vibrio fischeri ES114. J. Bac 22: 5223-5232
36. Dang H, Lovell CR. 2016. Microbial Surface Colonization and Biofilm Development in Marine Environments. Microbiol Mol Biol Rev 80:91–138.
37. Camacho-Chab JC, Lango-Reynoso F, Castañeda-Chávez M del R, Galaviz-Villa I, Hinojosa-Garro D, Ortega-Morales BO. 2016. Implications of extracellular polymeric substance matrices of microbial habitats associated with coastal aquaculture systems. Water (Switzerland) 8:369.
38. Mitra A, Mukhopadhyay S. 2016. Biofilm mediated decontamination of pollutants from the environment. AIMS Bioeng 3:44–59.
39. Yang Y, Liu W, Zhang Z, Grossart HP, Gadd GM. 2020. Microplastics provide new microbial niches in aquatic environments. Appl Microbiol Biotechnol 104:6501–6511.
40. Wang T, Wang L, Chen Q, Kalogerakis N, Ji R, Ma Y. 2020. Interactions between microplastics and organic pollutants: Effects on toxicity, bioaccumulation, degradation, and transport. Sci Total Environ 748.
41. Sonnenschein EC, Jimenez G, Castex M, Gram L. 2021. The Roseobacter-Group Bacterium *Phaeobacter* as a Safe Probiotic Solution for Aquaculture. Appl Environ Microbiol 87:1–15.
42. Buchan A, Neidle EL, Moran MA. 2004. Diverse Organization of Genes of the *B*-Ketoadipate Pathway in Members of the Marine Roseobacter Lineage. Appl Environ Microbiol 70:1658–68.
43. Newton RJ, Griffin LE, Bowles KM, Meile C, Gifford S, Givens CE, Howard EC, King E, Oakley CA, Reisch CR, Rinta-Kanto JM, Sharma S, Sun S, Varaljay V, Vila-Costa M, Westrich JR, Moran MA. 2010. Genome characteristics of a generalist marine bacterial lineage. ISME J 4:784–798.
44. Steen AD, Quigley LNM, Buchan A. 2016. Evidence for the Priming Effect in a Planktonic Estuarine Microbial Community. Front Mar Sci 3:6.
45. Quigley LNM, Edwards A, Steen AD, Buchan A, Fagervold SK. 2019. Characterization of the Interactive Effects of Labile and Recalcitrant Organic Matter on Microbial Growth and Metabolism. Front Microbiol 10:1–15.
46. Frank AM, Chua MJ, Gulvik CA, Buchan A. 2018. Functional Redundancy in the Hydroxycinnamate Catabolism Pathways of the Salt Marsh Bacterium *Sagittula stellata* E-37. Appl Environ Microbiol 84.
47. Waters CM, Lu W, Rabinowitz JD, Bassler BL. 2008. Quorum sensing controls biofilm formation in *Vibrio cholerae* through modulation of cyclic Di-GMP levels and repression of vpsT. J Bacteriol 190:2527–2536.
48. Liang F, Zhang B, Yang Q, Zhang Y, Zheng D, Zhang L, Yan Q, Wu X. 2020. Cyclic-di-GMP Regulates the Quorum-Sensing System and Biocontrol Activity of *Pseudomonas fluorescens* 2P24 through the RsmA and RsmE Proteins. Appl Environ Microbiol 86.
49. Srivastava D, Waters CM. 2012. A tangled web: Regulatory connections between quorum sensing and cyclic Di-GMP. J Bacteriol 194:4485–4493.
50. Loh J, Pierson EA, Pierson LS, Stacey G, Chatterjee A. 2002. Quorum sensing in plant-associated bacteria. Curr Opin Plant Biol 5:285–290.
51. Wagner VE, Bushnell D, Passador L, Brooks AI, Iglewski BH. 2003. Microarray analysis of *Pseudomonas aeruginosa* quorum-sensing regulons: Effects of growth phase and environment. J Bacteriol 185:2080–2095.
52. Antunes LCM, Ferreira RBRR, Lostroh CP, Greenberg EP. 2008. A mutational analysis defines *Vibrio fischeri* LuxR binding sites. J Bacteriol 190:4392–4397.
53. Buchan A, González JM, Moran MA. 2005. Overview of the marine *Roseobacter* lineage. Appl Environ Microbiol 71:5665–5677.

Appendix: Ongoing genomic and computational analysis in Y4I.

The work included in this appendix focuses on genetic and bioinformatic tools utilized to untangle the regulatory network governed by QS in Rhodobacterales sp. strain Y4I and does not appropriately fit into any of the preceding research chapters. Most of the preliminary work on CtrA was performed by Sarah Layne with the guidance of April C. Armes.

I. Identify T6SS homologs in Rhodobacterales sp. Y4I.

a) Identification of putative T6SS homologs in Y4I.

i) ***Method:*** We searched for the full suite of T6SS protein homologs in Y4I using Integrated Microbial Genome Joint Genome Institute (IMG JGI) database.

ii) ***Results:***

Table 5.1 Putative T6SS genes in Rhodobacterales strain Y4I based on COG families

Gene ID	Locus Tag	Annotated Gene Product Name	COG
647618729	RBY4I_3424	ATP-dependent Clp protease ATP-binding subunit ClpA (EC 3.4.21.92)	COG0542 - ATP-dependent Clp protease ATP-binding subunit ClpA
647619590	RBY4I_2485	ATP-dependent chaperone ClpB	COG0542 - ATP-dependent Clp protease ATP-binding subunit ClpA
647620384	RBY4I_162	type VI secretion ATPase, ClpV1 family	COG0542 - ATP-dependent Clp protease ATP-binding subunit ClpA
647620375	RBY4I_205	OmpA family protein	COG3455 - Type VI protein secretion system component VasF
647620392	RBY4I_151	type VI secretion-associated protein, ImpA family	COG3515 - Predicted component of the type VI protein secretion system
647620391	RBY4I_190	type VI secretion protein, VC_A0107 family	COG3516 - Predicted component of the type VI protein secretion system
647620381	RBY4I_163	conserved hypothetical protein	COG3517 - Predicted component of the type VI protein secretion system
647620390	RBY4I_222	type VI secretion protein, EvpB/VC_A0108 family	COG3517 - Predicted component of the type VI protein secretion system
647620387	RBY4I_227	type VI secretion system lysozyme-related protein	COG3518 - Predicted component of the type VI protein secretion system
647620386	RBY4I_180	type VI secretion protein, VC_A0110 family	COG3519 - Type VI protein secretion system component VasA
647620385	RBY4I_200	type VI secretion protein, VC_A0111 family	COG3520 - Predicted component of the type VI protein secretion system
647620376	RBY4I_167	type VI secretion protein, VC_A0114 family	COG3522 - Predicted component of the type VI protein secretion system
647620374	RBY4I_174	type VI secretion protein IcmF	COG3523 - Type VI protein secretion system component VasK

II. Determine if indigoidine can autoregulate synthesis of its own operon.

a) Characterization of indigoidine production under various growth conditions (temperature and medium)

i) ***Method:*** Indigoidine production was tested at various temperature ranges (4° C to 37° C) and on minimal media (marine basal medium [MBM] containing 10 mM Na acetate) using Y4I mutants. Mutants included in experimental design were chosen based on their previously reported indigoidine production or lack thereof (1, 2). There were primarily wildtype Y4I, the hyper pigmented *clpA*::TN5-Km^R, and the pigment null *igiD*::TN5-Km^R. Briefly, mid-exponential mutants were diluted and spread plate onto with YTSS and incubated at 4°, 20°, 25°, 30°, and 37° C *OR* were spread onto MBM with 10 mM Na acetate and incubated at 30° C. All plates were incubated for 38 hrs. Results reflect the observation in 3 biological replicates.

ii) ***Results:***

Table 5.2 Assessment of pigmentation in Y4I variants

Mutant Variant	AMB + 10mM Na Acetate Trial 1	AMB + 10mM Na Acetate Trial 2	4°C	20°C	25°C	30°C	37°C
Y4I	-	-	+	+	+	+	-
pgaR$^-$	-	NA	NA	NA	NA	NA	NA
phaR$^-$	-	NA	NA	NA	NA	NA	NA
igiD$^-$	-	-	-	-	-	-	-
clpA$^-$	-	+	+	+	+	+	+

+ = visual observation of pigmentation under tested condition; - = no visual presence of pigmentation' NA = not included in assay.

b) Determine dimethyl sulfoxide (DMSO) susceptibility of Y4I strains

i) Method: To utilize indigoidine for exogengous addition, we tested the susceptibility of wildtype Y4I and the *clpA* and *igiD* mutant strains to the organic solvent, dimethyl sulfoxide (DMSO) on agar plates and in broth culture. Briefly, we spread various concentrations (0 – 100 % in 10 % increments) of DMSO across YTSS agar plates. After allowing the plates to dry, we spot platted 10 µL of exponential phase culture onto agar plates in biological triplicates and allowed to incubate for 48 hrs at 30° C. DMSO was diluted with sterile water.

ii) ***Results:***

Table 5.3 Susceptibility to DMSO concentrations in Y4I variants

	DMSO Susceptibility Test					
	Plates			Liquid		
	Y4I	***igiD***	***clpA***	**Y4I**	***igiD***	***clpA***
100%	+	+	+	+	-	-
90%	+	-	+	+	-	-
80%	+	-	+	+	-	-
70%	-	-	-	+	-	-
60%	-	-	-	+	-	-
50%	-	-	-	+	-	-
40%	-	-	-	+	-	-
30%	-	-	-	+	-	-
20%	-	-	-	+	-	-
10%	-	-	-	+	-	-
0%	-	-	-	+	-	-

+ = visual observation of susceptibility in tested strain as determined by zone of clearing. under tested condition; - = no visual presence of pigmentation' NA = not included in assay.

III. Resolve the contribution of CtrA to the swim-stick modality, and therefore indigoidine production, in Y4I.

a) Generate knockout mutant using targeted mutagenesis approach.

I. ***Method:*** Successful integration of a small, PCR-amplified, *ctrA* fragment into the PCR cloning vector TA TOPO pCR 2.1 (Invitrogen, Carlsbad, CA) was made. The *ctrA*-containing plasmid was digested with BamHI and XhoI, liberating the fragment with compatible cohesive ends suitable for ligation into linearized pKNOCK-Km^R. Through biparental mating using with *E. coli* strain BW20767 the vector was introduced into Y4I. Transconjugates were counter-selected using marine basal medium (MBM) with p-hydroxybenzoate (POB) as the sole carbon source (per liter:1.5% (wt/vol) Sigma Sea Salts, 225 nM K2HPO4, 13.35 #M NH4Cl, 71 mM Tris-HCl (pH 7.5), 68μM Fe-EDTA, trace metals and vitamins) and kanamycin (50 μg/ mL) and allowed to incubate at 30°C for 2 days.

II. ***Results:*** We were unable to generate a knockout mutant in the *ctrA* gene. Given that CtrA has been demonstrated to essential in some Alphaproteobacteria, including a closely related member of the Roseobacter clade (3). It is possible that *ctrA* is an essential gene in Y4I.

b) Generate CtrA expression plasmid.

We aimed to modify an existing expression plasmid, pJBA21Tc, shown to work well in Alphaproteobaceria due its origin of replication (4, 5). This plasmid is reported to cleave X-gluc via GusA, resulting in a blue pigmentation distinct in color from indigoidine. However, GusA activity is constituently expressed due to the Paph promoter (6). We aimed to replace the Paph promoter in pJBA21Tc with the *ctrA* promoter in Y4I by incorporating restriction enzymes SphI and NdeI into *ctrA* promoter region, allowing for ligation of the *ctrA* promoter (ctrAp) in pJBA21Tc (**Figure 5.1**). This would result in an inducible promoter for the new plasmid vector.

I. ***Methods****:*

(1) *Sequence retrieval and annotation verification*. Genome sequences and *ctrA* amino acid sequences were retrieved from IMG JGI for the following organisms: *Caulobacter crescentus*, *Dinoroseobacter shibae*, *Rhodobacter capsulatus*, *Sinorhizobium meliloti*, and *Ruegeria* sp. KLH11, and Y4I. Genome and gene sequences (**Table 5.5**) were compared to Y4I using National Center for Biotechnology and Information (NCBI) blast tool (https://www.ncbi.nlm.nih.gov/). Domain comparisons revealed all genes shared a highly conserved OmpR domain (**Table 5.6**). BPROM (www.softberry.com) was used to identify putative promoter regions, specifically, the -10 and -35 regions (**Figure 5.2**).

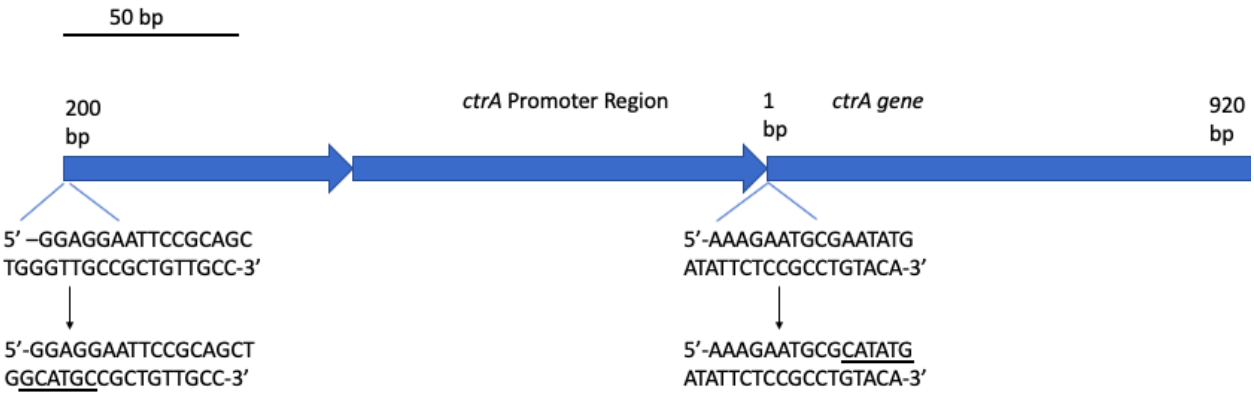

Figure 5.1 Schematic of ctrA promoter demonstrating nucleotide changes for incorporation of restriction enzymes.

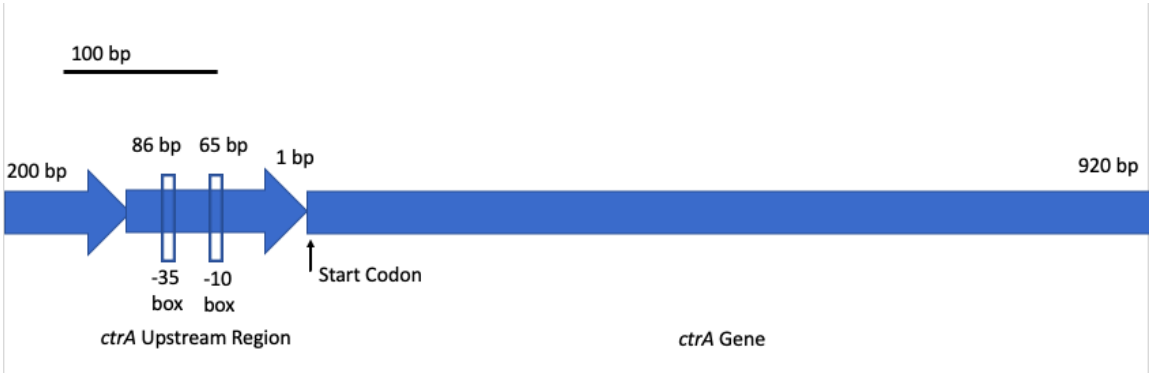

Figure 5.2 Visual representation of ctrA upstream region and gene with predicted promoter regions and lengths of the sequences. Bitscores for the -35 promoter consensus motif (5'-TTAACC-3') and -10 promoter consensus motif (5'-CATTAACTT-3') were 21 and 30, respectively.

(2) *Transformation of Y4I with pJBA21Tc.* The pJBA21Tc plasmid was extracted as per manufacturer's guidelines (QIAGEN, Venlo, Netherlands). Following plasmid extraction, pJBA21Tc was transformed into *E. coli* EZ180 via heat-shock and mated with Y4I. Confirmation of Y4I transformants containing pJBA21Tc in Y4I was performed via PCR using the *gusA* primers in table 5.4. Additionally, primers were designed and ordered in anticipation of performing rolling PCR on the pJBA21Tc plasmid to replace the constitutive promoter with the *ctrA* promoter region in Y4I (**Table 5.4**).

Table 5.4 Primers for CtrA expression plasmid

Primer Name	Sequence	TM
ctrA_F	CGGAATCACGGATTACGATT	59.8
ctrA_R	CCAGATTCGGTTTGGAAAAA	59.9
gusA_1F	ATGTTACGTCCTGTAGAAAC	56.3
gusA_1801R	TCATTGTTTGCCTCCCTGCT	60.4
gusA_outward	ATTCCACAGTTTTCGCGATC	58.4
ctrAp_24F	GGTGAAGAAGCGCTGAAAAC	60.4
ctrAp_178R	TGTTTCCCTCAGGTCTCGTT	60.4
ctrAp_FSphI	GGA GGA ATT CCG CAG CTG GCA TGC CGC TGT TGC C	76.7
ctrAp_RNdeI	AAA GAA TGC GCA TAT GAT ATT CTC CGC CTG TAC A	67.1

(3) *Colorimetric expression assay optimization.* Verification of a putative transconjugant was difficult to assess via PCR confirmation (**FIGURE 5.3**)**.** Instead, we modified X-gluc expression assays by X and Y et al to determine if the transconjugant carried the plasmid. Briefly, overnight cultures of WT Y4I, *E. coli* carrying pJBA21Tc and putative transconjugants were grown up in liquid YTSS. Strains carrying pJBA21Tc were grown in the presence of tetracycline (10 µg/mL). For liquid colorimetric assays, 1 mL overnight cultures were harvested, washed with 1.5 % sea salt solution and lysed as previously described (7). Following lysis, lysate was extracted and suspended in phosphate buffer (50 mM at pH 7.0) containing 5 mM DTT and 0.1% Triton X-100. 5 µL of X-gluc was added to this solution and incubated at 30°C for up to 24 hrs. Optical density of colorimetric expression was measured at 415 nm (OD_{415}) using a spectrophotometer. To assay colorimetric expression of *gusA* in solid-state cultures, we spread 100 µg/mL of X-gluc onto YTSS agar (1.5 %) to which we spotted 10 µL of exponential phase liquid cultures in duplicate and allowed to incubate for 24 hrs at 30°C (**Figure 5.4**).

II. ***Results*****:**

(1) Y4I possesses putative CtrA homolog

Table 5.5 NCBI Blast results comparing alphaproteobacterial CtrA amino acid sequence to

CtrA Protein Sequence	**Percent Match Identity to Y4I**	**E-value**
***C. vibrioides* CB15 >NP_421829.1**	74%	7e-102
***S. meliloti 1021* >NP_386824.1**	78%	5e-107
***D. shibae* DFL-12 >ABV93250.1**	91%	1e-121
***Rhodobacteraceae* bacterium KLH11 >EEE39107.1**	91%	3e-130
***R. capsulatus* SB1003 >ADE85408.1**	88%	4e-124

Table 5.6 Amino acid CtrA sequence blast results with NCBI database used for domain query.

Y4I CtrA Protein Sequence Match	Species Match	Percent Match Identity	E- value
***C. vibrioides* CB15 >NP_421829.1**	*Leisingera* sp. ANG-Vp Response Regulator transcription factor RefSeq: WP_039133034.1	100%	7e-163
***S. meliloti 1021* >NP_386824.1**	*Leisingera* sp. ANG-Vp Response Regulator transcription factor RefSeq: WP_039133034.1	100%	3e-162
***D. shibae* DFL-12 >ABV93250.1**	*Leisingera* sp. ANG-Vp Response Regulator transcription factor RefSeq: WP_039133034.1	100%	2e-161
***Rhodobacteraceae* bacterium KLH11 >EEE39107.1**	*Leisingera aquamarina* Response regulator transcription factor RefSeq: WP_027258794.1	99%	5e-173
***R. capsulatus* SB1003 >ADE85408.1**	*Leisingera aquamarina* Response regulator transcription factor RefSeq: WP_027258794.1	99%	5e-173

(2) Putative transconjugants containing pJBA21Tc in Y4I. Initial mating was unsuccessful, however, subsequent attempts performed by Cameron Moore, yielded two putative transconjugants. PCR verification was performed on plasmid extractions but yielded inconclusive results (**Figure 5.3**).

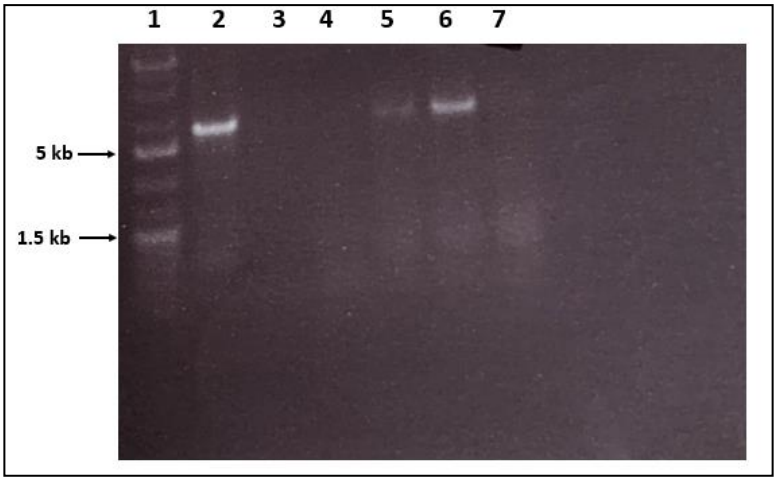

Figure 5.3 Transconjugant verification via PCR using gusA primers. Lane 1 harbored a 1 kb ladder for reference. PCR on plasmid extracts on the *E. coli* donor strain carrying pJBA21 (Lane 2), a no DNA negative control (lane 3) and putative transconjugants (lanes 4-7).

(3) Transconjugants demonstrate X-gluc activity in liquid colorimetric expression assays. In order to confirm PCR verification of the *gusA* gene, we performed colorimetric expression assays on potential transconjugates. Transconjugants resulted in a fraction of production of blue pigmentation indicative of GusA activity compared to donor *E. coli* strains (Figure 5.4).

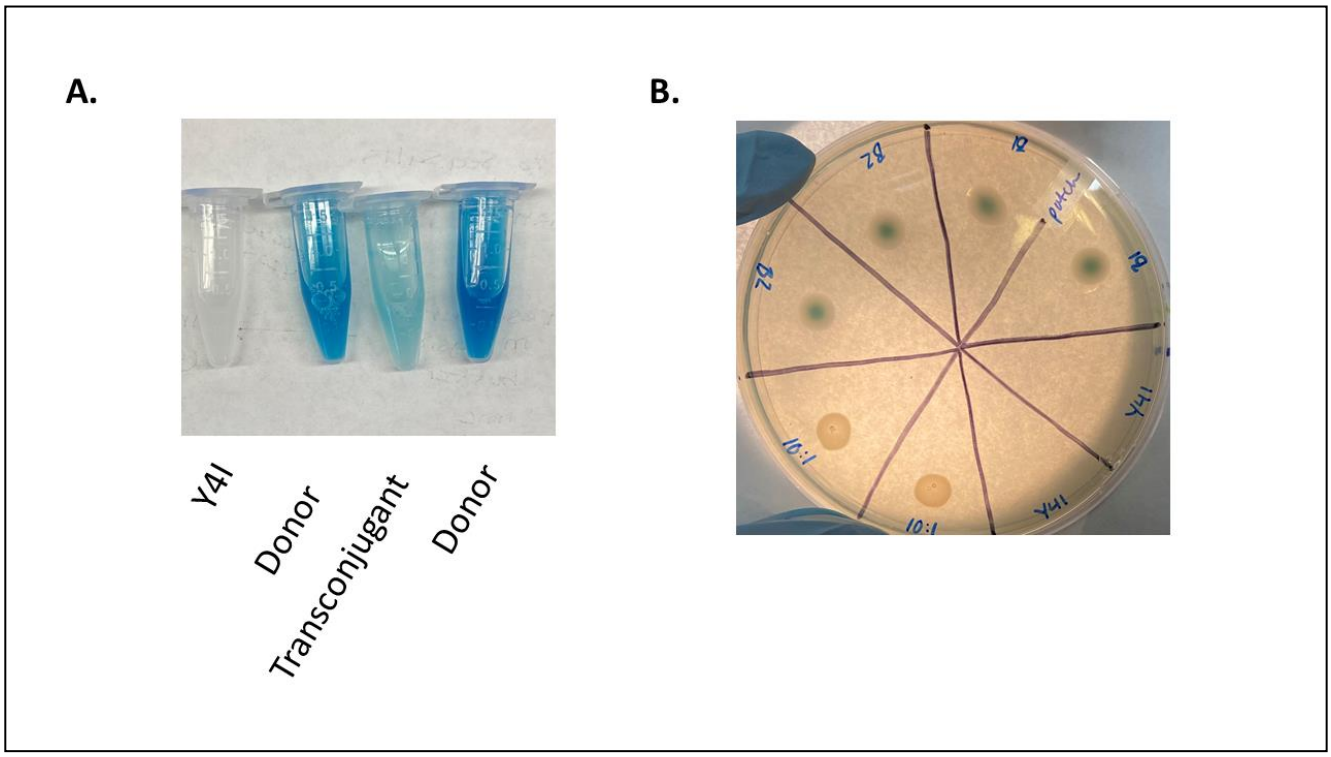

Figure 5.4 GusA activity as determined by liquid (A) and solid growth (B) colorimetric expression assays. GusA activity was determined by hydrolyzes of X-gluc resulting in blue coloration in liquid lysate (A) and in spot colonies on plate (B). GusA activity of transconjugants (labeled 10:1 in panel B) were compared to WT Y4I and two *E. coli* donor strains (labeled B1 and B2) as negative and positive controls respectively

.

References

1. Cude WN, Mooney J, Tavanaei AA, Hadden MK, Frank AM, Gulvik CA, May AL, Buchan A. 2012. Production of the antimicrobial secondary metabolite indigoidine contributes to competitive surface colonization by the marine roseobacter *Phaeobacter sp.* strain Y4I. Appl Environ Microbiol 78:4771–4780.
2. Cude WN, Prevatte CW, Hadden MK, May AL, Smith RT, Swain CL, Campagna SR, Buchan A. 2015. *Phaeobacter sp.* strain Y4I utilizes two separate cell-to-cell communication systems to regulate production of the antimicrobial indigoidine. Appl Environ Microbiol 81:1417–1425.
3. Zan J, Heindl JE, Liu Y, Fuqua C, Hill RT. 2013. The CckA-ChpT-CtrA Phosphorelay System Is Regulated by Quorum Sensing and Controls Flagellar Motility in the Marine Sponge Symbiont *Ruegeria* sp. KLH11. PLoS One 8:e66346.
4. Ramos HJO, Roncato-Maccari LDB, Souza EM, Soares-Ramos JRL, Hungria M, Pedrosa FO. 2002. Monitoring *Azospirillum*-wheat interactions using the *gfp* and *gusA* genes constitutively expressed from a new broad-host range vector. J Biotechnol 97:243–252.
5. Greer-Phillips SE, Stephens BB, Alexandre G. 2004. An energy taxis transducer promotes root colonization by *Azospirillum brasilense*. J Bacteriol 186:6595–6604.
6. Wielbo J, Skorupska A. 2001. Construction of improved vectors and cassettes containing *gusA* and antibiotic resistance genes for studies of transcriptional activity and bacterial localization. J Microbiol Methods 45:197–205.
7. Myronovskyi M, Welle E, Fedorenko V, Luzhetskyy A. 2011. β-Glucuronidase as a sensitive and versatile reporter in *Actinomycetes*. Appl Environ Microbiol 77:5370–5383.

VITA

April Christine Armes (Mitchell) was born in Lanett, Alabama to Ronald and Tina Mitchell in the month of February. April's passion for microbiology began before she knew the word microbiology. She pretended to be every type of doctor a five-year old knew about, which admittedly is only a medical doctor and dentist. April dreamed of becoming a doctor, but she did not become the type of doctor she thought she'd be.

April attended the University of Alabama in pursuit of her dream of becoming a pediatric doctor. During her education, April was met with many hardships. One of these hardships was the tragic loss of her mother in 2009. After which, April suffered many injuries of the emotional, physical, and academic variety. After receiving criticisms and discouragement from her advisors, April changed her major to nursing. Had circumstances not been what they were, April's determination would have superseded any negative remarks to her academic success.

During her education in the College of Nursing at The University of Alabama, April encountered a microbiology course and began to connect the dots to what made her so passionate about pursing a degree in the medical field in the first place. Enchanted with the subject matter, April absorbed every lesson. She even watched microbiology content for fun! Eventually, she stumbled upon the idea that bacteria could talk to one another, but not before another tragedy struck.

April's father passed away in 2012. Prior to this, her plan had been to get her nursing degree and move back home to care for her father as he aged. After all, he was a widowed empty nester. The grief of the death of her father hit April differently than it had her mother. This time, April poured herself into her studies. At the library with her microbiology textbook in hand was the only place April felt safe during that time of her life. Realizing she now had the freedom to choose who she wanted to be and was no longer shackled to the idea of caring for her father, April firmly decided that she would attend graduate school to further pursue her love for microbiology.

Changing course with a year left before her education was complete (this time now as a Bachelor of Science in Biology), April quickly secured a research position in a microbiology lab. April worked in the PhycoLab under Dr. Juan Lopez-Bastista at The University of Alabama where she learned molecular techniques. April's first major project in the PhycoLab was optimizing DNA extraction methods for a gelatinous deep-sea algal, Verdigellas peltata, thought to be an evolutionary link between gelatinous matrix derived algal species and flagellated algal species. April explored many different methods to extract DNA, including freezing the algae with liquid nitrogen and manually disrupting its cells, using commercially available kits, and finally using phenol chloroform. Much to her dismay, none of these methods yielded much success when it came to amplifying the Rubisco operon. Needless to say, pulling a 200 ft deep gelatinous algal species up from the ocean floor without maintaining pressure or proper storage upon surfacing did not give April a prime specimen to work with in the first place. Nonetheless, she persevered.

April attended her first scientific conference where she had the opportunity to meet the founder of chemical communication, Dr. Edward O. Wilson. April presented her research on Verdigellas peltate DNA extraction methods at the First Annual Southeastern

Biogeochemistry Symposium (SBS) in Atlanta, Ga later that year. At SBS, April met students from the Microbiology Department at The University of Tennessee who represented the second largest University in attendance. There, April expressed her interest in cell-to-cell communication with one of the students from The University of Tennessee who encourage her to meet with her advisor, Dr. Alison Buchan.

April Armes started her graduate career in the Fall of 2014 and joined the Buchan lab in December of that year. After joining Dr. Buchan's lab, April worked on the projects outlined in this dissertation including determining the hierarchical regulation governing antimicrobial production via cell-to-cell communication in a competitive member of the Roseobacter clade, Rhodobacterales strain Y4I. As she grew into an independent scientist, April merged two projects in the Buchan lab to understand how cell-to-cell communication influences a multispecies biofilm. During her graduate career, April was a teaching assistant and was awarded an excellence in teaching award during the Covid19 pandemic, she presented her research at both local conferences including ASM branch meetings and SBS and national conferences as often as she could, and received a fellowship to as a summer intern at the Center of Disease Control and Prevention where she created standards for detecting botulism toxin using Matrix-Assisted Laser Desorption/Ionization-Time Of Flight (MALDI-TOF) mass spectrometry. April hopes to one day return to the CDC in continuation of her scientific career.